NASA/TM-2009-xxxxxx

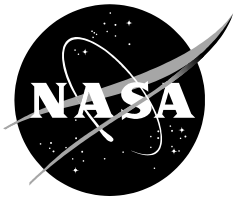

C-9 and Other Microgravity Simulations

Summary Report

Report prepared by
Space Life Sciences Directorate
Human Adaptation and Countermeasures Division
NASA Johnson Space Center, Houston

Lyndon B. Johnson Space Center
Houston, Texas

September 2009

THE NASA STI PROGRAM OFFICE . . . IN PROFILE

Since its founding, NASA has been dedicated to the advancement of aeronautics and space science. The NASA Scientific and Technical Information (STI) Program Office plays a key part in helping NASA maintain this important role.

The NASA STI Program Office is operated by Langley Research Center, the lead center for NASA's scientific and technical information. The NASA STI Program Office provides access to the NASA STI Database, the largest collection of aeronautical and space science STI in the world. The Program Office is also NASA's institutional mechanism for disseminating the results of its research and development activities. These results are published by NASA in the NASA STI Report Series, which includes the following report types:

- TECHNICAL PUBLICATION. Reports of completed research or a major significant phase of research that present the results of NASA programs and include extensive data or theoretical analysis. Includes compilations of significant scientific and technical data and information deemed to be of continuing reference value. NASA's counterpart of peer-reviewed formal professional papers but has less stringent limitations on manuscript length and extent of graphic presentations.

- TECHNICAL MEMORANDUM. Scientific and technical findings that are preliminary or of specialized interest, e.g., quick release reports, working papers, and bibliographies that contain minimal annotation. Does not contain extensive analysis.

- CONTRACTOR REPORT. Scientific and technical findings by NASA-sponsored contractors and grantees.

- CONFERENCE PUBLICATION. Collected papers from scientific and technical conferences, symposia, seminars, or other meetings sponsored or cosponsored by NASA.

- SPECIAL PUBLICATION. Scientific, technical, or historical information from NASA programs, projects, and mission, often concerned with subjects having substantial public interest.

- TECHNICAL TRANSLATION. English-language translations of foreign scientific and technical material pertinent to NASA's mission.

Specialized services that complement the STI Program Office's diverse offerings include creating custom thesauri, building customized databases, organizing and publishing research results . . . even providing videos.

For more information about the NASA STI Program Office, see the following:

- Access the NASA STI Program Home Page at http://www.sti.nasa.gov

- E-mail your question via the Internet to help@sti.nasa.gov

- Fax your question to the NASA Access Help Desk at (301) 621-0134

- Telephone the NASA Access Help Desk at (301) 621-0390

- Write to:
  NASA Access Help Desk
  NASA Center for AeroSpace Information
  7115 Standard
  Hanover, MD 21076-1320

NASA/TM-2009-xxxxxx

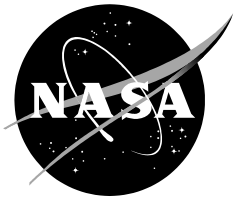

C-9 and Other Microgravity Simulations

Summary Report

Report prepared by
Space Life Sciences Directorate
Human Adaptation and Countermeasures Division
NASA Johnson Space Center, Houston

National Aeronautics and Space Administration
Lyndon B. Johnson Space Center
Houston, Texas

September 2009

PREFACE

This document represents a summary of medical and scientific evaluations conducted aboard the C-9 and other NASA-sponsored aircraft from June 2008 to June 2009. Included is a general overview of investigations manifested and coordinated by the Human Adaptation and Countermeasures Division. A collection of brief reports that describe tests conducted aboard the NASA-sponsored aircraft follows the overview. Principal investigators and test engineers contributed significantly to the content of the report, describing their particular experiment or hardware evaluation. Although this document follows general guidelines, each report format may vary to accommodate differences in experiment design and procedures. This document concludes with an appendix that provides background information concerning the Reduced Gravity Program.

Acknowledgments

The Space Life Sciences Directorate gratefully acknowledges the work of the Sharon Hecht, Jacqueline M. Reeves, and Elisabeth Spector for their outstanding editing support and contribution to the overall quality of this annual summary report.

Available from:

NASA Center for AeroSpace Information
7115 Standard Drive
Hanover, MD 21076-1320
Phone: 301-621-0390 or
Fax: 301-621-0134

National Technical Information Service
5285 Port Royal Road
Springfield, VA 22161
703-605-6000

This report is also available in electronic form at http://ston.jsc.nasa.gov/collections/TRS/

C-9 and Other Microgravity Simulations
Summary Report – September 30, 2009

National Aeronautics and Space Administration
Lyndon B. Johnson Space Center

Prepared by: _____ _____
Noel C. Skinner, M.S. Date
C-9 Coordinator
Wyle Integrated Science and Engineering Group

_____ _____
Wanda L. Thompson, R.N., BC, NMCC Date
Alternate C-9 Coordinator
JES Tech, LLC

Approved by: _____ _____
Jeannie L. Nillen, MT(ASCP) Date
Manager
Human Adaptation and Countermeasures Group
Wyle Integrated Science and Engineering Group

Approved by: _____ _____
Todd T. Schlegel, M.D. Date
Technical Monitor
Human Adaptation and Countermeasures Office
Reduced Gravity Program
NASA Johnson Space Center

CONTENTS

Acronyms

A-IgG	anti-immunoglobulin G
ABF	Anthropometry and Biomechanics Facility
AC	alternating current
ADUM	Advanced Diagnostic Ultrasound in Microgravity
AP	Advanced Projects [group]
ARGOS	Active Response Gravity Offload System
ASEP	American Society of Exercise Physiologists
AVI	audio visual interface
BCI	blood count instrument
CEV	crew exploration vehicle
CFD	computational fluid dynamics
CG	center of gravity
CH	Cooper-Harper
CITML	California Institute of Technology Micromachining Laboratory
CMO	Crew Medical Officer
CMRS	Crew Medical Restraint System
COM	center of mass
CPHS	Committee for the Protection of Human Subjects
CPR	cardio-pulmonary resuscitation
CTSD	Crew and Thermal Systems Division
CxP	Constellation Program
DSO	Detailed Science Objective
Eg	Earth gravity
EPSP	EVA Physiology, Systems, and Performance [Project]
ESPO	EVA Systems Project Office
ET	endotracheal
EVA	extravehicular activity
ExPC	Exercise Physiology and Countermeasures [Project]
HACD	Human Adaptation and Countermeasures Division
HRF	Human Research Facility
HSC	Hele-Shaw Cell
ICF	immune complex formation
ICP	intracranial pressure
IEEE	Institute of Electrical and Electronic Engineers
IgG	immunoglobulin G
IKA	intubation kit-airway
ILMA	intubating laryngeal mask airway
IOP	intraocular pressure
ISM	industrial, scientific, and medial
ISS	International Space Station
IST	Integrated Suit Test
IV	intravenous
JSC	Johnson Space Center

LCD	liquid crystal display
LED	light-emitting diode
Lg	lunar gravity
LIPO	lithium polymer
LOCAD PTS	Lab-On-a-Chip Applications and Development Portable Test System
Med Ops	Medical Operations
MRI	magnetic resonance imaging
MRT 7	West Virginia University Microgravity Research Team
NBL	Neutral Buoyancy Laboratory
NEEMO	NASA Extreme Environment Mission Operations
NMT	Noninvasive Medical Technologies Inc.
PC	personal computer
PCR	polymerase chain reaction
PEG	polyethylene glycol
PET	pressure equalization tube
PI	Principal Investigator
PLSS	Portable Life Support System
PMD	pressure measurement device
PMT	photon multiplication tube
POGO	prevention of coupled structure propulsion instability
psi	pounds per square inch
RGO	Reduced Gravity Office
RH	relative humidity
RPE	rating of perceived exertion
SAMS	Space Acceleration Measurement System
SAR	specific adsorption rate
SEM	standard error of mean
TSAS	Tactile Situation Awareness System
TSH-ES	triaxial sensor head-Ethernet standalone
UHCL	University of Houston, Clear Lake
UNC	University of North Carolina
USB	universal serial bus
USP	United States Pharmacopeia
UV	ultraviolet
WVU	West Virginia University
ZERO-G®	Zero Gravity Corporation

Overview of Reduced-gravity Flight Activities Sponsored by the Human Adaptation and Countermeasures Division

As a summary for the year, 7 weeks were specifically reserved for flights sponsored by the Human Adaptation and Countermeasures Division (HACD) from June 2008 to June 2009. In addition, we were able to obtain seating during 5 weeks for funded customers alongside Education Outreach Program participants. A total of 35 flights with approximately 40 parabolas per flight were completed. The average duration of each flight was 2 hours. The Reduced Gravity coordinator assisted principal investigators and test engineers of 26 different experiments and hardware evaluations in meeting the necessary requirements for flying aboard the C-9 or other NASA-sponsored aircraft and in obtaining the required seating and floor space. HACD customers purchased a total of 374 seats. The number of seats supported and number of different tests flown by flight week are provided below:

Flight Week	Seats	No. Tests Flown	Sponsor
2008			
June 24–25	5	1	Education Outreach Program
July 17–18	8	2	Education Outreach Program
July 22–25	25	3	HACD
August 29	5	1	HACD
September 9–10	12	2	HACD
November 21	8	4	HACD
December 9–12, 17	108	1	HACD
2009			
January 13–16	29	6	Education Outreach Program/HACD
January 13	18	1	HACD
February 24–17	26	3	Education Outreach Program/HACD
March 4, 5, 10–13, 27	126	1	HACD
March 31–April 1	4	1	Education Outreach Program

Support was provided to the Education Outreach Program during weeks in June and July 2008 as well as in January, February, March, and April 2009 to undergraduate students and educators from participating universities or middle and high schools. A large ground crew from the respective academic institution supported the in-flight experiments.

Other HACD-sponsored flight opportunities are scheduled for weeks during August and September 2009. Additional flights will be added throughout the remainder of calendar year 2009 to accommodate customers as needs arise.

Medical and Scientific Evaluations during Parabolic Flights

TITLE

Education Outreach Program – Investigation of Viscous and Capillary Fingering through a Hele-Shaw Cell in Microgravity

FLIGHT DATES

June 24–25, 2008

PRINCIPAL INVESTIGATORS

Emily Calledrelli, West Virginia University (WVU)
Alan Talbot, WVU
Greg Duckett, WVU
Gavin Hall, WVU

CO-INVESTIGATORS

Andrew Harner, WVU
Jesse Phillips, WVU
Eileen Reiff, WVU
Corey Snyder, WVU

FACULTY ADVISORS

John Kuhlman, WVU
Donald Gray, WVU

GOAL

The proposed experiment will test the phenomena of capillary fingering and viscous fingering in a 2-phase immiscible flow under the conditions of microgravity and hypergravity.

INTRODUCTION

The term capillary fingering refers to the fingering created when the initial velocity of injection is small and capillary forces are more dominant than viscous forces. These fingers tend to be smaller and wider than those produced by viscous fingering. In comparison, viscous fingering occurs when a less viscous fluid is driven at high velocity through a more viscous defending fluid. The term "viscous fingering" refers to the instabilities at the interface of a 2-fluid flow (Homsy, 1987). While the major driving force for viscous fingering is difference in viscosity, other forces, such as gravity and surface tension, have influence on the propagation of the fingers (Homsy, 1987). Although there are different types of fingering, the categories considered here are primarily viscous and capillary. The given experiment studied this phenomenon under conditions of variable gravity.

Viscous fingering was first studied by Hill in 1952. A 1-dimensional analysis was performed by having a gravitationally driven vertical flow. Another way to think of a 1-dimensional flow is a single line or slice of fluid. Gravity and viscous-stabilizing flows were investigated. Another early development was by Chouke et al. in 1959. Chouke was the first scientist to include surface tension effects. He used 1-dimensional flows to find equations relating viscosity, surface tension, velocity, and gravity to the viscous fingering phenomenon. In 1958, Saffman and Taylor also found similar results (Homsy, 1987). Viscous fingering can be studied through various methods or geometries of injection and growth patterns. The most commonly investigated are radial propagation, a 5-point pattern with a source in the middle of a square with sinks on all 4 corners, and, as will be studied here, the 2-dimensional linear case.

The injection of a fluid with lower viscosity into one with higher viscosity can commonly occur in technological applications. For instance, the insertion of air into water and oil into water are both common fluid pairs that can potentially produce viscous fingering. A better grasp of the physics governing the development of fingering patterns will help to control the fluid behavior in such applications. For example, changes in fuel injection can yield better combustion efficiency. The fuel injected can be controlled and engineered so there is a maximum uniformity mixing and atomization, allowing the combustors in jet engines to become more environmentally friendly. The process also can be used to describe the propagation of a flame, which could be instrumental in subduing fires in microgravity environments. As a flame expands, it takes on a fingering profile similar to those in the proposed experiment.

There also can be an improvement in the efficiency of carbon dioxide sequestration, and the secondary extraction of materials from the earth, such as oil, can be optimized. More specifically, after the majority of oil is drilled from the earth, this secondary extraction process is used. The process of injecting carbon dioxide into the earth (which can be analyzed as a porous medium in which carbon dioxide flows through and disperses into viscous fingering) is commonly used to extract oil around a drill site (Saffman, 1986). As more information is developed about the fingering patterns, we can better answer many questions, such as (1) what will happen to the

carbon dioxide underground over time, and (2) are there small fingers of oil that are mixed into the sand and not extracted?

In the future, there are plans for lunar mining. This secondary extraction process could also be used to extract minerals from the moon more effectively, where gravitational levels are about 1/6 that of Earth gravity. Not only can this process be used for extracting minerals, but also possibly to control the underground storage of materials for a lunar space station. If technology allows, one day there could be mining on an asteroid as well.

In the context of these applications, it is beneficial to study the fractal behavior of the fingering patterns in flipped Hele-Shaw Cell (HSC)-PM and HSC, and the injection HSC. It was hypothesized that the flow patterns created at the interface in both the flipped HSC and HSC-PM would be similar given that the equations that govern both flows are analogous. Within the flipped HSC and HSC-PM, at higher viscosity ratios, the number and dispersion of capillary fingers were hypothesized to increase. During microgravity, the 2 fluids within the flipped HSC and HSC-PM should not have displaced one another. However, if capillary fingers were created, it would have been due to forces other than gravity. Within the injection HSC, viscous fingering, as opposed to capillary fingering, was hypothesized to occur. Lastly, increasing the injection flow rate was assumed to create a greater number and dispersion of the viscous fingers.

The given experiment involved 2 major components. The first part included 2 pairs of HSCs that were flipped about a common axis to analyze the behavior of possible capillary fingering for varying levels of gravity. The second part of the experiment consisted of a low-viscosity fluid injected into a high-viscosity fluid within an HSC. The goal of this part of the experiment was to simulate the flow through a 2-dimensional porous medium and to study the behavior of viscous fingering in varying gravity levels.

The first part of this experiment involved 2 sets of closed HSC pairs with 1 HSC in each set containing a porous medium. These were used to study the propagation of fingers, expected to be driven by capillary forces, in a closed 2-immiscible-fluid system without injection. The propagation of fluids through one another was based on a buoyancy force due to the 2 different fluid densities. In this portion, there were 2 different test pairs. Each test pair consisted of an HSC and an HSC-PM. Within each set, both the HSC-PM and the HSC contained identical fluid viscosity ratios. However, the 2 different HSC test pairs had different fluid-viscosity ratios. During the test period, the flows within each set were assumed to have similar patterns.

An additional objective for the first part of the experiment was to investigate the flow during hypergravity. During the pullout when gravity increased from near zero to nearly 2 G, the exchanging of liquids (the denser liquid falling towards the bottom) was expected to create a viscous fingering pattern. As the gravitational force increased, this fingering pattern was predicted to occur at a faster rate and with longer fingers. The team also predicted that with a higher viscosity ratio, the amount and dispersion of fingers would increase.

Viscous fingering, which was analyzed in the second portion of the proposed experiment, commonly occurs in 3-dimensional porous media, such as when water is absorbed in a sponge or

when carbon dioxide is injected into an oil field to enhance oil recovery. The 3-dimensional phenomenon is complex to analyze due to the complexity of the geometry and the governing equations. In addition, because of the small pore sizes and opaque nature of the 3-dimensional porous media, it is quite difficult to obtain experimental data. Sir Geoffrey Taylor (1958) overcame this dilemma in 1956 when he discovered that the flow through a porous medium could be modeled by flow through an HSC, and that the equations that govern both are similar (Saffman, 1986).

The WVU Microgravity Research Team investigated this injection flow in the second part of the experiment in hopes of improving knowledge of how viscous fingering affects flow patterns in porous media for varying gravity levels. The team predicted to observe viscous fingering, as opposed to capillary fingering, and also the development of fractal patterns at higher injection rates within the injection HSC. Lovoll et al. (1983) state that fast displacements can cause a fractal pattern to develop in the flow. The team suspected that microgravity conditions would cause the fingering patterns to be more sporadic as the propagation had one less force (gravity) governing it. As seen from equations above, the pressure drop in the flow was also expected to be negative as the factor, G, would be zero.

Another objective of both experiments was to describe the flow behavior qualitatively. Fingering patterns depend on many factors, some of which were measured in this experiment. Finger patterns propagate in different patterns. Saffman and Taylor (1958) first found that a single finger dominates the flow because of what they called shielding. They explained shielding as the tendency of a finger to grow in the direction of the pressure gradient. A finger that is larger is more apt to grow and, thus, shield its neighbors from growing, causing the instabilities to get larger as time proceeds. Surface tension acting at the tips of the fingers also has a great deal to do with how they spread. As the surface tension decreases, the once-steady finger becomes unstable because of the area the finger now covers. This finger then splits at the tip and the new, smaller fingers are stable. One will shield the other, and then eventually will have to tip-split as well. Saffman (1986) found that as a finger width approached one-half of the total width of the test section, the finger engaged in side-splitting rather than tip-splitting (Homsy, 1987). The pattern of shielding then tip-splitting and repeating may be a form of fractal growth. Fractals are patterns in nature that continue as the frame or view is reduced until it becomes infinitesimal, or behaves the same at any scale.

METHODS/RESULTS

To come to a final experiment apparatus, the West Virginia University Microgravity Research Team attempted many different designs for each of the systems involved in the experiment. These include the HSC design, the porous media choice, the mechanism to flip the capillary-driven HSCs, the injection system used to test the viscosity driven HSCs, and the injection flow rate control.

The first and most important subsystem of the experiment was the HSC design. Many hours were spent brainstorming, constructing, and testing different HSC ideas to achieve the best results possible for the experiment. The materials, dimensions, and adhesives that were involved all needed to be considered when determining the best design for the HSC. Glass, LEXAN®, and

Plexiglas® were tested, and Plexiglas® was chosen for its weight, durability, and the fact that it is hydrophobic. The thickness of outside plates of Plexiglas® used was 0.25 in. Several sizes of HSCs were considered, and a final size was chosen based on the strength needed for the Plexiglas® sides and viewing of fingers. The flipped HSCs were 6 in×8 in on the outside, 0.5-in borders and a gap of 0.0625 in for the test area. The injection HSCs were 5.5 in×11.5 in on the outside with the same 0.5-in borders, and a gap of 0.062 in. This small gap created an environment in which the fluids could interact with one another in a constant area. Designing the gap was a tricky process, because it was imperative that the gap remain sealed. To make this gap, the team tried using a rubber gasket as a seal between 2 compressed Plexiglas® plates but still had leakage. The team then tried different adhesives and a thin frame-like Plexiglas® sheet to make this gap. Finally, the team used acrylic glue, which was satisfactory in sealing the HSC. For the flipped HSCs, small holes were placed in opposite corners to fill and drain the HSCs when appropriate. Injection HSCs had 1 hole specially made at the top for injection and 3 holes at the bottom for drainage.

Porous media were researched, and many different options were purchased. BBs, buckshot, sewing beads, and acrylic spheres were considered. The acrylic spheres were chosen for their size and hydrophobic nature. These spheres had a diameter of 0.0625 in.

A flipping mechanism was needed to test capillary fingering. The mechanism design consisted of a hand crank used to flip a central axis connected to all 4 flipped HSCs. This hand crank could be used from the outside by an operator and held the HSCs at 180-degree intervals. A stepper motor was considered for automation, but not integrated due to unnecessary complication and time constraints.

For the injection subsystem, the team chose to use an air compressor plug to inject air through an inflatable ball while keeping the HSC sealed. The excess fluid pushed down by the air would travel up a manometer-like pressure equalization tube (PET) in microgravity. This would then refill the HSC when reentering gravity. This was very different from the originally designed system and other evolving ideas. Such systems included the use of fluid-separating membranes, multiple fluid tanks to refill the HSC, multiple injection sites, and expanding bladders to relieve pressure and control excess fluid.

Varying the flow rate was achieved through the use of a variable power supply. By changing the voltage of the power supply, the rate of injection from the air compressor could be controlled. The voltage range was from 0 volts to 17.5 volts. A fully constructed experiment setup follows.

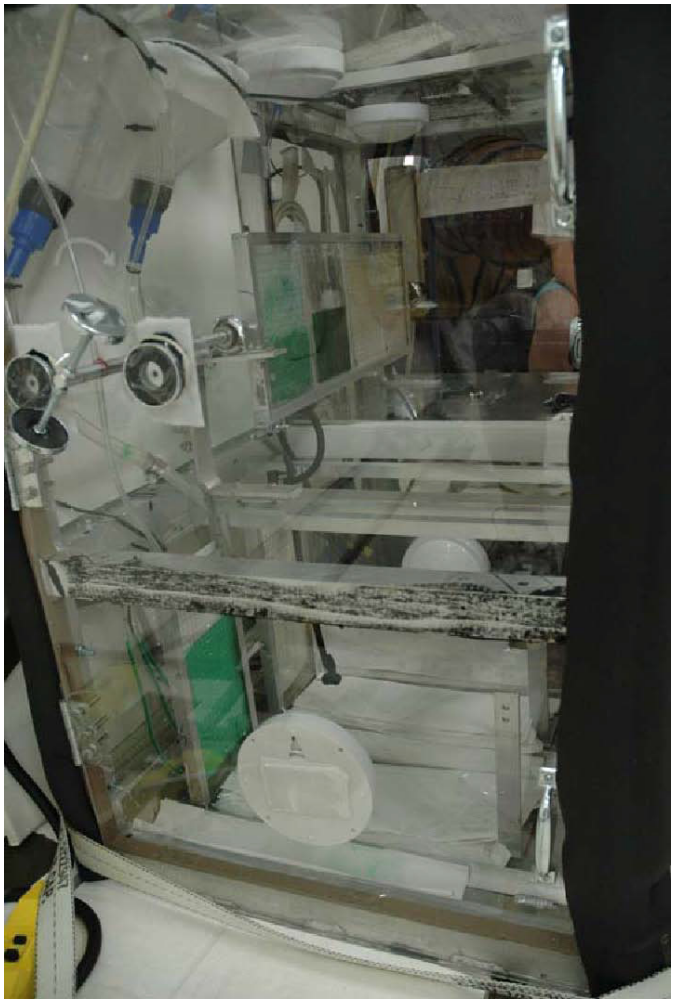

Side view of completed experiment.

After construction, the experiment was flown aboard the C-9 aircraft. MRT 7 was unsuccessful in collecting video recordings on either flight day (reasons and solutions to these problems are listed in the conclusions section to help prevent this from happening to future teams). The team's only data from the plane were from member observations during flight.

The compressors did not release any air while in flight for either day, thus there were no observations made for the injection HSCs. Some things were taken from the flipped HSCs, even though it was very hard for an observer to see the HSCs from the outside because of the enclosure constructed to help with lighting. On the first day, flyers saw little action during microgravity in the flipped HSCs, as expected. In the water and air HSC with no porous media, there were mixtures of air pockets and water globules floating throughout the HSC. The oil and glycerin HSC had little instabilities, but did have a slightly curved interface. Because of lighting, no observations could be made in either porous-media HSC. The second day, flyers saw similar results. The water and air with no porous media were observed to be stable with no fingers and only slight instabilities probably caused by plane vibrations. The oil and glycerin with no porous media showed similar results. The water and air with porous media did have very small fingers during microgravity, probably either residual from the constant flipping or driven by the surface

tension of the bead pack. Once again, no observations could be made from the oil and glycerin with porous media HSC because of poor lighting. The second day, flyers also attempted to observe the HSCs in hypergravity conditions. The water and air with no porous media fell extremely fast and no fingers were seen by the naked eye. The oil and glycerin with no porous media did have some long-thin fingers with almost no tip-splitting. The water and air with porous media had many fingers that moved quickly and branched off in many directions. Finally, the oil and glycerin with porous media could not be observed, again because of poor lighting.

For some visual data, the team did a ground run using the same fluids, injection rates, and equipment that were used for the experiment in microgravity. Flipped HSCs showed hypothesized results. The water and air with no porous media interaction moved very quickly in this 1-G environment, and swirled instead of fingered. The water and air with porous media interaction had some slow individual fingers. The oil and glycerin with no porous media also showed some fingering. The oil and glycerin with porous media was very hard to see, but had some fingers. These fingers are known to be capillary fingers, because the capillary numbers of these interactions are very low. This is because the velocities were zero to start and very low even when well into the interaction.

From this ground run, many observations were made pertaining to the relationship between the flow rate and finger geometry or fluid and finger geometry in the injection HSCs. The voltage was varied from 5 volts to 17.5 volts in 2.5-volt increments. From the video, it was observed that as voltage increased in the oil and air fluid pair HSC, the finger length increased and finger width decreased. There was also much more tip-splitting and side-branching fingers. In some rare cases at higher voltages, multiple fingers were observed. At higher voltages, finger growth would invert and go back toward the source of the air. Increased flow rate displaces the defending fluid more rapidly, which allows the fingers produced by the invading fluid to be longer and narrower. This increased speed of finger propagation also catalyzes the effect of tip-splitting of these narrowed fingers.

In the HSC with water as the defending fluid, the findings were almost completely opposite. This interface was much more stable, in general, with most of the instabilities on the interface being prevalent but with no large fingering. At smaller injection rates, fingers did occur, but, at larger rates, only a “saw tooth” effect on a relatively flat interface occurred. The “saw tooth” effect could have been caused by inherent vibrations from the mechanical motion of the air compressor. This effect was more apparent in the water HSC, because the defending fluid was less viscous, causing the defending fluid to fill the void caused by the injected air more quickly, thus producing fewer long fingers.

Individual injection runs were analyzed in more depth using the fluid properties, the ground run video, and dimensionless numbers. In the first set of data for the oil and air injection, the voltage was set at 5 volts. This resulted in a finger velocity of 0.297 meters per second. This velocity was found by taking the time for finger growth and dividing by the average finger length. This method is an approximation, as the video software used did not allow video to be viewed frame by frame and there was no zoom availability. In addition to this velocity, values were researched for the viscosity of the invading fluid (air) and the surface tension between the 2 fluids (air and oil).

These values were 1.82×10^{-5} Pascal-seconds and 0.047 Newtons per meter. These were used to find the capillary number, which was 1.150×10^{-4}. This is larger than the reference value of 10^{-5} meaning that this interaction was driven by viscous forces. The viscosity ratio was then calculated using a value of 4.425×10^{-3} Pascal-seconds for the viscosity of oil. This ratio was found to be 243.13. Visual inspection showed a tip split into 2 fingers and 2 main-side branches emanating from the main finger.

Another injection run was analyzed, this one at 12.5 volts. The velocity was found to be 0.521 meters per second and the capillary number was 2.017×10^{-4}. This also was larger than the reference value and, thus, driven by viscous forces. Of course, the viscosity ratio was the same. Visual inspection showed 1 main finger with a smaller, secondary finger. The main finger had 17 side branches and 1 tip split.

The same voltages were analyzed for the water and air injection. With the viscosity of air at 1.82×10^{-5} Pascal-seconds and the surface tension between the water and air equaling 0.07286 Newtons per meter, the capillary number can be could be calculated using the velocity. Since the velocity was 0.1099 meters per second for the 5-volt run, the capillary number is 2.745×10^{-5}. For the 15-volt run, the velocity was 0.3533 meters per second and the capillary number was 8.825×10^{-5}. These numbers are only slightly larger than the reference value, so theory says that these interactions show a stable interface, which was observed. The flow was driven by capillary and viscous forces, so a viscosity ratio needed to be calculated. The viscosity of water is known to be 1×10^{-3} Pascal-seconds, meaning the viscosity ratio was 54.95.

When comparing the 2 separate-fluid interactions, many interesting numerical observations were made. The velocity was found to be slower in the air-into-water injection. This was due to the air being distributed evenly across the cell in this injection instead of concentrated in 1-slim finger, as in the air into oil injection. The capillary numbers were larger in the air-into-oil injection, which was anticipated because this interaction was known to be driven by viscous forces, whereas the “air-into-water” injection numbers were near the boundary. Finally, as the viscosity ratio increased, the fingering complexity increased. This was consistent with theory.

In comparing the varying voltages, other similar numerical observations were made. In the air-into-oil injection as voltage was increased, velocity increased, and the capillary number and fingering thus increased. This was because this injection was driven by capillary forces, and these forces were greater with the increased velocity. The opposite occurred in the air-into-water injection. As the velocity was increased, the capillary number increased, but the fingering decreased and the flow was more uniform. This is because as capillary fingering turned to viscous fingering, a smooth interface was observed and the increased velocity brought the flow closer to this boundary.

CONCLUSION

There was no successful video data collection for either of the 2 flight days, due to technical difficulties. While there was a lack of data received during flight by WVU MRT 7, the team did learn many valuable lessons that could be readily applied if this experiment were chosen for re-

flight. The issues that arose can mainly be attributed to lack of experience and unforeseen electrical/mechanical problems; most, if not all, of these have very simple solutions.

The first and foremost problem occurred within the data recording interface. Four cameras were used for the experiment: including 2 standard-definition JVC camcorders and 2 high-definition JVC camcorders. JVC uses a battery conservation safeguard that automatically shuts down the camera when the liquid crystal display (LCD) viewfinder is closed. Whether this function is good or bad, it is a very strange function and, unfortunately, the team was not expecting this, resulting in zero data from the first flight day. On the second day, the viewfinders were kept open, but, unfortunately, the batteries ran out on all camcorders prior to the first parabola. In hindsight, this catastrophe could be easily have been prevented by using extended-life batteries, which will be purchased for future camera use. Alternatively, the 2 newer, high-definition cameras can be operated with alternating current (AC) power provided from the power strip on the aircraft. However this function is unavailable for the 2 older, standard-definition cameras.

The next issue, which dealt with the fluid reactions, could be avoided with a more exact assembly. The HSC containing the porous medium had a gap that was slightly larger than the diameter of the beads used to form the porous medium. This caused the beads to arrange in approximately 1.5 layers instead of only 1 layer. This created extra space and irregularities in the bead pack, as shown following.

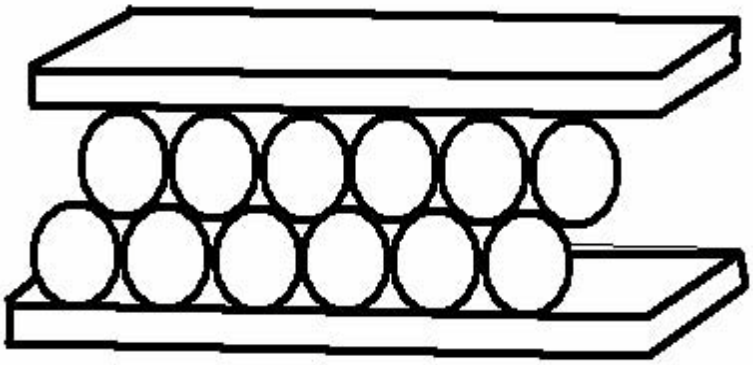

By observation, the team was also led to believe the beads were close enough so the surface tension between the fluid and the bead material drove the flow more than the fluid interaction, which was not the goal of the experiment.

These problems could be solved a number of ways, including the use of a mill for construction of all HSCs. Using a mill will ensure, to a very small tolerance, that the HSCs will be just wide enough to fit the beads, thus leaving no gaps between the beads and the glass. Another approach would be to have porous-medium HSCs with machined cylinders through the test area instead of a bead pack. An example of an ideal bead pack follows.

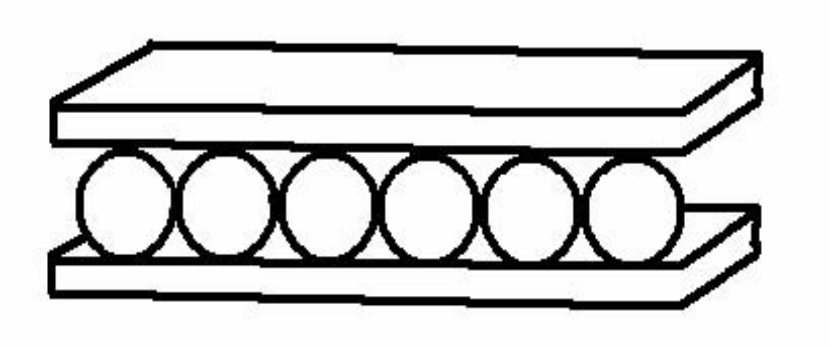

This would definitely eliminate the double stacks and gaps, and possibly eliminate most of the surface-tension-driven flow. The only negative of this idea is the feasibility. If it can be made, it is a much better approach.

There was another problem with fluid reaction, specifically the visual aspect. The fluid pair choice of glycerin and oil seems to be the root of the problem. The colors of these 2 fluids were so close that it was hard to distinguish the interface. Thus, if 1 fluid could be dyed, such as water with food coloring with a dye that will not change its properties significantly; this would be an easy solution. If not, new fluid pairs must be chosen. The reaction between this pair was also very slow, and the time during microgravity and hypergravity was not sufficient for a complete reaction to occur. In addition, a numerical value for surface tension between the 2 fluids could not be located, so some theoretical numbers could not be calculated. Overall, a new fluid pair would be the easiest solution.

Finally, the most intriguing and unforeseen problem was with the compressors. Both flight days, just prior to flight, the air compressors were tested while in the plane and were functional. Yet, at altitude, they did not work. They were connected to a variable power supply and the range of voltages and currents (0 amps to 10 amps and 0 volts to 18 volts) were tried on both days, but to no avail. The team investigated this and found that the only electrical requirement for high-altitude compressors was less power. A website, which was found by the team, said, “The efficiency of air compression depends on air temperature, atmospheric pressure, and relative humidity. The rating of an air compressor therefore depends on ambient conditions. This aspect should be taken in to account if an air compressor is used in very cold weather, very wet weather or at a high altitude.” With the compressors working on the ground, the team knew that there was enough power in the variable power source, thus less power could be achieved and was tried in flight. The team then tested many different models of air compressors in a pressure chamber at WVU, in the Mechanical and Aerospace Engineering Department, to see whether the change in pressure with altitude was the source of the problem. Compressors were individually placed in the chamber and connected to a 12.97-volt, 1-amp battery and turned on. The pressure inside the chamber was then lowered to near-vacuum, and observations were recorded. In each case, the compressors worked but at a slightly lower flow rate. The team thought this pressure difference was the root of the problem but through this test that theory was disproved. At the time of submission, the team is still investigating why this failure occurred. One possibility is the plane’s power was sufficient while grounded, with power coming from the ground, yet not sufficient while in flight. The easiest solution would be not to use air compressors and instead use a more

simple air injection system. This could be a syringe primed with air and mechanically plunged using some sort of motor to ensure injection rate consistency. The rest of the system could be the same with the air release tube at the top and pressure equalization tubing. The syringe would have an air reserve with a check valve to reset. A pressure vessel could also be an option, but the safety of the team and other members aboard the flight would have to be considered.

Even with no video data of the experiment in microgravity, the team got valuable flight experience with this experiment. If chosen for re-flight, the experiment could be greatly improved and valuable data could be obtained from it. This team's experience will greatly improve the success of future teams.

REFERENCES

1. Baker, Gregory L., and Jerry P. Gollub. Chaotic Dynamics, An Introduction, New York: Cambridge University, 1990.
2. Broyles, B. Scott, R. Andrew Shalliker, Djamel E. Cherrak, and Georges Guichon. "Visualization of Viscous Fingering in Chromatographic Columns." Journal of Chromatography 822 (1998): 173-187.
3. Chen, Ching-Yao, and Shu-Wei Wang. "Interfacial Instabilities of Miscible Fluids in a Rotating Hele-Shaw Cell." Flight Dynamics Research 30 (2002): 315-330.
4. Ferer, M. C. Ji, G. S. Bromhal, J. Cook, G. Ahmadi, D. H. Smith. "Crossover from Capillary Fingering to Viscous Fingering For Immiscible Unstable Flow: Experiment and Modeling." Physical Review E 70 (2004): 016303-1-016303-7
5. Ferer, M., W. N. Sams, R. A. Geisbrecht, and Duane H. Smith. "Crossover from Fractal to Compact Flow from Simulations of Two-Phase Flow with Finite Viscosity Ratio in Two-Dimensional Porous Media." Physical Review E 47 (1993): 2713-2723.
6. Gleick, James. Chaos: Making a New Science New York: Penguin Books, 1987.
7. Homsy, G. M. "Viscous Fingering in Porous Media," Annual Review of Fluid Mechanics 19 (1987):271-309
8. Kawaguchi, Masami, Kyoko Makino, and Tadaya Kato. "Viscous Fingering of Silica Suspensions in Polymer Solutions: Effects of Viscoelasticity and Gravity." Physica 246 (1997): 385-398.
9. King, P. R. "The Fractal Nature of Viscous Fingering in Porous Media," J. Phys. A: Math Gen. 20 (1987): L529-534
10. Kuang, Jun, Tony Maxworthy, and Philippe Petitjeans. "Miscible Displacements between Silicone Oils in Capillary Tubes." European Journal of Mechanics B/Fluids 22 (2003): 271-277.
11. Lovoll, Grunde, Yves Meheust, Knut Jorgen Maloy, Evyind Aker, and Jean Schmittbuhl. "Competition of Gravity, Capillary, and Viscous Forces during Drainage in a Two-Dimensional Porous Medium, A Pore Scale Study." Energy 30 (2005): 861-872.
12. Maxworthy, T. "Bubble Formation, Motion and Interaction in a Hele-Shaw Cell." Journal of Fluid Mechanics 173 (1986): 95-114.
13. Orr, Franklin M. Jr. Scale-Up of Miscible Flood Processes United States. Department of Petroleum Engineering Stanford University: 1993.
14. Raudkivi, A. J. and R. A. Callander. Analysis of Groundwater Flow New York: Halested Press, A Division of John Wiley and Sons, Inc., 1976.

15. Saffman, P. G. “Viscous Fingering in Hele-Shaw Cells.” Journal of Fluid Mechanics 173 (1986): 73-94.
16. Saffman, P.G. Vortex Dynamics New York: Cambridge University Press, 1992.
17. Saffman, P.G., G.I. Taylor. “The Penetration of a Fluid into a Porous Medium or Hele-Shaw Cell Containing a More Viscous Fluid.” Proc. Roy. Ssc. London. Ser. A 245 (1958): 312-329.
18. Saghir, M. Z., O. Chaalal, and M. R. Islam. “Numerical and Experimental Modeling of Viscous Fingering during Liquid-Liquid Miscible Displacement.” Journal of Petroleum Science and Engineering 26 (2000): 253-262.
19. Shalliker, R. Andrew, Heather J. Catchpoole, Gary R. Dennis, and Georges Guiochon. “Visualizing Viscous Fingering in Chromatography Columns: Viscosity Solute Plug.” Journal of Chromatography 1142 (2007): 48-55.
20. Sheorey, Tanuja, and K. Muralidhar. “Isothermal and Non-Isothermal Oil-Water Flow and Viscous Fingering in a Porous Medium.” International Journal of Thermal Sciences 42 (2003): 665-676.
22. Tanveer, S. “Surprises in Viscous Fingering.” Journal of Fluid Mechanics 409 (2000): 273-308.
23. Verruijt, A. Theory of Groundwater Flow New York: Gordon and Breach Science Publishers, 1970.
24. Wooding, R. A. “Growth of Fingers at an Unstable Diffusing Interface in a Porous Medium or Hele-Shaw Cell.” Journal of Fluid Mechanics 39 (1969): 477-495.
25. Yang, Z. M., Y. C. Yortsos, and Dominique Salin. “Asymptotic Regimes in Unstable Miscible Displacements in Random Porous Media.” Advances in Water Resources 25 (2002): 885-898.
26. Zhang, Jian-hua, and Zhen-hua Liu. “Study of the Relationship between Fractal Dimension and Viscosity Ratio for Viscous Fingering with a Modified DLA Model.” Journal of Petroleum Science and Engineering 21 (1998): 123-128.

PHOTOGRAPHS

JSC2008EO48595
JSC2008EO48698
JSC2008EO48600
JSC2008EO48621
JSC2008EO48624
JSC2008EO48628 to JSC2008EO48629
JSC2008EO48634 to JSC2008EO48635
JSC2008EO48659
JSC2008EO49248 to JSC2008EO49249
JSC2008EO49167 to JSC2008EO49170
JSC2008EO49152 to JSC2008EO49159
JSC2008EO49146
JSC2008EO49135

VIDEO

- Zero-G flight week 6/23–6/27/08, Master #: 738978

Videos are available from the Imagery and Publications Office (GS4), NASA JSC.

CONTACT INFORMATION

Emily Calandrelli
ecalandr@mix.wvu.edu

TITLE

Aerosol Deposition in Fractional Gravity:
Risk Mitigation for Martian and Lunar Habitats

FLIGHT DATES

July 21–25, 2008
September 8–10, 2008
February 24–27, 2009

PRINCIPAL INVESTIGATOR

G. Kim Prisk, University of California, San Diego

CO-INVESTIGATORS

Chantal Darquenne, University of California, San Diego
I. Mark Olfert, University of California, San Diego

GOAL

The inhalation and deposition of small particles in the lungs is a health concern here on Earth and future space travelers risk detrimental health consequences from particle inhalation. Because gravity affects the deposition of particles in the lung, in microgravity or in the reduced gravity of the Moon and Mars inhaled particles are left in suspension in the airways, and can be transported deeper into the lung where they reach the sensitive alveolar region. On the Moon and Mars, it is believed that much of the dust is highly reactive, which may exacerbate its potential for lung damage. Because it is electrostatically charged, lunar and Martian dust sticks to spacesuits and could be tracked into habitats and subsequently inhaled.

OBJECTIVES

The deposition of aerosols from the environment in the lung presents a health risk. For particles larger than 0.5 micron, such deposition is strongly influenced by gravitational sedimentation. In microgravity, deposition by gravitational sedimentation is absent, and, as a consequence, airway particle concentrations are higher than in 1 G, thus enhancing aerosol transport to the alveolar region of the lung. The presence of previously unaccounted for complex mixing patterns in the periphery of the lung, combined with high alveolar aerosol concentrations, results in high deposition in this sensitive region of the lung in microgravity. Similar effects are expected in the fractional gravity environments of the Moon and Mars.

The dust on the surface of Mars is highly oxidative in nature, due to the ultraviolet (UV) environment on the surface. Mars dust is also electrostatically charged, and so will tend to stick to the outside of spacesuits and be tracked into habitats. The lung, with its huge exposed surface area, is highly vulnerable to adverse effects resulting from exposure to Mars dust.

We propose a multifaceted approach involving human and animal experiments, combined with sophisticated modeling, to provide a path to assessing the health risk of dust exposure in habitats on both the Moon and Mars, addressing risk No. 7 in the Bioastronautics Critical Path Roadmap. Such an assessment has profound implications on the degree of engineering (and, thus, cost) that will be required to limit the risk of such exposure to the inhabitants of these habitats. We will address the following hypotheses and objectives:

1. That total aerosol deposition in the human lung in fractional gravity will be higher than predicted by existing models (as is the case in microgravity), and that a higher-than-predicted alveolar deposition will result in these circumstances. Using the NASA Microgravity Research Aircraft, we will non-invasively measure both the total and the regional deposition of inert particles (0.5 microns to 2 microns) in humans in fractional-G corresponding to that on the surface of the Moon and Mars.
2. That aerosol deposition in the lungs of spontaneously breathing rats in fractional-G will be more peripheral (closer to the alveoli) than in 1 G. We will expose spontaneously breathing rats to fluorescently and magnetically labeled particles of varying sizes (between 0.5 microns and 2 microns) in 1 G, and in fractional-G corresponding to surface of the Moon and Mars, and measure the specific sites of regional deposition in the lungs using both fluorescent confocal microscopy and magnetic resonance imaging (MRI) techniques.

3. We will couple existing sophisticated computational fluid dynamics (CFD) models of the upper airways of humans to our model of the alveolar region of the lung to predict aerosol deposition under conditions matching those of the experiments performed in humans. In rats, we will use detailed 3-dimensional images of the rat bronchial tree to develop an upper airway CFD model that, used in conjunction with an appropriately scaled alveolar model, will predict aerosol deposition under conditions matching those of the experiments performed in rats.

METHODS AND MATERIALS

Human Studies in Fractional-G

In the past we have measured both total and regional aerosol deposition in humans in 1 G and in microgravity (see Preliminary Data). The results of those studies highlighted the nonlinear nature of aerosol deposition of small (~1 μm) particles as a function of G-level (Darquenne et al., 1997). Thus, to accurately determine particle deposition in fractional-G, direct measurements are required.

Total Deposition

Protocol overview: We will measure total deposition of 0.5-μm and 1-μm particles in the lungs of subjects in 1 G and at fractional-G levels corresponding to the surface of the Moon and Mars (termed 1/6 G and 1/3 G for the sake of convenience). Total deposition will be measured during controlled tidal breathing, and, as was the case in our previous studies in microgravity (Darquenne et al., 1997), we will select data during stable G-level periods after allowing sufficient time at that G-level for deposition to stabilize (2 to 3 breaths). We will study 6 subjects.

Equipment: Deposition data will be collected by using equipment that is similar to that used in a previous study (Darquenne et al., 1997). The subject breathes from a reservoir through a non-rebreathing valve. Aerosol concentration and flow rate are measured at the mouth using a photometer and a pneumotachograph, respectively. A diffusion dryer is located between the photometer and the mouthpiece. The system is heated to body temperature to prevent water condensation. Data are recorded on a laptop personal computer (PC) equipped with a data acquisition subsystem.

Central and Alveolar Deposition (SA1b)

Protocol overview: The proposed protocol will be the same as that used in our previous studies of bolus deposition and dispersion (Darquenne et al., 2000, 1998, 1999). The subject will perform the standardized maneuver described in Preliminary Studies, and a 70-mL bolus will be inserted in the inspiration at one of the preselected penetration volumes (V_p) using the equipment shown in the Facilities and Equipment section. During the subsequent expiration, the exhaled bolus will be recorded.

We will measure deposition, dispersion (change in bolus half-width), and bolus mode shift. We can designate a volume below end inspiration for the bolus (the penetration volume, V_p), and propose to measure aerosol bolus parameters at each of 3 V_p (200 mL, 500 mL, and 1,200 mL). We will use 2 particle sizes (0.5 μm and 1 μm) at 1 G and in 1/6 G. As was the case before, measurements will be performed in triplicate on a total of 6 subjects.

***Equipment**:* The equipment, which will be the same as that used for previous studies, uses the same photometer and pneumotachograph system used in the total deposition studies. In brief, a pneumatically controlled sliding valve allows the subject to breathe either filtered room air, or allows inspiration through a tube prefilled with a bolus of aerosol. By actuating the sliding valve at the appropriate point during inspiration, the bolus can be delivered at any desired penetration volume with an accuracy of ±100 mL. A full description can be found in previous publications (Darquenne et al., 1998).

Rat Studies in Fractional-G

We propose to determine the degree of deposition and the location of inhaled particles in the lungs of spontaneously breathing rats, and compare the deposition patterns in 1 G and in fractional-G levels corresponding to the surface of the Moon and Mars. Our hypothesis is that in the fractional-G environments, total deposition may be somewhat reduced, but those particles that do deposit will do so more peripherally. In humans, more peripheral deposition results in particles avoiding the mucociliary system and, in the case of oxidative particles, could increase oxidative damage to the lung.

By performing these studies in rats, we can subsequently use anatomical and state-of-the-art imaging techniques to determine the exact site and degree of deposition, providing otherwise unavailable validation for the CFD models. We expect to be able to experimentally demonstrate alterations in the heterogeneity of particle deposition between G-levels.

***Protocol**:* We propose to expose on the NASA Microgravity Research Aircraft spontaneously breathing, restrained rats to fluorescent-labeled and MRI-labeled particles during periods of fractional-G corresponding to the surface of the Moon and Mars. During 1 G and during the hyper-G phase of parabolic flight, the animals will breathe filtered air, and while the aircraft is in fractional-G they will be exposed to particle-laden air for head-only particle exposure for a cumulative exposure period of approximately 20 minutes. At the completion of the flight, the animals will be euthanized and the lungs preserved. The lungs will be returned to San Diego for MRI of particle location, and for slicing and confocal microscopy of fluorescent particle location (see below). We propose to use 3 different particle sizes (0.5 μm, 1 μm, and 2 μm), matching those used in the human studies (see above). We will require 2 flights per size and G-level (10 rats per condition) for a total of 12 flights.

***Exposure techniques**:* Five rats (adult male Wistar, with a body weight in the range 200 g to 250 g) will be simultaneously restrained in head-out plastic cones (Sweeney et al., 1991) in individual sealed plethysmograph chambers. When the animal breathes, changes in box pressure occur as inspired air is warmed and humidified in the respiratory tract, allowing the calculation of tidal volume and breathing frequency (Jacky, 1978, 1980). An identical reference chamber will be used, and differential pressure between the plethysmograph and the reference chamber will be measured (Jacky, 1978, 1980). This will eliminate difficulties associated with changes in cabin pressure in the aircraft. The chambers will be ventilated continuously by drawing either filtered cabin air or particle-laden air through them at approximately 250 mL/min (Sweeney et al., 1991).

The inlet path for the ventilation will be such that it impinges directly onto the nose region of the restrained rats. This arrangement will allow us to rapidly switch the inlet flow between filtered (particle-free) air and particle-laden air drawn from a reservoir into which particles in suspension have been aerosolized during the period of hypergravity immediately preceding the fractional-G parabola. During 1 G and during the hyper-G phase of parabolic flight, the animals will breathe filtered air, and while the aircraft is in fractional-G they will be exposed to particle-laden air for head-only particle exposure. The fractional-G time available to us in the aircraft is about 35 seconds to 40 seconds for 1/6 G and approximately 45 seconds to 50 seconds for 1/3 G, giving a cumulative exposure period of about 20 minutes assuming 30 seconds (which will be recorded) of fractional-G exposure time can be used per parabola. Control studies on the ground (1 G) will be performed after the fractional-G studies, allowing us to match the timing of the exposures to those that occurred during the flights (a delayed synchronous control approach). Importantly in the context of this proposal, Pinkerton et al. (1993) demonstrated in 1-G exposure times of 15 minutes to 30 minutes, deposition of 1.0-μm microspheres throughout the bronchial tree and alveoli of spontaneously breathing rats.

At the completion of the flight, the animals will be anesthetized by intraperitoneal injection of pentobarbital; the trachea will be cannulated and connected to a pressure source to permit setting of intratracheal pressure. The caudal vena cava will be cannulated, and the carotid arteries and veins will be cut to permit perfusion fixation. Physiologic buffered saline will first be infused for 5 minutes to clear blood from the lungs, followed by fixative for 15 minutes as described by Pinkerton (1993). Intratracheal pressure will be maintained at 9 mmHg, providing for a lung volume approximating functional residual capacity.

RESULTS/DISCUSSION

The July 2008 flight week provided a good test of the new rat plethysmograph system. In flight, we obtained good breathing pattern signals and experience on dosing the animals with large-diameter particles. Based on preliminary results, very low deposition of large (~5 micron) particles occurred, even in reduced gravity.

The September 2008 flight week was cut short (2 flights only) as a result of Hurricane Ike. Good technical quality data were obtained on both days. Preliminary data show a significant deposition of 1-micron particles in the flight lungs. Because of the reduced flight schedule that week, a further week of flight is planned.

In the February week, we performed an additional data collection on the human studies in which we studied the combined effects of reduced gravity and reduced gas density. This was outside the originally planned studies but was occasioned by the recent definition of the low-density atmosphere for a lunar base. Studies were performed on 8 subjects with technically good results. No scientific results are yet available.

CONCLUSION

Reduced gravity results in a more peripheral site of deposition of fine particulate matter in the human lung compared to 1 G (see Darquenne et al., 2008).

Further conclusions from more recent studies are pending data analysis.

REFERENCES

1. Darquenne C, Paiva M, Prisk GK. Effect of gravity on aerosol dispersion and deposition in the human lung after periods of breath-holding. *J Appl Physiol;* 89:1787–1792, 2000.
2. Darquenne C, Paiva M, West JB, Prisk GK. Effect of microgravity and hypergravity on deposition of 0.5- to 3-μm-diameter aerosol in the human lung. *J Appl Physiol;* 83:2029–2036, 1997.
3. Darquenne C, West JB, Prisk GK. Deposition and dispersion of 1 μm aerosol boluses in the human lung: Effect of micro- and hypergravity. *J Appl Physiol;* 85:1252–1259, 1998.
4. Darquenne C, West JB, Prisk GK. Dispersion of 0.5-2 μm aerosol in micro- and hypergravity as a probe of convective inhomogeneity in the human lung. *J Appl Physiol;* 86:1402–1409, 1999.
5. Darquenne C, Prisk GK. Deposition of inhaled particles in the human lung is more peripheral in lunar than in normal gravity. *Eur J Appl Physiol*; 10:687-695, 2008. DOI: 10.1007/s00421-008-0766-y.
6. Jacky JP. A plethysmograph for long-term measurements of ventilation in unrestrained animals. *J Appl Physiol;* 45:644–647, 1978.
7. Jacky JP. Barometric measurement of tidal volume: effects of pattern and nasal temperature. *J Appl Physiol;* 49:81–86, 1980.
8. Peterson JB, Prisk GK, Darquenne C. Aerosol deposition in the human lung periphery is increased by reduced-density gas breathing. *J Aerosol Med Pulm Drug Delivery*; 21:159–168, 2008. DOI: 10.1089/jamp.2007.0651.
9. Pinkerton KE, Gallen JT, Mercer RR, Wong VC, Plopper CG, Tarkington BK. Aerosolized fluoresecent microspheres detected in the lung using confocal scanning laser microscopy. *Microsc Res Tech;* 26:437–443, 1993.
10. Steinbrook RA, Feldman HA, Fencl V, Forte VA, Gabel RA, Leith DE, Weinberger SE. Naloxone does not affect ventilatory responses to hypoxia and hypercapnia in rats. *Life Sci;* 34:881–887, 1984.
11. Sweeney TD, Leith DE, Brain JD. Restraining hamsters alters their breathing pattern. *J Appl Physiol;* 70:1271–1276, 1991.

PHOTOGRAPHS

JSC2008E053799 to JSC2008E053805
JSC2008E055848 to JSC2008E055856
JSC2008E055495 to JSC2008E055503
JSC2008E055806 to JSC2008E055817
JSC2008E116053 to JSC2008E116056
JSC2008E116059
JSC2008E116089 to JSC2008E116090
JSC2008E118213 to JSC2008E118218
JSC2009e047919 to JSC2009e047924
JSC2009e048098 to JSC2009e048107
JSC2009e047944 to JSC2009e047956

JSC2009E048256 to JSC2009E048273
JSC2009E048797 to JSC2009E048820

VIDEO

- Zero-G flight week 7/22–7/25/08, Master nos.: 306440, 306441
- Zero-G flight week 9/9–9/10/08, Master no.: DV1721
- Zero-G flight week 2/23–2/27/09, Master no.: DV1998

Videos are available from the Imagery and Publications Office (GS4), NASA JSC.

CONTACT INFORMATION

G. Kim Prisk, Ph.D., D.Sc.
Department of Medicine - 0931
University of California, San Diego
9500 Gilman Drive
La Jolla, CA 92093-0931
kprisk@ucsd.edu

TITLE

Determination of Variables, such as Lap Restraint, on the Effects of Measuring Seated Height in a Microgravity Environment

FLIGHT DATES

July 25, 2008
August 28, 2008
January 16, 2009

PRINCIPAL INVESTIGATOR

Sudhakar Rajulu, Ph.D, NASA Johnson Space Center

CO-INVESTIGATOR

Karen Young, Lockheed Martin

GOAL

The goal of this experiment was to ensure that the collection of seated-height data was accurate, and that the subject was properly restrained to the seat with minimal gap between the subject and the seat pan. To test the methodology and procedures developed for the on-orbit experiment, a simulated microgravity evaluation was proposed. The simulated microgravity evaluation presented in this report was a precursor to the payload experiment on board the shuttle to measure the effect of microgravity on spinal elongation in a seated configuration. This evaluation obtained data to (a) ensure that the lap restraint provided sufficient restraint to eliminate any gap between the subject's gluteal surface and the seat pan, and (b) document and verify that the lap restraint tension did not affect seated-height measurements in microgravity.

OBJECTIVES

1. To collect seated-height anthropometric data while experiencing microgravity to ensure an accurate seated-height measurement will be collected during the on-orbit experiment: Spinal Elongation and its Effects on Seated Height in a Microgravity Environment.
2. To collect force and pressure data of how much a subject is loading the seat while restrained.
3. To update the crew procedures and hardware design as necessary for the in-orbit experiment.

METHODS AND MATERIALS

This experiment was performed on the microgravity aircrafts C-9 and ZERO-G®. Three flights occurred during which approximately 50 parabolas during each flight simulated lunar and microgravity conditions during each flight. However, since the payload experiment will be performed in microgravity, it was the data from the microgravity parabolas that were of most interest. The data collected during these 3 flights were seated height, force data, and pressure data.

The test setup included: the shuttle seat, a load cell plate, an X-Sensor pressure pad, an anthropometer, and data acquisition systems. The shuttle seat was secured to the aircraft floor facing the starboard side of the aircraft. Attached to the shuttle seat was a standard anthropometer (figure 1). For Flights 1 and 2, a standard anthropometer was attached to the seat pan and secured by tape to the back of the chair. However, during Flight 3, a prototype of the flight hardware anthropometer was used, which attached to the top of the seat back in the same manner as the headrest (figure 2). During all 3 flights, a load cell plate and X-Sensor pressure pad were secured to the seat pan of the shuttle seat. The load cell plate and X-Sensor pressure pad were connected through a series of cables to the data acquisition systems located on the computer rack. The load cell plate, or force plate, collected only the vertical force applied by the subject, and the pressure pad collected the pressure applied by the subject, resulting in the outline of the buttock and thighs.

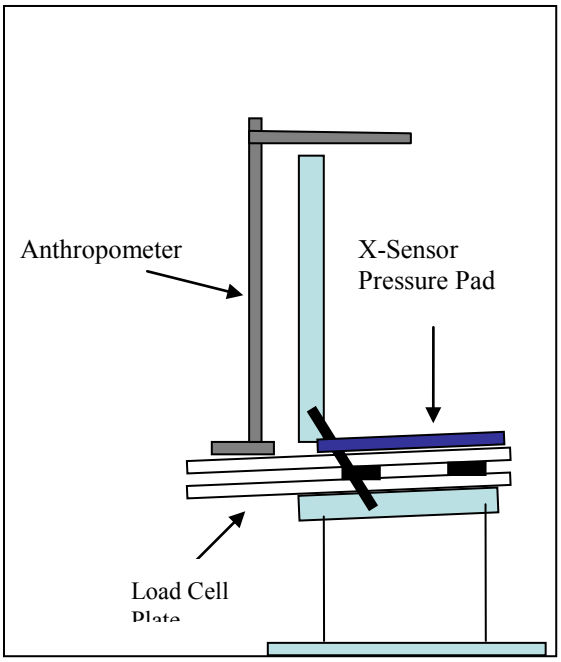

Figure 1. Equipment layout during Flights 1 and 2.

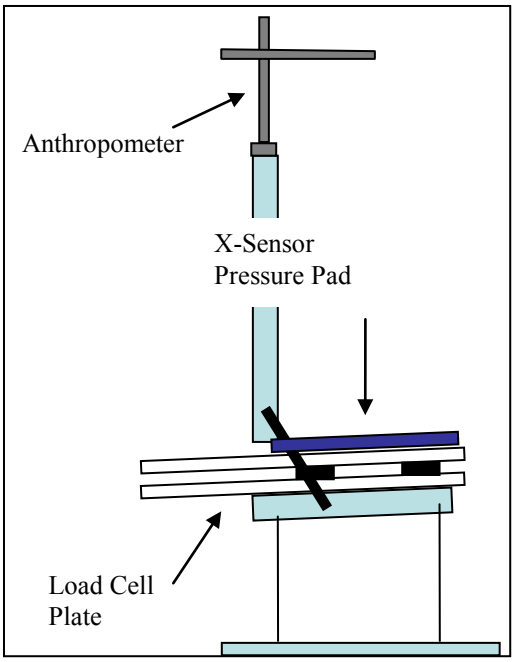

Figure 2. Equipment layout during Flight 3.

During the simulated microgravity parabolas, the subject was seated in the shuttle seat and restrained for the collection of pressure, force, and seated-height data. The subject remained seated during several consecutive parabolas; the number of consecutive parabolas varied between subjects.

During the first flight, only 1 restraint system was examined: 3 points of the current 5-point harness. The 3-point harness included the use of the crotch buckle and 2 pelvis straps. Data were collected for 4 subjects during Flight 1. The second flight examined multiple restraint systems: the 3-point harness, the 3-point harness with leg strap, the 3-point harness with leg and lap straps, the 3-point harness with loose buckle, and the 3-point harness with a foam insert. During the second flight, the 3-point harness was adjusted to wrap around the seatback support bars. Four subjects participated in Flight 2. However, only 2 of these subjects participated in Flight 1. To compare across restraints, the 3-point harness examined during Flight 1 was also examined during Flight 2 for those subjects who did not fly during Flight 1. The third flight, Flight 3, tested the prototype anthropometer assembly and the 3-point harness wrapped around the seatback support bars. Data were collected for 3 subjects; all 3 subjects participated in Flight 1, and 2 of the subjects also participated in Flight 2.

Seated-height data were collected during all 3 flights for each restraint system examined. The seated-height data were used to validate which restraint system secured the subject to the seat pan with the smallest amount of variability between the measurements. To ensure minimal variability to the measurement, all measurers followed a standard procedure. Once in microgravity, the measurer ensured the subject was looking straight and lowered the tyne of the anthropometer to the middle of the subject's head, ensuring proper contact with scalp of the head, and collected the seated-height measurement.

RESULTS

During all flights, seated-height measurements and pressure data were collected. During Flight 1 and Flight 3, force data and the aircraft acceleration also were collected. However, this analysis will focus on the seated-height measurements collected during microgravity parabolas.

Flight 1

The ranges of seated-height measurements collected during Flight 1 varied from 1.1 cm to 5.6 cm. The variability in the seated-height measurements indicates that the subjects were not tightly restrained to the seat and that the subjects were not in complete contact with the seat pan. The subjects also reported the lack of restraint; the subjects often felt as though their buttocks were floating off of the seat in microgravity, even with the lap restraint tightened as far as the restraint system would allow.

The results from Flight 1 demonstrate that the current 3-point harness used in its nominal configuration was not sufficient to ensure contact between the subject and the seat pan to collect consistent seated-height measurements. The restraint system must restrain the subject properly so that the seated-height measurements are consistent. Inconsistent measurements will adversely affect the amount of spinal growth that is reported to the designers, which may impact crew safety and crew fit with the seats, suits, and vehicle after exposure to microgravity.

Flight 2

From Flight 1 it was realized that the 3-point harness in its nominal configuration was not sufficient to restrain the subject. As a result, other methods of restraints were explored during Flight 2, namely:

- Flight 1 – 3-point configuration
- Flight 1 – 3-point configuration with a foam insert under the buckle
- A 3-point harness with a loose buckle and a Velcro® leg strap
- Flight 2 – 3-point harness configuration
- Flight 2 – 3-point configuration with Velcro® leg strap
- Flight 2 – 3-point configuration with Velcro® leg and lap straps

According to the seated-height measurements collected during Flight 2, the seated-height range verified that the Flight 2 configuration restrained the subject(s) more effectively than the Flight 1 configuration. The greatest range in seated height for subject 1 was 0.5 cm for Flight 2 (3-point with leg and lap configuration) compared to 1.4 cm for Flight 1. This indicates that the subject was better restrained in the seat for Flight 2 than for Flight 1. For subject 2, the range decreased from 2.3 cm to 0.3 cm. This shows that with the modification of the restraint belts, the consistency increased. Looking at the 3 different types of restraints and the range of measurement variation, the data indicate that the addition of the leg and lap straps minimized the seated-height range, except for subject 1. This would signify that the addition of a leg and lap strap may be necessary to restrain the subject to the seat and allow for accurate seated-height measurements. However, when comparing the average seated-height measurements for each configuration, the seated-height measurements did not vary greatly. The difference in the average seated heights can be accounted for by the variation that occurs while collecting anthropometric measurements

using traditional methods; i.e., manual measurements using an anthropometer (0.6 cm). Therefore, based on the subjects from Flight 2, any Flight 2 restraint configuration would be satisfactory to collect seated-height measurements in microgravity and restrain the subject to the seat pan.

Flight 3

Flight 3 tested the Flight 2's 3-point harness configuration in addition to the use of the prototype anthropometer to be used during shuttle missions. The prototype anthropometer attaches to the seatback in the same manner as the headrest. In addition to testing the 3-point harness, the subjects were also asked to look up, down, and straight forward to determine whether the head position affected the seated height. During Flight 3, it was also apparent that the operator and subject must work together to ensure that the restraint system is tight against the subject's pelvis. Several times the restraint was not completely tight, and the subjects responded by stating that they were not cinched down completely and felt as if they were floating. As opposed to the first 2 flights in which 1-seated-height measurement was collected per parabola, Flight 3 collected multiple seated-height measurements during a single parabola (after the first 11 parabolas).

When the subjects were loosely restrained versus tightly restrained with the 3-point harness, the range of the seated-height measurements decreased. Subject 2's measurement range decreased from 1.4 cm to 0.6 cm due to tightening of the restraint system. All 3 subjects' seated-height ranges were similar when they were tightly restrained (0.6 cm, 0.6 cm, and 0.7 cm), indicating that when tightly restrained the variation in seated height was due to the effects of microgravity and the variation in collecting manual measurements.

Based on the limited amount of data collected during Flight 3, in which the subjects changed their head orientation from looking forward, down, and up, the seated-height measurements did change for subject 1 and subject 2. When comparing looking forward to looking down, there was a greater increase in seated height for subject 1 compared to subject 2. This resulted from subject 2 drastically looking down as opposed to subject 2 who did not drastically look down at the floor. This relative difference in head orientation was not seen when the subjects looked up. Therefore, the difference in seated heights when the subjects looked up versus looking forward was very small, 0.2 cm and 0.4 cm, respectively, for subjects 1 and 2. Another factor that may explain the small variation in seated-height values when looking up was the location on the head where the measurement was collected. The measurements may not have been collected from the most superior location on the head but, rather, from the middle of the head. From the results of looking down, it can be assumed that if the subjects drastically looked up and the measurement was collected at the most superior location on the head, the seated-height measurements would be affected the same as when the subjects drastically looked downward. If the seated height of the payload experiment were to be recorded when the subjects were not looking forward, the results from the study that would be given to the designers and used to update Constellation's Human System Interface Requirements would be over-calculated, impacting crew safety, crew selection, and anthropometric requirements.

DISCUSSION

Flight 1

Two lessons learned while collecting seated-height measurements during Flight 1 were: (1) to make sure the subject is looking straight forward, and (2) to make sure the subject is in the center of the seat. Often, subjects perceived that they were looking forward but were actually looking slightly downwards. Also, there were times when the anthropometer was not positioned in the middle of the subject's head due to that subject's positioning on the chair. Therefore, the measurer needs to instruct subjects as to how to move their torsos/heads so that the anthropometer measures to the middle of the top of the head. The 2 lessons learned can affect the measurement of seated height by providing more accurate data. Without accurate data, the impact of spinal elongation on seat positioning and fit may pose risks to crew safety. The effectiveness of the crew may be reduced due to impaired access to displays and controls, and selected crewmembers may not fit into seats following exposure to microgravity. The inaccurate data could also be fed to the designers and into the requirements for crew exploration vehicle (CEV) and future vehicles, habitations, and spacesuit components.

Flight 2

During this flight, the 3-point-harness-waist straps were adjusted to wrap around the seatback support bars; this increased the consistency in measurements and the contact between the subject and the seat. The subjects felt better restrained with this configuration than with the configuration of Flight 1. However, the average seated heights results from this flight demonstrated that additional straps were not necessary. Therefore, additional hardware was not needed for the on-orbit activity. The decision was made to proceed with the Flight 2's 3-point-harness configuration for on-orbit activities; wrapping the restraint belts around the seatback joint.

Flight 3

Using the prototype anthropometer during Flight 3 resulted in little variability during parabolas and decreased the inconsistencies of using a standard anthropometer taped to the load cell plate. Also, using the Flight 2's 3-point harness configuration decreased the delta for seated height due to the tightening of the restraint. During Flight 3, several seated-height measurements were collected when the restraint was not completely tight, resulting in a greater range than when the restraint was pulled tight around the subject's pelvic/waist area. The lack of tightness led to inconsistencies within the seated-height measurements. As a result, a lesson learned from Flight 3 is that after the subject gets in the seat and is buckled, the operator must pull the side straps as tight as he/she can to ensure the subject is in contact with the seat pan.

Comparing the average seated height for the 3-point-harness-restraint system for all 3 flights, it was determined that the Flight 3 configuration improved the variability compared to Flight 1. Flight 2 had the smallest seated-height range but had the fewest seated-height measurements for each subject; subject 1 had 2 measurements, and subject 2 had 3 measurements.

CONCLUSION

In conclusion, the microgravity flights were pertinent to the spinal elongation payload experiment. Flight 1 verified that the current 3-point-harness system was not sufficient to provide adequate contact between the seat pan and the subject. Flight 1 also provided insight into some

possible procedural problems that may occur. The lessons learned during Flight 1 were: (1) the subjects often perceived that they were looking straight when they were looking slightly downward, and (2) the operator should confirm that the subject is in the center of the chair so that the anthropometer measures to the middle of the head. These lessons learned have been included in the crew procedures, ensuring that crewmembers are aware of these issues and that testers can position the subjects as necessary to achieve an accurate seated-height measurement.

After learning that the current restraint system was not sufficient, 7 alternative restraint systems were examined during Flight 2. The results from Flight 2 indicated that a restraint on the lower thighs and a restraint that is anchored from behind the seatback will pull the subject down and back into the seat, thereby reducing variability in the seated-height measurement. Therefore, the recommendation given to the hardware designers after Flight 2 was to include a leg strap and an additional lap strap into the next restraint system prototype to be investigated during Flight 3. However, the seated-height data from Flight 2 proved that the variability between the Flight 2's 3-point harness, the 3-point harness with a leg strap, and the 3-point harness with the leg and lap straps was minor. Therefore, due to time and schedule constraints, the decision was made by the principal investigative team not to develop any additional hardware.

With the restraint system decided on, Flight 3 examined the design of the prototype anthropometer and operationally verified the restraint method for crew procedures. Installing and operating the prototype anthropometer was also verified during Flight 3 for crew procedures; the installation and operation of the anthropometer was found to be straightforward. One lesson learned during Flight 3 was that the lap straps of the restraint must be tight against the subjects' pelvis/waist to reduce the amount of variability in the seated-height measurements.

The 3 microgravity flights allowed the principal investigation team to explore the best methodology for collecting seated-height data. The seated-height data collected during the microgravity flights assisted with crew procedures, data collection methodology, and hardware design. The lessons learned from the microgravity flights will aid in successfully and accurately collecting seated-height data that can be used by the CEV designers to accurately design for the amount of spinal lengthening due to microgravity. The spinal lengthening that crewmembers experience may affect crew safety, crew selection, and design requirements. If the designers do not have the correct data for spinal lengthening, a crewmember may not have enough clearance on reentry to allow for the appropriate vibration and stroke volume, or may not properly fit into the reentry suit, therefore affecting that crewmember's safety and the safety of the other crewmembers.

REFERENCES

1. Anthropometric Source Book Vol. I: Anthropometry for Designers. (NASA 1024). Edited by Staff of Anthropology Research Project, Webb Associates, Yellow Springs, Ohio, 1978.
2. Human-Systems Integration Requirements (HSIR), CxP 70024. NASA, Houston, TX 2007.
3. Thornton W, Hoffler G, Rummel J. Anthropometric Changes and Fluid Shifts. In Johnston, R. and Dietlin, L. (Eds.), *Biomedical Results from Skylab* (pp. 330–338), 1977. Washington, DC: NASA.

4. Thornton, W. and Moore, T. Height changes in microgravity. In: *Results of the Life Sciences DSOs Conducted aboard the Space Shuttle 1981-1986* (pp. 55–57). Biomedical Research Institute, Houston, TX, 1987.
5. Brown J. (1975). ASTP002: Skylab 4 and ASTP Crew Height. Retrieved December 28, 2007, from NASA Life Sciences Data Archive Website: http://lsda.jsc.nasa.gov.
6. Gordon CC, Bradtmiller B, Churchill T, Clauser CE, McConville JT, Tebbetts I, Walker R. *1988 Anthropometric Survey of U.S. Army Personnel: Methods and Summary Statistics.* Final Report, NATICK/TR-89/044, Natick, Massachusetts, 1989.

PHOTOGRAPHS

JSC2008E055472 to JSC2008E055494
JSC2008E105506 to JSC2008E105524
JSC2009E018274 to JSC2009E018302

VIDEO

- Zero-G flight week 7/22–25/08, Master nos. : 306440, 306441
- Zero-G flight week 8/27–29/08, Master no.: 307073
- Zero-G flight week 1/13–16/09, Master no.: 734616

Videos are available from the Imagery and Publications Office (GS4), NASA JSC.

CONTACT INFORMATION

Sudahahkar Rajulu, Ph.D.
NASA Lyndon B. Johnson Space Center
Mail Code: SF3
Houston, TX 77058
281-483-3725

TITLE
C-9 Space Medicine Familiarization Flight

FLIGHT DATE
July 25, 2008

PRINCIPAL INVESTIGATORS
Heather Van Velson, Wyle Integrated Science and Engineering Group
Bob Tweedy, Barrios

CO-INVESTIGATORS
David Ham, Wyle Integrated Science and Engineering Group
Faith Knudsen, Wyle Integrated Science and Engineering Group
Michelle Urbina, Wyle Integrated Science and Engineering Group
Corinne Williams, Wyle Integrated Science and Engineering Group

TEST OBJECTIVE

Familiarize Medical Operations (Med Ops) personnel with the effects of microgravity on medical equipment and procedures, as well as the required process for conducting a C-9 flight.

INTRODUCTION

The space medicine familiarization flight provided Med Ops personnel with a better understanding of the effects of microgravity for use of medical procedures. Specifically, the time allotted on this flight was used to study intravenous (IV) fluid insertion, intubation, and cardio-pulmonary resuscitation (CPR) in microgravity. Personnel who understand the limitations of medicine in a microgravity environment can use this knowledge to assist astronauts in a medical contingency or on-board training, design space-friendly medical equipment, and write procedures to better explain how to overcome the difficulties of operating medical equipment in microgravity.

METHODS AND MATERIALS

Preflight, all flyers were required to attend a C-9 Familiarization Training Session. At this training session, flyers were briefed on the bodily effects of the C-9, as well as given the opportunity to practice all procedures to be performed while flying on the C-9. Materials and procedures are explained thoroughly below.

INSTRUMENTS

The procedures and materials were divided into 3 stations: (1) intubation, (2) IV fluid insertion, and (3) CPR administration.

Intubation Station

The intubation station was composed of a plastic-human-upper body and the on-board airway subpack and intubation kit-airway (IKA) pack. Two methods of intubation were practiced: (1) intubating laryngeal mask airway (ILMA) device with an endotracheal tube and (2) laryngoscope with an endotracheal tube.

IV Fluid Insertion Station

The IV station consisted of a plastic-human arm, with fluid-filled tubes that substitute as veins, and the IV administration subpack on board the International Space Station (ISS).

CPR Station

The CPR station consisted of a life-sized, plastic dummy named Rescue Randy, attached via straps to the Crew Medical Restraint System (CMRS). CPR was practiced in 3 positions: (1) beside the patient, (2) straddled on patient, and (3) inverted position.

PROCEDURES

All personnel were trained on the following procedures prior to flight. Procedures used are detailed in the following attachments:

Attachment 1 – ILMA Insertion

Attachment 2 – Intubation with Laryngoscope
Attachment 3 – IV Insertion

RESULTS

Intubation Station

Due to the number of co-investigators as well as the limited time (30 seconds) of microgravity per parabola, only the ILMA insertion procedure was able to be followed. The dummy was intubated successfully on the first try, with lungs inflating properly on ventilation with the Ambu bag.

During intubation, the ease of losing small objects that "float away" was definitely noticed. While everything is conveniently strapped down into the pack, recently used objects can float away during the procedure if not specifically placed in a secure position. In addition, on board the ISS, the patient would be strapped to the CMRS; this would require the Crew Medical Officer (CMO) to be strapped onto the CMRS by the patient's head. This aspect of the procedure was not able to be practiced.

IV Fluid Insertion Station

The insertion of an intravenous catheter was achieved using the given procedure. The most difficult part of this procedure was securing the body of the IV administrator. However, placing legs underneath the metal table proved to be an efficient method for securing the co-investigator's body. Unfortunately, this table is not present on board the ISS.

The propensity for small objects to float away was also noticed during IV insertion. The management of sharp objects was taken seriously, but could be a concern in a true microgravity environment, given the ease for losing such objects.

CPR Station

All 3 stances of CPR administration were attempted. The inverted CPR was the fastest and most convenient method of CPR, as the other 2 options require coordination of straps for the CMO. Given the nature of a cardio-pulmonary emergency, the co-investigator would recommend attempting inverted CPR first for expediency.

DISCUSSION

The C-9 Space Medicine Familiarization Flight proved very useful, and test objectives were met. Med Ops personnel will now better relate to the challenges related to microgravity, as well as be equipped to improve the future of space medicine.

The lack of body control was one of the most difficult aspects of microgravity. With medicine, the needs for gross and fine motor control are extremely important. Certainly, extended time in microgravity would allow one to adapt to such an environment. However, the acquisition of fine motor control in microgravity may never be as simple as in a gravitational environment.

Losing small objects was another difficult aspect of working in microgravity. Even one small miscalculation in how well an object is strapped down can lead to losing that object.

Both of these realizations will help the co-investigator in dealing with real-time calldowns from the crew on board the ISS. Medical operations personnel can better suggest methods of practicing medicine in microgravity in the event that a crewmember asks. The situational awareness also extends beyond medicine into all procedures that the crew performs. The time spent on the C-9 was invaluable in acquainting the co-investigator with the challenges of microgravity.

CONCLUSION

The objectives of the C-9 Space Medicine Familiarization Flight were met. All co-investigators appreciated the exposure to microgravity and will use the lessons learned to benefit the future of space medicine.

Attachment 1 – ILMA Insertion

TOP

AIRWAY (ILMA)

1. Unstow from Med Locker:
   Airway Subpack – 17,18

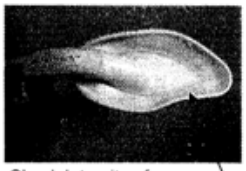

2. Check Integrity of
   ILMA Cuff
   Inject 8 cc air;
   confirm inflation;
   deflate cuff
   Cuff tip must be in shape above.
   Apply Surgilube to bottom of cuff
3. Insert cuff in mouth and rub Surgilube on roof of mouth

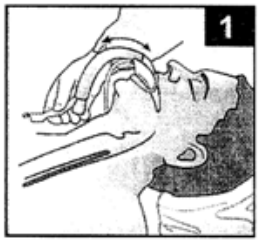

4. While maintaining contact with the roof of mouth, hug chin while inserting the ILMA.

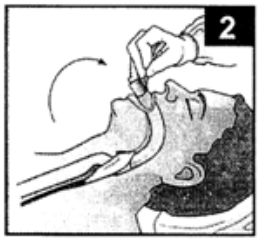

5. Inflate mask, w/o holding tube or handle:
   sm = 30 cc; lg = 40 cc

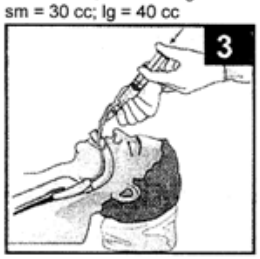

6. Provide ventilation using the AMBU Bag
7. Contact Surgeon prior to Endotracheal ET tube insert
8. Lubricate the ET tube with Surgilube. Hold tube with black line facing the ILMA handle.
9. Holding ILMA handle, gently insert ET tube into the metal shaft.

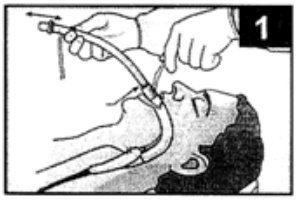

10. Advance ET tube (24 cm for small; 26 cm for large).
11. Inflate the ET tube cuff (8-10 cc): confirm placement w/ Stethoscope.

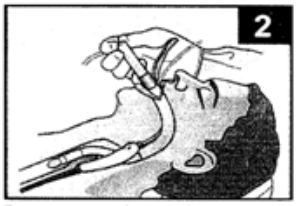

12. Remove all air from ILMA cuff. Remove tracheal tube connector and ease the ILMA out by gently rotating towards neck.
13. Use stabilizing rod to keep ET tube in place; remove ILMA until ET tube can be grasped above the teeth.

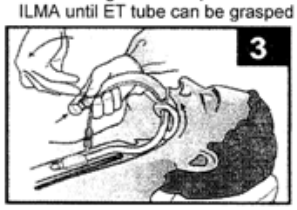

14. Remove the stabilizing rod and gently unthread the cuff valve of the ET tube.
15. Replace the ET tube connector.

16. Attach AMBU Bag to ET tube and give the patient two breaths.
17. Check for breath sounds in both lungs; reposition ET tube until breath sounds confirmed.
18. If successful, tape ET tube securely in place.

Attachment 2 – Intubation with Laryngoscope

1. Remove endotracheal (ET) tube from package.
   - ✓ Leave metal stylet inside ET tube.
2. Lubricate cuffed end with Xylocaine® jelly.
3. Fill syringe with 10 cc air.
4. Insert syringe into one-way valve/pilot balloon on ET tube, inflate balloon, check integrity.

5. Deflate balloon, leave syringe connected with balloon deflated.
6. Extend laryngoscope blade to 90-deg position.
   √ Light is on.
7. Open mouth with fingers of right hand, with laryngoscope in left hand. Insert laryngoscope blade into right side of mouth, displacing tongue to left.

WARNING
Avoid pressure on lips, teeth.

8. Advance laryngoscope blade into space between base of tongue, epiglottis.
9. Lift tongue forward with laryngoscope blade tip to expose vocal cords.
10. Advance cuffed end of ET tube along right side of mouth into trachea until entire cuff is about 1 cm below vocal cords.
11. Holding ET tube in place, remove laryngoscope.

WARNING
Firmly hold ET tube in place until proper placement is confirmed and tube is taped.

12. Inflate ET tube cuff with syringe until it feels tight (6–10cc), remove stylet.
13. With mask removed, connect Ambu bag to ET tube to resume ventilation as soon as possible.
    - ✓ Squeeze bag until chest rises.
    - ✓ Allow passive exhalation.
    - ✓ Repeat every 5 seconds.
14. Verify ET tube placement.
    - ✓ View patient's lungs:
      - ✓ If evenly rising then good placement; continue to step 15.
      - ✓ If only one lung rising or one lung rises more than the other, tube is inserted too far into one lung; deflate and move out 1 to2 cm.
      - ✓ Check for evenly rising lungs.
      - ✓ If yes, continue to step 15.
      - ✓ If no, remove tube and go back to step 6.
      - ✓ If stomach inflates, deflate and remove tube and go to step 6.
15. Ventilate for 30 seconds, then remove Ambu bag.

Attachment 3 – IV Insertion

1. Tear off 4 pieces of tape approximately 4 in. long.
2. Remove cap (not rubber port) from saline bag. Remove protective cap from spike of IV administration set.
3. Make sure IV administration set roller clamp is closed.
4. Insert saline bag into IV pressure infusor and inflate.
5. Tie tourniquet tightly around upper arm and locate vein.
6. Don non-sterile gloves (optional).
7. **Pretend to do this step:** Clean a wide area over vein with an iodine pad by starting in the center and moving outward in expanding circles; fan to dry.
8. Remove 16G catheter from package. Twist the Teflon® piece (around the needle) to loosen.

9. Capture vein between thumb and index finger of nondominant hand.
10. With needle bevel up, puncture skin over vein.
11. Slightly drop angle of needle and insert 1 to 2 mm more to ensure Teflon® catheter is properly placed in vein.
12. While holding needle stationary, advance Teflon® catheter into vein.
13. While holding Teflon® catheter with needle in place, remove tourniquet.
14. Apply pressure on vein (above end of catheter tip) with finger; remove needle and quickly attach Y-type catheter (on IV administration set) to the Teflon® catheter.

DO NOT open roller-clamp
No fluid is allowed to be transferred

15. Dispose of needle in sharps container.
16. Secure IV tubing like a "chevron" on the arm with tape.
17. Assemble Tubex injector and "administer drugs" into Y-type catheter.

PHOTOGRAPHS

JSC2008E055775 through JSC2008E055805

VIDEO

- Zero-G flight week 7/22–7/25/08, Master nos.: 306440, 306441

Videos are available from the Imagery and Publications Office (GS4), NASA JSC.

CONTACT INFORMATION

Robert Tweedy
Wyle Integrated Science and Engineering Group
1290 Hercules Suite 120
Houston, TX 77058
Robert.Tweedy-1@nasa.gov

TITLE
FASTRACK

FLIGHT DATES
September 9–10, 2008

PRINCIPAL INVESTIGATORS
Robert Soler, The Bionetics Corporation
Larry Chew, University of Florida
Luis Moreno, The Bionetics Corporation

GOALS/OBJECTIVES

The goals of the zero-G experiments included specific tests to verify the FASTRACK engineering unit prior to fabrication of the flight units. Three investigations were conducted in conjunction with FASTRACK. The first FASTRACK middeck locker housed the Space Acceleration Measurement System (SAMS) hardware. This hardware has previously flown on numerous space shuttle missions and is currently being used on the ISS. The SAMS hardware was used to collect acceleration data in various locations on the FASTRACK hardware. The second FASTRACK middeck locker housed an experiment looking at the phenomenon of Faraday-wave interface in 2 non-mixable fluid interfaces. The third experiment included 1 component (a receiver) that flew in the SAMS locker and received transmissions from the N^cIQ noncontact sensor unit that was worn by one of the FASTRACK flyers.

Major goals of the study

- To demonstrate the FASTRACK engineering unit interfaces and operational procedures for use on parabolic flights
- To validate the performance of rack systems and power support in the microgravity environment prior to the fabrication of flight units
- To collect baseline characterization data of the microgravity environment in the FASTRACK payload accommodations using SAMS instrumentation and test experiments that have previously flown
- To conduct a fluid dynamics experiment to study the Faraday-wave interface in 2 non-mixable fluid interfaces
- To conduct a test of the N^cIQ hardware to provide hemodynamic status monitoring in a variable gravity environment

METHODS AND MATERIALS

FASTRACK

The 2 single-middeck-locker FASTRACK configuration was used for the zero-G flights (figure 1). The overall FASTRACK dimensions are 24 in×24 in×36 in, and the overall weight is 300 lbs. The FASTRACK rack structure is made from 80/20 extrusion hardware, which is lightweight, has superb material quality (6105-T5 aluminum and carbon steel), has a drop-lock feature that makes it vibration-proof, and has proven structural integrity as well as fastener application quality. The middeck lockers are mounted to the FASTRACK frame via back plates. The back plate bolt patterns and fasteners are the same as those used to mount the lockers to the space shuttle or to the ISS EXPRESS Racks. In addition to the 2 middeck lockers, a support drawer located at the bottom of the FASTRACK structure contained all supporting electrical equipment as well as a front panel to serve as a user interface for FASTRACK and its experiments. The FASTRACK was mounted to the aircraft using ZERO-G®-provided bolts.

Figure 1. FASTRACK mounted to ZERO-G® aircraft floor.

SAMS

The SAMS hardware has previously flown on numerous space shuttle missions and is currently in use on the ISS. The triaxial-sensor-head, Ethernet-standalone (TSH-ES) component was flown during the FASTRACK zero-G campaign (figure 2).

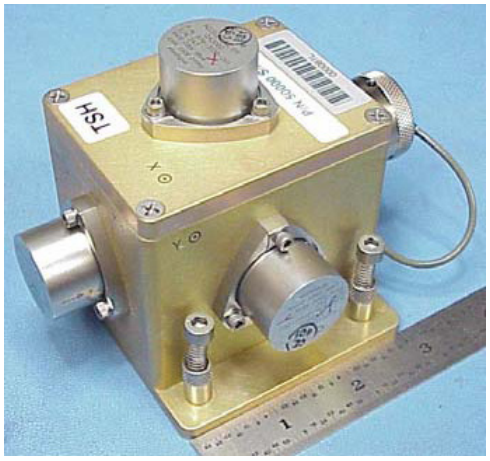

Figure 2. Triaxial sensor head-Ethernet standalone.

The TSH-ES consists of 3 analog accelerometers and 3 temperature sensors. It senses acceleration and provides a digital signal to the control unit via Ethernet. The TSH-ES has internal processing capabilities, which allow it to interface directly with the SAMS laptop. The SAMS laptop was located in the first FASTRACK middeck locker. The TSH-ES is attached using 4 integral spring-loaded captive screw assemblies with nut retainers. It was attached to a different location on FASTRACK for each flight day. All 4 fasteners were used to secure the

TSH-ES to provide a fail-safe condition as well as to ensure a rigid connection between the TSH-SE and the FASTRACK. A TSH-SE cable, which connected the TSH-SE to the SAMS laptop, contained all power and data connections.

Faraday-Wave Interface Experiment

The Faraday-wave-interface experiment was located in the second FASTRACK middeck locker (figure 3). Each experiment run used a petri dish filled with 30 mL of liquid. The petri dish was glued shut. One petri dish contained water, the second petri dish contained a mixture of water and oil, and the third and fourth petri dishes contained a mixture of water and corn starch. A single petri dish flew each day; petri dishes were replaced on subsequent flight days. All Faraday-wave equipment was mounted to a wood box. The front of the box had a hinged panel to enable the operator to switch out memory cards on the video camera during the flights. With the exception of the video camera, all powered equipment associated with the Faraday-wave experiment ran on three 9-volt batteries. A function generator (small, portable), an amplifier (from a computer speaker box), and a 4-in speaker were beneath the petri dish to generate the ripples on the liquid interfaces. The video camera was mounted next to the petri dish to record data; a small lamp was used to illuminate the area. The Faraday-wave-interface experiment did not interface with the FASTRACK support drawer or the lithium polymer (LIPO)-32 battery pack. Prior to the start of parabolas, the user opened the middeck locker door and turn on the power switch to the Faraday-wave equipment and the video camera. The middeck locker door was closed during the parabolas. The middeck locker door was opened again on completion of the parabolas to power down the experiment and video camera. There were no other in-flight operations associated with this experiment.

Figure 3. An operator performs a status check of the Faraday-waves experiment during the parabolic flights.

N^{c}IQ™ Experiment

The N^{c}IQ experiment used commercially available, off-the-shelf hardware provided by Noninvasive Medical Technologies Inc. (NMT) (figure 4). The N^{c}IQ uses patented technology to measure the reflected electrical signal length from anatomical structures in motion. The signal generated by the N^{c}IQ is integrated into the NMT IQ algorithm, and the following hemodynamic parameters are measured: cardiac output, heart rate, respirations, and life score. The N^{c}IQ noncontact sensor is 3 in×1 in×4 in and weighs less than 6 oz. The N^{c}IQ noncontact sensor, which does not require skin contact for proper operation, was worn in the pocket of the operator during the parabolic flights.

Figure 4. N^{c}IQ Noncontact Sensor.

The N^{c}IQ noncontact sensor operates on an internal 4.7-volt non-rechargeable battery manufactured by Inspired Energy (Model NC2040HD). The N^{c}IQ noncontact sensor transmits data to a data manager receiver that was located inside the locker containing the SAMS laptop (figure 5). The data manager receiver was attached to the inside of the middeck locker using Velcro. The N^{c}IQ noncontact sensor produces a fixed, single-frequency, sinusoidal signal in the 902 MHz to 928 MHz ISM [industrial, scientific, and medial] frequency band, which is typically centered at 915 MHz (similar to a cellular phone). The signal was applied for 30 seconds for a 2-minute measurement process for a 25% duty cycle, which follows the standards and exposure restrictions set by the Institute of Electrical and Electronic Engineers (IEEE) Std. C95.1™-2005. The calculated specific absorption rate (SAR_{peak}=5.8419 mW/Kg, $SAR_{nominal}$=1.4605 mW/Kg for 10 grams of tissue) maximum for the N^{c}IQ noncontact sensor is <4% of the limit (Basic Restriction SAR=160 mW/Kg for 10 grams of tissue). The data manager receiver operates on AA alkaline batteries and can receive a signal from the noncontact sensor as far away as 500 ft, with or without a line of sight.

Figure 5. N^{c}IQ data manager receiver.

RESULTS

1. FASTRACK: The engineering unit interfaces and operational procedures were successfully demonstrated. The FASTRACK rack system and power support were successfully validated in the microgravity environment. This enabled the FASTRACK team to evaluate the FASTRACK design prior to fabricating the flight units.
2. SAMS: The SAMS accelerometer data were collected without issue and provided valuable insight into the forces applied to different locations on the FASTRACK hardware during parabolic flight.
3. Faraday Waves: The Faraday-waves experiment had several technical glitches that prevented experiment success. The adhesive holding the petri dish cover to the petri dish base was not always adequate to contain moisture. A small amount of liquid was released from the petri plate on the first flight day, and the experiment had to be shut down to prevent damage to the Faraday-waves hardware. The video camera was unable to film the Faraday waves in the petri dish due to the liquid obscuring the view through the petri dish cover during parabolas. While the results of this experiment were disappointing, the Faraday-waves investigators' team had several lessons learned that they will incorporate if the experiment is to be repeated in the future.
4. N^{c}IQ: The N^{c}IQ hardware performed very well overall. The N^{c}IQ user wore the noncontact sensor inside his/her flight suit pocket. This worked well for most of the parabolas, although data dropouts between the noncontact sensor and the receiver did occur. The N^{c}IQ equipment has been tested in a variety of extreme conditions. The additional testing in microgravity has helped to further define the ruggedness and accuracy of this hardware in extreme conditions.

CONCLUSION

As per previous experience, parabolic flights have proven invaluable in testing hardware designs and performance in microgravity. The validation of the FASTRACK design gives the engineering team the confidence that the current design will meet the future microgravity requirements for this hardware. The validation that the N^{c}IQ can provide reliable and accurate data while in the subjects' pocket in microgravity conditions gives the manufacturer further data to show that its hardware is reliable in a wide variety of environments.

PHOTOGRAPHS

JSC2008E116066 to JSC2008E116067
JSC2008E116081 to JSC2008E116078
JSC2008E118171 to JSC2008E118177

VIDEO

- Zero-G flight week 9/9–9/10/08, Master no.: DV1721

Videos are available from the Imagery and Publications Office (GS4), NASA JSC.

CONTACT INFORMATION

For more information on the FASTRACK or SAMS hardware, contact:
Robert Soler
The Bionetics Corporation
Kennedy Space Center, FL
(321) 861-3047
Robert.R.Soler@nasa.gov

For more information on the Faraday Waves experiment, contact:
Larry Chew, Ph.D.
University of Central Florida
Phone: (407) 924-3179
Email: teducators@hotmail.com

For more information on the $N^{c}IQ$ hardware, contact:
Luis Moreno, M.D.
The Bionetics Corporation
Kennedy Space Center, FL
Phone: (321) 867-3827
Email: Luis.A.Moreno@nasa.gov

TITLE

Noninvasive Ophthalmic Nerve Sheath Diameter and Intraocular Pressure Responses to Microgravity

FLIGHT DATE

November 21, 2008

PRINCIPAL INVESTIGATOR

Doug Hamilton, M.D., Ph.D., Wyle Integrated Science and Engineering Group

GOALS

- Refine the human factors for eye exams using ultrasound and applanation tonography while observing ophthalmic morphometrics in response to microgravity and hypergravity.
- Map human ophthalmic nerve changes in response to physiologic maneuvers.
- Determine human choroid thickness changes in response to microgravity
- Measure intraocular pressure changes in response to microgravity.

INTRODUCTION

In past parabolic flights provided by the Reduced Gravity Office (RGO), Med Ops has performed a variety of ultrasound research objectives. Med Ops and the Advanced Diagnostic Ultrasound in Microgravity (ADUM) research team engaged in a broad range of experiments and testing in clinical and research uses of ultrasound with the RGO and on the ISS (Chiao et al., 2005; Hamilton et al., 2004). As related to human testing of ophthalmic ultrasound in parabolic flights, the ADUM team has had some limited exposure on the previously flown C-9 aircraft. Additionally, Med Ops experimented with visualization and mapping of the ophthalmic nerve sheath to investigate the correlation between nerve diameter and intracranial pressures (ICPs). This project was based on seminal work by Dr. Blavias et al., which demonstrated that ICP correlates with optic nerve diameters as seen by ultrasound (Newman et al., 2002). In this experiment, the Med Ops team directly measured ICP and changed the ICP in the animal (pig) while the nerve diameter was monitored with high-frequency ultrasound at micro- and hypergravity on board the C-9.

Zero Gravity Corporation (ZERO-G®) presented Med Ops with an opportunity to fly scientific research in their aircraft provided that the potential experiment required limited labor and resources. The Med Ops team designed an experiment that offered valuable data and used minimal resources. Despite a compendium of prior work, including the ADUM experiments, data are still very limited on the human factors of eye ultrasound exams in a microgravity environment. The team designed an experiment looking at changes in the human eye during microgravity.

The protocol and corresponding documentation was drafted, presented, and approved by the NASA JSC Committee for the Protection of Human Subjects (CPHS). After approval, events on the ISS sparked an interest and led to a last-moment change to the protocol.

The principal investigator (PI), Dr. D. Hamilton, was informed by one of his collaborators, Dr. C. Gibson, NASA JSC Optometrist, regarding ophthalmic changes occurring in astronauts that appeared to be specific to microgravity exposure. These physiologic changes involved decrease in near visual acuity, choroid (inner vascular layer of tissue behind the retina), and nerve edema. Direct intraocular pressure (IOP) measurements on the eye were taken using the applanation tonography protocol currently being flown on the ISS. In previous parabolic flight experiments, IOP measurements had been successfully performed by Dr. Gibson and Dr. Tom Mader during parabolic flight aboard KC-135 aircraft (DSO [Detailed Science Objective] 472). With these events in mind, the PI, Dr. Gibson, and the Med Ops team rationalized that perhaps ultrasound also could be used to assess choroid changes as it is available in the Human Research Facility (HRF) aboard the ISS. But, could the choroid changes actually be seen with ultrasound in microgravity? IOP, nerve, and choroid thickness change correlation has never been compared in

humans in a microgravity environment. Since both IOP and ultrasound testing modalities are available in the ISS, the experiment was refined to include IOP measurements for correlation with ultrasound measurements. The addition of a tonometry measurement protocol was approved by the NASA JSC CPHS by expedited review.

METHODS AND MATERIALS

Ultrasound was digitally captured in still frames and audio visual interface (AVI) loops using a portable ultrasound device with an 18-MHz, broad-band-linear probe manufactured by Biosound Esaote Inc. Video output from the ultrasound machine was recorded to a digital video recording device to serve as (1) a back-up data saving plan, and (2) a record of the entire data collection process. Ultrasound gel manufactured by Aquasonic Inc. was applied to the closed eyelid of the volunteer subject. IOP measurements were taken using a TONO-PEN AVIA® made by Reichert International. Prior to applanation for IOP data collection, volunteer subjects were treated with a single drop of proparacaine 0.5% (anesthetic eye drops).

During mapping of the optic nerve diameter and Doppler measurement of blood flow into the eye, the volunteer subjects performed controlled Valsalva and Muller maneuvers by blowing and sucking, respectively, into a pressure measurement device (PMD). The PMD is a negative and positive pressure-breathing device designed to monitor and store the pressure effort from breathing into the mouthpiece, built by Wyle Integrated Science and Engineering Group.

The experiment was videotaped with both mounted and handheld video cameras. This experiment consisted of 60 parabolas, all of which were microgravity.

The team for the experiment consisted of 1 TONO-PEN/PMD operator, an ultrasound operator, and a volunteer subject. There were 3 volunteer subjects who participated for 20 parabolas each. Each subject was also participating in a separate experiment on the plane and, therefore, was not exclusively dedicated to the eye experiment. This reduced the amount of resources needed for completion of the experiment. All subjects had identical testing on the ground the week prior to flight testing. During a 20-parabola set in flight, ultrasound was performed for the first 15 parabolas and IOP using the TONO-PEN was performed for the last 5 parabolas on each of the 3 volunteer subjects.

Parabolas 1–15: Ultrasound

Ultrasound monitoring with intermittent color-flow Doppler and pulse-wave Doppler continued on the eye throughout the microgravity phase of the parabola and into the hypergravity phase. The volunteer subject was coached to stare a forward gaze with the contra lateral eye. Due to the very short phases of microgravity and dynamics of the eye, quality images would be impossible to reacquire by removing the probe during hypergravity phase and reapplying it again at the top of the parabola. The safety and comfort of each volunteer subject was monitored by both operators and a dedicated flight crewmember who was (1) seated in the experimentation area and (2) in communication with the flight crew, as needed. The TONO-PEN operator acted as the PMD operator during the physiologic maneuvers of Valsalva and Muller. While the optic nerve was being scanned, the subject blew into the mouthpiece of the PMD and was coached to maintain a

consistent 30 mmHg for Valsalva or negative 30 mmHg for Muller for the duration of the parabola.

Ultrasound operator scanning the optic nerve over the eyelid with a high-frequency linear probe.

During parabolas when the TONO-PEN/PMD operator was not engaged with human testing, applanation was done on an eye simulator Eyetech Ltd. This is the identical device that was used to train the ISS crew in applanation tonography and is a pressure modulator with 3 controlled settings. This simulator acted as a control for the IOP experiment.

Parabolas 16–20: IOP Measurements

After parabola 15, the subject wiped his/her eye free of ultrasound gel, and the ultrasound operator placed 1 numbing drop into the right eye just as the parabola was going into the hypergravity phase. The TONO-PEN/PMD operator performed applanation tonometry at the top of the microgravity portion of parabolas 16 through 20. The IOP was successfully measured 1 to 2 times per parabola, depending on the length of each parabola. Parabolas ranged in length from 10 seconds to 17 seconds.

TONO-PEN/PMD operator performing applanation on the cornea of the anesthetized eye measure intraocular pressure.

RESULTS/DISCUSSION/CONCLUSION

The results of this investigation are not finalized, and additional analysis of the ultrasound images has yet to be complete. However, the IOP measurements are complete and show minimal pressure increases in parabolic flight. Ophthalmologist Dr. T. Mader (currently practicing in

Anchorage, AK) had flown an earlier version of the TONO-PEN in an experiment for NASA on KC-135 aircraft (DSO 0472). He communicated that this minimal change is largely due to the reduced time in zero gravity. Previous flight experiments on the KC-135 have also shown that there was a more significant increase in ocular pressure because the exposure to microgravity was longer. NASA JSC Optometrist Dr. C. Gibson agrees, and has added that the fluid shift was not as prolonged for this investigation; therefore, the pressure in the eye did not have enough time to elevate as in previous experiences on the KC-135. The parabolas for this flight were exceptionally short intervals, which reduced exposure to microgravity and, thus, also reduced the physiologic effects normally observed on volunteer subjects.

The choroid, which was the original area of interest, was identified with ultrasound. This is an initial effort in determining whether the choroid could be visualized in microgravity and by no means should be considered a final product but, rather, an influential forward progress. Additional data are needed to show conclusively that this vascular bed changes with acute changes in gravity. The significance of changes in the choroid structure may be statistically relevant with a larger subject population. Our study consisted of 3 subjects total, and the final results are pending completion. The initial data are interesting and reproducible with the single experienced operator for both the ultrasound and tonometry. The dynamics and human factors involved have not been completely refined due, in part, to the fact that the volunteer subjects had a difficult time holding a forward gaze during the flight. Without mechanically "fixing" the gaze, it seems likely that this may be a factor that cannot be changed, and additional data takes could be helpful in deciding whether alternative gazes yield similar results. The images with "off-axis gaze" were readily attainable and could potentially capture the region, which is the area of the back of the eye that we were trying to acquire. We are currently collaborating with Dr. Tom Mader, Ophthalmologist from Anchorage, AK (previously mentioned), and eye ultrasound expert, Professor Dr. Anastas Pass from the University of Houston in our interpretation of the data.

REFERENCES

1. Chiao L, Sharipov S, Sargsyan AE, Melton S, Hamilton DR, McFarlin K, Dulchavsky SA. Ocular examination for trauma; clinical ultrasound aboard the International Space Station. *J Trauma*; 2005.
2. Hamilton DR, Sargsyan AE, et al. Sonographic detection of pneumothorax and hemothorax in microgravity. *Aviat Space Environ Med*; 2004.
3. Newman WD, Hollman AS, et al. Measurement of optic nerve sheath by ultrasound: a means of detecting acute raised intracranial pressure in hydrocephalus. *Br J Ophthalmol*; 2002.
4. Referenced communication from Dr. Gibson NASA ophthalmologist: Vision Changes and the Possible Etiology of Choroidal Folds in Microgravity: NASA Studies: Dr. Tom Mader, Anchorage Alaska and Dr. C. Robert Gibson, NASA.
5. DSO 0472: Intraocular Pressure, KC-135 experiment. Meehan RT, Charles JB, Taylor GR, Mader TH, Bagian JP, Gibson CR, Caputo M, Hunter N.

PHOTOGRAPHS

JSC2008E147963 to JSC2008E147965
JSC2008E147967
JSC2008E147978 to JSC2008E147983
JSC2008E147994 to JSC2008E147996
JSC2008E148005 to JSC2008E148006

VIDEO

- Zero-G flight week 11/18–11/21/08, Master nos.: 881350, 881289, 881290

Videos are available from the Imagery and Publications Office (GS4), NASA JSC.

CONTACT INFORMATION

Kathleen Garcia
Advanced Projects Group
Wyle Integrated Science and Engineering Group
1290 Hercules Avenue
Suite 120 (MC: W1C)
Houston, TX 77058
(281) 212-1364
kgarcia@wylehou.com

TITLE

Performance of a Portable Blood Count Instrument in a Microgravity Environment

FLIGHT DATE

November 21, 2008

PRINCIPAL INVESTIGATORS

Yu-Chong Tai, Ph.D., California Institute of Technology
Victor Hurst IV, Ph.D., Wyle Integrated Science and Engineering Group

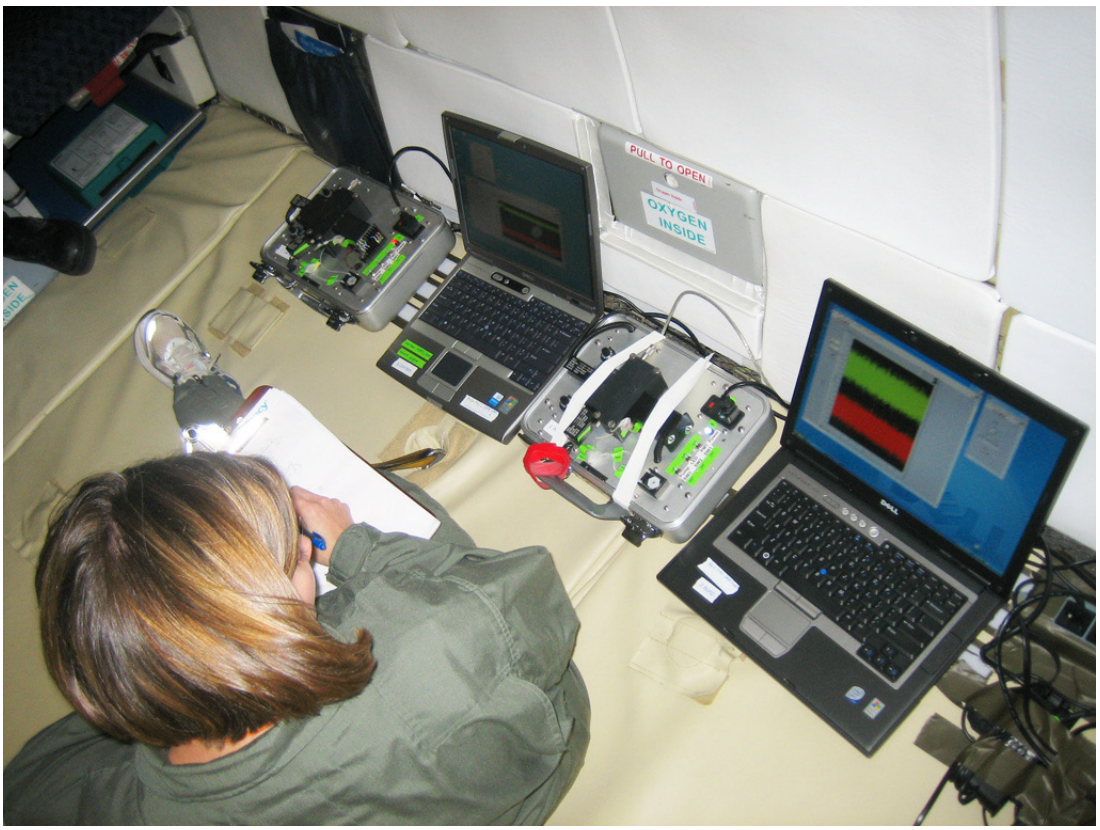

GOAL

To validate the principle of a portable blood count instrument prototype in microgravity environment and to determine whether the performance is comparable to that of ground-based testing.

INTRODUCTION

The purpose of this study is to perform a protocol evaluation of the portable blood count instrument (BCI) to determine whether the principle of the BCI works under the microgravity environment, and whether the performance of the instrument is the same as that seen in ground-based testing. The California Institute of Technology Micromachining Laboratory (CITML) co-operated with the Advanced Projects (AP) group of Wyle Integrated Science and Engineering Group (Houston) to conduct this evaluation.

Blood count is an important medical test that is known to supply a rapid assessment of diseases such as anemia, infection, inflammation, acute radiation syndrome, and immunosuppression. The test provides a useful health-monitoring method for astronauts, especially when they experience stress or are exposed to radiation during space missions. However, the commercially available blood counters are usually heavy and bulky and occupy a volume greater than 10^5 cm^3. This is a concern considering that space missions require small-sized medical instruments due to limited on-board space.

To address this concern, CITML has been tasked to develop and demonstrate an automated portable BCI that is easy for astronauts to operate in space (Zheng et al., 2008). A prototype BCI has been recently designed and tested in a terrestrial environment (figure1). Fluorescence-based microflow cytometry is employed to count the number of cells in the blood sample, and a micro-fluidic device is used as a disposable cartridge for detection. A blue-light-emitting diode (LED) is used as the excitation source (figure 2). The excitation light is filtered and condensed onto the detection zone of the micro-device. The blood sample is drawn through the micro-device by a mini-peristaltic pump. The fluorescence signal from the stained blood cells is collected, split into 2 colors, and measured by 2 photon-multiplication tubes (PMTs). Blood count, including both leukocyte absolute count and a lymphocyte ratio, can be conducted with this portable BCI prototype.

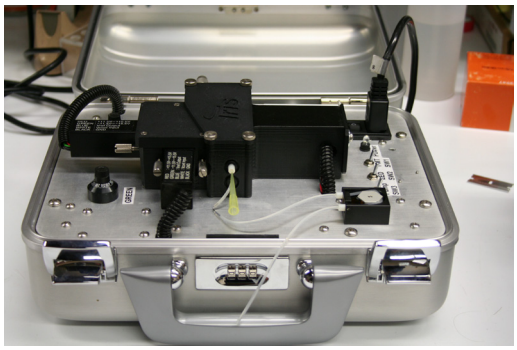

Figure 1. The prototype BCI.

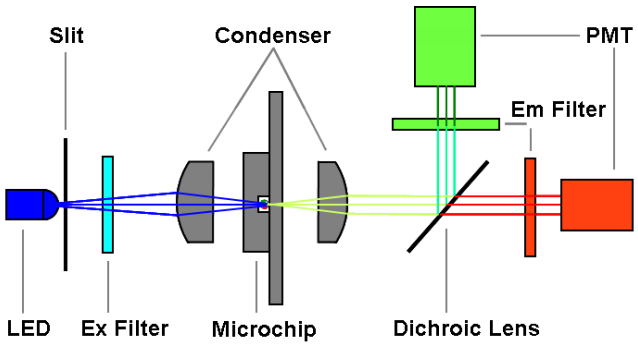

Figure 2. The optical configuration of the BCI.

To assess the feasibility of using the BCI under microgravity environment, the CITML and the AP group conducted and evaluated blood counts with blood samples from healthy donors using the BCI prototype devices during parabolic flight aboard the ZERO-G® Corporation aircraft.

OBJECTIVE

To validate the principle of a portable BCI prototype in the microgravity environment and determine whether the performance is comparable to that of ground-based testing.

METHODS AND MATERIALS

Two BCI prototype devices were used in the flight test. One BCI was used to test a blood sample while the other BCI performed a control test using fluorescent beads. For the blood sample, a volume of 100 µL of human blood from a healthy donor was stained with 100 µL Acridine Orange solution (concentration 200 µg/mL) for 5 minutes under room temperature, and then diluted to a total volume of 1,500 µL with Ficoll-Paque. For the control sample, green fluorescence beads (5-µm diameter) were diluted with Ficoll-Paque to a concentration of 10^5 beads/µL and a total volume of 1,500 µL. Samples were prepared and loaded onto the BCI prototypes during the on-ground preparation just before take off of the aircraft.

The tests were started by turning on the BCI prototypes after the aircraft took off. The data of the detected signals were recorded on 2 laptop computers connected to the BCI prototype with universal serial bus (USB) cables (figure 3). The starting time of the test was recorded by a flight crewmember from AP (figure 4) to ensure that the test time could be synchronized with the acceleration data during the 60-parabola-flight time. The acceleration data were recorded by a separate accelerometer on the rack on the flight. All of the data were saved and analyzed afterwards.

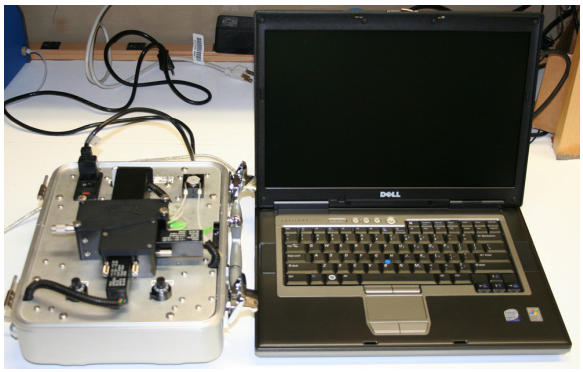

Figure 3. The BCI prototype and the laptop computer for data recording.

Figure 4. Flight crew turned on the BCI and recorded the test starting time.

RESULTS/DISCUSSION/CONCLUSION

Preliminary analysis of the data shows that the portable BCI prototype worked under the reduced-gravity environment. The fluorescence signal of the blood cell count showed no observable difference from the results of ground tests. The low-environment pressure (~6 pounds per square inch [psi] versus 14 psi atmosphere pressure) during the flight test reduced the pumping

efficiency of the peristaltic pump used in the BSI prototype. The power of the pump should be increased for future flight tests. The data will be formally analyzed and written up by the CITML for peer review.

ACKNOWLEDGMENTS

The CITML would like to acknowledge the following groups for their support with flight preparation and execution for this evaluation: Advanced Projects at Wyle Integrated Science and Engineering Group, and the NASA JSC RGO.

REFERENCES

1. Zheng S, Kasdan HL, Fridge A, Tai Y-C. Blood cell analysis using portable flow cytometer with microfluidic chips as cartridge. In: Proceedings of the 12th International Conference on Miniaturized Systems for Chemistry and Life Sciences (microTAS'08), San Diego, Calif., October 12–16, 2008.

PHOTOGRAPHS

JSC2008E147966
JSC2008E148007 to JSC2008E148008

VIDEO

- Zero-G flight week 11/18–11/21/08, Master nos.: 881350, 881289, 881290

Videos are available from the Imagery and Publications Office (GS4), NASA JSC.

CONTACT INFORMATION

Yu-Chong Tai, Ph.D.
(626) 395-8317
Electrical Engineering
California Institute of Technology
1200 East California Boulevard, MC 163-93
Pasadena, CA 91125
vctai@mems.caltech.edu

TITLE

Effectiveness of Needleless Vial Adaptors for Drug Administration in a Microgravity Environment

FLIGHT DATE

November 21, 2008

PRINCIPAL INVESTIGATORS

Melinda J. Hailey, RN, BSN, Wyle Integrated Science and Engineering Group
Tina M. Bayuse, PharmD, Wyle Integrated Science and Engineering Group

GOALS

- Identify appropriate size vial required to withdraw a defined drug volume.
- Identify hardware that facilitates withdrawal of the appropriate volume of drug from vial (blunt cannula with syringe, needleless valve, syringe size, etc.).
- Identify fluid properties of ISS-related medications that would prevent withdrawal of medication from vial using identified hardware (viscosity, foaming, particulate formation, etc.).
- Video record procedure used to withdraw medication from a vial into a syringe for use with on-orbit procedure.

INTRODUCTION

The current system for injectable medications aboard the ISS has experienced a materials failure that requires a new system for injectable medications to be identified and flown. It is desired that this new system will fly medications for injection in their original manufacturer packaging. This will allow the system to comply with United States Pharmacopeia (USP) guidelines while minimizing the frequency of resupply due to medication expiration. However, this change will require crew to draw liquid medications for injection from a glass vial into a syringe prior to injection.

This experiment will evaluate the effectiveness of various needleless-vial adaptors to facilitate the withdrawal of liquid medication from a glass medication vial into a syringe for injection within a microgravity environment. Other parameters to be assessed include determining the ability to withdraw the required amount of medication, and whether this is dependent on vial size, liquid viscosity, or the total volume of fluid within the vial. Liquid medications proposed for flight on the ISS will be used for this experiment.

DISCLAIMER

The content of this report should not be considered final and binding. Formal review and evaluation of all data collected will be the subject of final reports and publications when deemed appropriate. The content of this report should permit the reader to become familiar with the procedures followed and the preliminary observations and lessons learned. This document neither endorses nor rejects the performance of any commercial products used.

Medications for injection are commercially available in a variety of forms including glass/plastic single-dose vials, glass/plastic multi-dose vials, and prefilled syringes. Whenever possible, it is desired that injectable medications for use on the ISS be delivered in a prefilled syringe to limit the need for astronauts to manipulate the medication prior to administration. However, the healthcare market is constantly evolving based on new evidence sources and changing standards of care, meaning that medications are not consistently available at the desired strengths or volumes in the same packaging over a period of time.

Figure 1. Carpuject® syringe (current method of injectable meds on the ISS).

Figure 2. Single-dose and multi-dose medication vials (current method of injectable meds on the ISS).

Figure 3. Commercially prepared pre-filled medication syringes.

In the event medications must be supplied in a vial, a system is required that allows for the safe withdrawal of medication from the vial into a syringe for administration. Traditionally, this method of withdrawal requires the use of a needle. In an effort to limit risk of inadvertent needle sticks, the healthcare marketplace has a variety of needleless-vial adaptors that allow direct connection of a syringe to a medication vial, eliminating the need for a needle to pierce the vial septum. These vial adaptors, in some instances, can also offer the protection of a re-sealable, swabbable barrier, thus preventing inadvertent contamination of medications from repeated withdrawals over a period of time. For ease of training and in an attempt to minimize multiple variations of hardware, it is desired that the hardware of choice be a single system that is effective for use no matter what vial size or syringe is selected.

OBJECTIVE

Identify issues related to the withdrawal of liquid medication for injection from a glass medication vial into a syringe within a microgravity environment using a needleless-vial adaptor.

METHODS AND MATERIALS

A market survey of needleless-vial adaptors was performed, and a representative sample was obtained for further evaluation. A small group consisting of a pharmacist, engineers, and nurses evaluated the narrowed field of hardware and identified 3 primary pieces of hardware for further testing. The original experiment design was based on 1-G ground-testing of 3 different vial adaptors followed by microgravity testing of the 2 best candidates. Due to a shipping delay, 1 of the 3 vial adaptors was unable to be obtained in time for ground/inflight testing. Please refer to the Future Studies section for further information on this hardware.

It was also desired to evaluate the volume of air and its behavior in prefilled medication syringes packaged by the manufacturer. Four sample medications were obtained for observation during the flight.

Figure 4. Cap vial adaptor.

Figure 5. Spike vial adaptor.

Figure 6. Blunt cannula vial adaptor.

1-G ground-testing was completed using medications in similar volume and concentration to those currently flown on the ISS. The experiment was designed to be evaluated within 60 parabolas, lasting approximately 20 seconds each, with testing divided into 3 segments: Segment 1 – Cap-vial adaptor testing; Segment 2 – Spike-vial adaptor testing; Segment 3 – Video documentation of the procedure steps required to withdraw medication from the vial into the syringe. Two participants were used to conduct the ground and flight testing, with the first participant assembling hardware and the second participant withdrawing the medications during the microgravity portion. Two fixed video cameras were used to document the experiment, and 2 handheld cameras were used intermittently throughout the flight. Still images were also captured at various stages of the experiment. Feedback on each medication and device was captured by activated microphones attached to both participants. Materials were immobilized using Velcro® and foam blocks for safety during periods of aircraft turbulence and during microgravity portions of the flight. Sharp objects (i.e., plastic vial adaptors, medication vials) were disposed of in a sharps container attached to the table used in the experiment. Any liquids that were inadvertently released during microgravity portions of the flight were captured using towels secured to the work surface. A postflight debriefing was conducted by the 2 flight evaluators, and still photographs were taken of problematic hardware/vials.

RESULTS/DISCUSSION/CONCLUSION

The microgravity portion of testing highlighted 3 areas of focus when attempting to draw up a medication in microgravity in addition to revealing information on the vial adaptors tested. Specific areas for discussion are: (1) fluid isolation in medication vial, (2) withdrawal of medication into syringe and use of air injection into the vial for pressure equalization, and (3) air/fluid separation in a syringe.

Figure 7. Fluid isolation in medication vial (cap vial adaptor testing).

Fluid isolation in the medication vial: In all instances, the medication vials were spiked with a syringe/vial adaptor assembly prior to fluid isolation in vial. Maneuvers were used to facilitate separation of air and fluid in the vial while moving fluid to the end of the vial that was closest to the septum. These fluid isolation maneuvers may be achieved in multiple ways, all of which, based on experience of fluid management in microgravity, may be performed according to the preference of the astronaut. If vial adaptors and syringes are attached to a vial before fluid is isolated in the vial, consideration of how that vial is manipulated should be based on the stability of the assembly attachment. Holding the vial in hand to prevent "slinging" of the vial off the adaptor is a recommended action. Alternatively, fluid isolation can be performed prior to attaching the syringe/vial adaptor assembly. Limitations of the ZERO-G® flight prevented analysis of microbubbles in solution created by launch forces, and it is anticipated that this will be more of an issue in a sustained microgravity environment compared to this test flight.

Figure 8. Withdrawal of medical into syringe (spike vial adaptor testing).

Withdrawal of medication into syringe: Terrestrial practices for medication withdrawal from a non-vented vial require injection of an equivalent amount of air as the expected medication volume prior to inverting the vial and withdrawing liquid. This practice eliminates the resistance

of the syringe plunger pulling against a higher vial pressure as the drug is withdrawn. In microgravity, this rationale is still valid; however, the injection of additional air into the vial creates a multitude of microbubbles and increases the volume of medication mixed with air that must be withdrawn to achieve the desired drug volume in syringe. This practice is more likely to be required when using vials >30 mL in size and injection volumes >10 mL. It is felt that, based on the microgravity flight, the practice of air injection is more of a hindrance than help.

Figure 9. Trapping of fluid in medication vial due to flight adhesion (spike vial adaptor testing).

It was found that single-dose-medication vials present a problem in accessing the entire drug volume required for administration. At issue is the manufacturer's air bubble in the vial. In microgravity, this air bubble traps fluid along the sides and base of the vial despite effective air/fluid separation prior to medication withdrawal. Manufacturers typically provide some overfill of the vial, but this volume is not predictable. Terrestrially, any fluid that is not immediately at the septum may be "chased" using a needle that can be manipulated to the liquid bubble. Both vial adaptors tested limited this ability to chase pockets of medication in the vial either due to the locking mechanisms on the vial top or the length of the spike. The spike-vial-adaptor length was also limiting in vials holding <3 mL of fluid. The spike length (in relation to where the fluid ports on the spike) was too long to allow access to all the fluid in the vial. Use of single-dose vials without the ability to "chase" fluid risks the possibility of the inability to access all the desired medication from the vial.

Figure 10. Air/fluid separation in syringe.

Air/fluid separation in syringe: Due to dead space within vial adaptors, some air will inevitably be mixed into medications as they are withdrawn into a syringe, despite effective fluid isolation in vial. This air, combined with any microbubbles that are possibly still in solution, will require a second effort on the part of the astronaut to isolate fluid in the syringe prior to medication administration. Selection of a syringe size larger than the volume required is considered to be helpful so that a larger volume than necessary may be withdrawn followed by fluid and air being isolated and then extra air ejected from syringe.

In the prefilled syringes packaged by the manufacturer, the air volume within the syringe varied. This was due to varying fluid volumes in each of the syringes as well as to different packaging. During 2 parabolas, it was noted that the air in each of the prefilled syringes separated to form smaller air bubbles. Fluid/air isolation techniques were evaluated. It was decided that the presence of air within these syringes would not pose a problem for medication administration in microgravity once the isolation technique was used.

Hardware selection: While advantages can be observed for both pieces of hardware, it was felt that the cap vial adaptor was the superior choice of the 2 pieces of hardware. The cap serves as a physical barrier between the septum and the environment, which would be helpful, especially for multi-dose vials that might be restowed within the ISS medical kits. Its smaller diameter spike is also markedly superior in perforating the rubber septum without causing displacement that causes leakage. The spike is short enough that it sits close to neck of the vial, making the fluid bolus more accessible. It was found that the larger dead space in the spike vial adaptor caused problems when attempting to withdraw the total volume of medication from vials containing 2 mL or less of fluid. Additionally, the diameter of the spike-vial adaptor was so large that, in some instances, it totally displaced the septum of the vial, causing leakage and risk of drug contamination.

Learning points from the study:

1. Air injection into a vial makes air/fluid isolation for withdrawal challenging.
2. Medication withdrawal from a vial requires three distinct steps: fluid isolation in vial, fluid withdrawal from vial, and fluid isolation in syringe to achieve final medication volume for injection. These distinct steps should be emphasized in procedure documentation and training practices.
3. Fluid viscosity is not a limiting factor in vial adaptor selection.
4. Medications evaluated within this flight do not present issues with particulates or disabling foaming properties within the microgravity environment.
5. When reconstituting medications from powder, it is suggested that a lower concentration and higher volume should be considered for ease in medication withdrawal into a syringe. This study evaluated 3 volumes of ceftriaxone diluted with lidocaine or a normal saline solution.

Limitations of the study:

1. Aircraft cabin pressure was reported to be variable during flight but averaged approximately 7 psi. ISS cabin pressure has a higher range of 10.7 psi to 15.2 psi
2. Parabola length was too short to evaluate all of the steps required to withdraw medications from a vial, taking into consideration fluid bubble management. These steps are required in

full sequence in microgravity to fully assess the time impact required to withdraw the medications. Microgravity portions of parabolas were also variable and unpredictable.
3. Bubbles and microbubbles that could be formed during the agitation of launch and subsequent continuous microgravity could not be realized in this study due to the pullouts.
4. Difficulty in shipments prior to flight eliminated the testing of the blunt cannula-vial adaptor. It is felt that this hardware should be given consideration in a future reduced-gravity flight due to its low volume of dead space, small packaging size, and ability to be manipulated within the vial.
5. It was desired to have a second day of flight to evaluate parameters assessed on this first flight and modify testing procedures using lessons learned.

Future studies:
It is desired that a future flight be scheduled to evaluate the cap-vial adaptor against the blunt cannula, especially as it relates to use of single-dose vials compared with larger-volume multi-dose vials. An additional flight would be used to further refine the procedure steps required for fluid isolation, with focus specifically on fluid isolation within a syringe.

ACKNOWLEDGMENTS

The investigators would like to acknowledge the following groups for their support with flight preparation and execution for this evaluation: Advanced Projects at Wyle Integrated Science and Engineering Group, NASA JSC Medical Operations Group, and the NASA JSC Pharmacy. Finally, the investigators also acknowledge the valued support and guidance from the NASA JSC RGO.

PHOTOGRAPHS

JSC2008E147960 to JSC2008E147962
JSC2008E147968 to JSC2008E147977
JSC2008E147985 to JSC2008E147993
JSC2008E147997 to JSC2008E147998
JSC2008E148001 to JSC2008E148004

VIDEO

- Zero-G flight week 11/18–11/21/08, Master nos.: 881350, 881289, 881290

Videos are available from the Imagery and Publications Office (GS4), NASA JSC.

CONTACT INFORMATION

Melinda J. Hailey, RN, BSN
HMS Instructor, Space Medicine Training
Wyle Integrated Science and Engineering Group
1290 Hercules Avenue
Suite 120 (MC:W1A)
Houston, TX 77058
(281) 212-1355
Melinda.j.hailey@nasa.gov

Tina M. Bayuse, Pharm.D.
Lead Pharmacist, JSC Pharmacy
Wyle Integrated Science and Engineering Group
NASA-Johnson Space Center
2101 NASA Parkway (MC: SD38)
Houston, TX 77058
(281) 244-1632
Tina.M.Bayuse@nasa.gov

TITLE

Integrated Parabolic Flight Test: Effects of Center of Gravity and Mass on the Biomechanics, Kinematics, and Operator Compensation of Exploration Tasks in Lunar Gravity

FLIGHT DATES

December 9–12, 17, 2008
January 13, 2009
March 4–5, 2009
March 10–12, 2009
March 27, 2009

PRINCIPAL INVESTIGATOR

Michael L. Gernhardt, Ph.D., NASA Johnson Space Center

CO-INVESTIGATORS

Jeff Patrick, NASA Johnson Space Center
Sudhakar Rajulu, Ph.D., NASA Johnson Space Center

GOALS

This test was a continuation of the Constellation Program (CxP) Extravehicular Activity (EVA) Systems Project Office (ESPO- sponsored testing series that is being conducted to enable the development of optimized design requirements for the next-generation lunar EVA suit. ESPO initiated this series of tests aimed at understanding human performance and suit kinematics under a variety of simulated lunar EVA conditions. The test series is a collaborative effort among the Crew and Thermal Systems Division (CTSD), the EVA Physiology, Systems, and Performance (EPSP) Project, the Anthropometry and Biomechanics Facility (ABF), and the Exercise Physiology and Countermeasures (ExPC) Project of the HACD. The goal of the studies is to systematically evaluate the individual contributions of suit weight, mass, center of gravity (CG), pressure, and kinematics and determine their relative contributions to the overall metabolic cost, biomechanics, and required operator compensation associated with performing ambulation and exploration tasks in spacesuits.

OBJECTIVES

The objectives of this study in the testing series were to:

1. Compare the results to testing performed on the NASA JSC prevention of coupled structure propulsion instability (POGO) partial-gravity system during Integrated Suit Test (IST)-1 and IST-2.
2. Assess the effects of varying the suit weight while keeping CG and mass constant.
3. Assess the effects of varying the suit mass while keeping CG constant.
4. Assess the effect of varying the suit CG while keeping mass and weight constant.

METHODS AND MATERIALS

The study protocol was designed to evaluate the objectives through subject performance of ambulation and exploration tasks similar to those performed during prior POGO tests. The protocol for the study was reviewed and approved by the NASA JSC Committee for the Protection of Human Subjects. Subjects were provided written informed consent and a layman's summary before participating in the study. Seven astronaut subjects took part in the study, with subjects nominally flying 3 times to complete all conditions. Data were collected during 14 flights, with each flight consisting of approximately 60 parabolas. Two flights were designated as engineering flights to ensure the efficacy of the planned protocols and data collection techniques. Testing was performed both unsuited and suited. The suited portions of the test used the Mark III Advanced Space Suit Technology Demonstrator (MK-III).

The tasks performed were walking, kneeling and recovering, shoveling, and rock pickup (figure 1). The test conditions consisted of 3-suit masses (195 lbs, 265 lbs, and 400 lbs assessed at zero-G to 17-G and a constant CG), 3-suit weights (simulated by 0.1-G, 0.17-G, and 0.3-G parabolas at a constant suit mass of 265 lbs and a constant CG), and 3 CGs (1 being near a standard subject's natural CG and 2 further high and aft, all assessed at 400 lbs and 0.17-G; figure 2). A matrix of the test conditions is shown in Table 1.

Figure 1. Subjects performing study tasks; clockwise from top left: walking, kneeling and recovering, shoveling, and rock pickup.

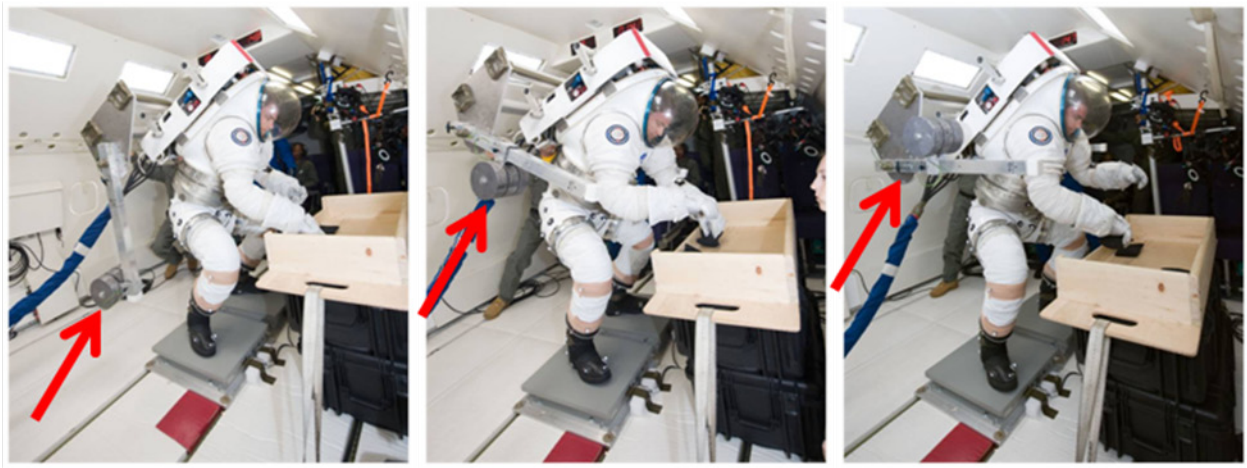

Figure 2: Subject performing rock pickup task with mass/CG rig configured for different CGs; arrows point to differences in position of weights on rig in each configuration; left to right: backpack, CTSD, and POGO CG.

Table 1. Matrix of Test Conditions

Varied Mass Testing	**Suit Mass** **g-level** **1-g Suit Weight** **CG**	195 lbs 0.17-g 195 lbs ~CTSD	265 lbs 0.17-g 265 lbs ~CTSD	400 lbs 0.17-g 400 lbs CTSD
Varied Weight Testing	**Suit Mass** **g-level** **1-g Suit Weight** **CG**	265 lbs 0.1-g ~87 lbs ~CTSD	265 lbs 0.17-g 265 lbs ~CTSD	265 lbs 0.3-g ~620 lbs ~CTSD
Vaired CG Testing	**Suit Mass** **g-level** **1-g Suit Weight** **CG**	400 lbs 0.17-g 400 lbs Backpack	400 lbs 0.17-g 400 lbs CTSD	400 lbs 0.17-g 400 lbs POGO

Note: Red and green matching denotes the same condition; those conditions are shown twice for descriptive purposes only; the condition was only performed once across Phase I & Phase II

For each tested condition, the walking task was performed during 4 parabolas, shoveling for 2 parabolas, rock pickup for 2 parabolas, and kneeling and recovering for 1 parabola. During a parabola dedicated to a particular task, the task was nominally performed twice.

Motion-capture camera systems were used along with biomechanics markers to capture the gait characteristics and kinematics of the subjects as they performed tasks. Force plates also were used to collect vertical ground reaction force during walking and to provide input for determination of stability while performing the shoveling and rock pickup tasks. Since the duration of parabolas does not allow for accurate direct metabolic rate measurement, subjective ratings of perceived exertion (RPEs) were collected. Results from the ground-based series of tests on the POGO produced a correlation between RPE and metabolic rate that can be used for metabolic rate estimations. Finally, ratings of modified Cooper-Harper (CH) were collected to determine the amount of operator compensation required for the subjects to perform the task. The modified CH scale allows subjects to be their own control as ratings are given in reference to their own ability to perform the task in a 1-G shirtsleeve environment.

RESULTS

The results of this study are being assessed at the time of this publication. Efforts are under way to address the objectives through analysis of the collected data and comparison of the results to those from the EVA Walkback Test, ISTs-1, -2, and -3, as well as Neutral Buoyancy Laboratory (NBL) and NASA Extreme Environment Mission Operations (NEEMO) (9–13) tests.

DISCUSSION

This test series is developing a parametric understanding of the interrelationships among suit weight, mass, pressure, and CG as well as crew anthropometrics and performance while defining the limitations and correction factors associated with each testing environment. This test was designed to validate earlier testing performed on the POGO and to provide guidance for the

design of other reduced-gravity simulator projects such as the Active Response Gravity Offload System (ARGOS). The results will also provide new insights into the effects of CG on suited performance. The outcomes of this testing series will contribute to the development of informed, evidence-based recommendations for suit weight, mass, CG, pressure, and kinematic constraints that optimize human performance in partial-gravity environments.

PHOTOGRAPHS

JSC2008e153248 to JSC2008e153320
JSC2008e153964 to JSC2008e154052
JSC2008e154246 to JSC2008e154355
JSC2008e154555 to JSC2008e154987
JSC2008e156756 to JSC2008e156809
JSC2009e017642 to JSC2009e039509
JSC2009e051206 to JSC2009e051302
JSC2009e052024 to JSC2009e052133
JSC2009e053532 to JSC2009e053564
JSC2009e053650 to JSC2009e053702
JSC2009e053721to JSC2009e053867
JSC2009e054097 to JSC2009e054235
JSC2009e062376 to JSC2009e062586

VIDEO

None

CONTACT INFORMATION

Michael L. Gernhardt, Ph.D.
NASA Johnson Space Center
2101 NASA Parkway
Houston, TX 77058
281-244-8977
michael.l.gernhardt@nasa.gov

TITLE

Education Outreach Program – Human Immune Complex Formation Rates in Microgravity

FLIGHT DATES

January 13–14, 2009

PRINCIPAL INVESTIGATORS

Branyun Bullard, University of North Carolina (UNC) Pembroke
Lane Guyton, UNC Pembroke
Michelle Godwin, UNC Pembroke
Tamra Henderson, UNC Pembroke
Lisa Walters, UNC Pembroke
Lindsay Willis, UNC Pembroke
Timothy Ritter, UNC Pembroke

CO-INVESTIGATOR

Siva Mandjiny, UNC Pembroke

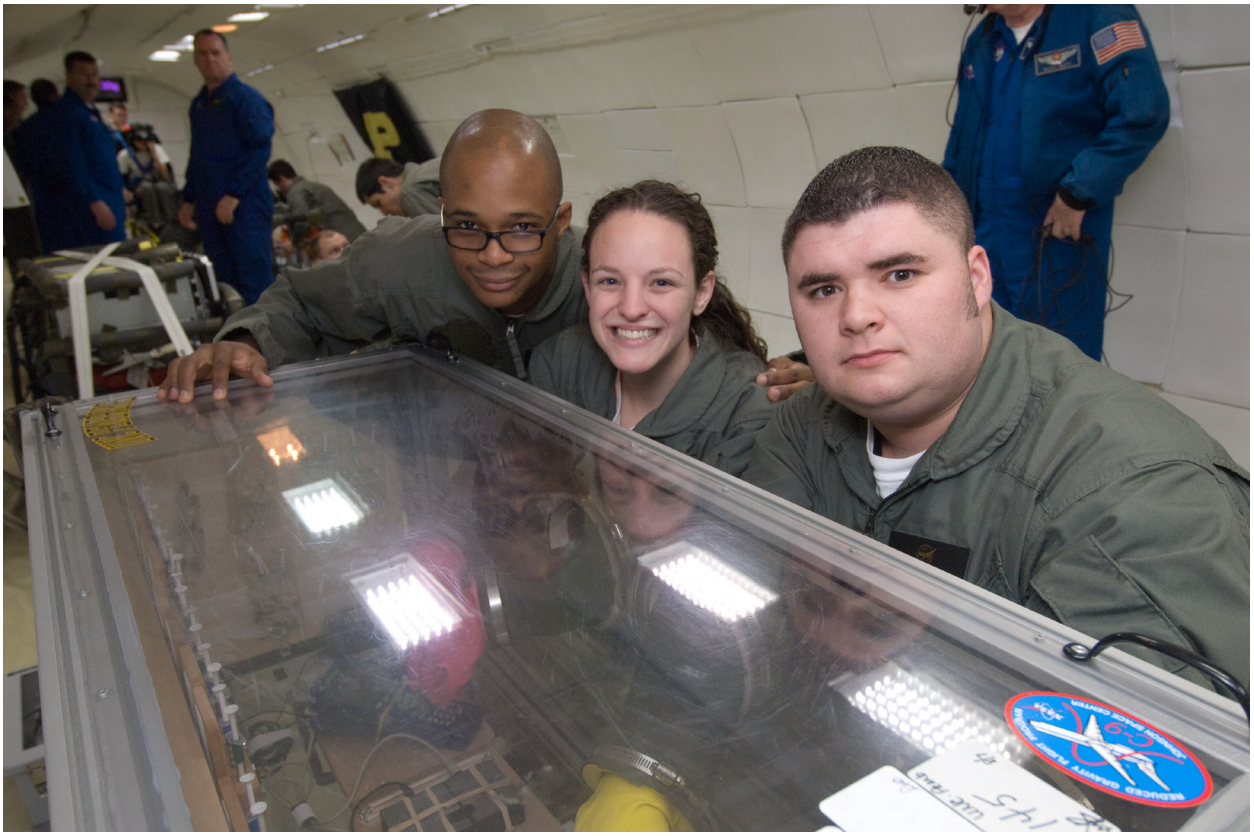

GOAL

It has been determined during the past decades of space travel that the human immune system is compromised during extended periods in the environment of orbital flight. The goal of our research was to determine what effect the force of gravity has on the rate at which immune complexes are formed.

OBJECTIVES

We considered the following question for our principal investigation with this project: "What is the dependency, if any, of immune complex formation rates on gravitational force?" We hypothesized that gravitational forces would change the convection flow within the fluid, thus preventing the immune molecules from interacting the way they normally do. Thus we predicted that the reaction rate would decrease in a reduced-gravitational environment due to less molecular interaction. In an attempt to prove our hypothesis, our research group, The Weightless Lumbee's from The University of North Carolina at Pembroke, conducted a human immune complex formation reaction in the zero-G portions of the parabolic flight path flown by the NASA research aircraft. The reaction rates from these flight samples were then compared to ground-truth experiments.

METHODS/MATERIALS

To study the formation of immune complexes in vitro, we observed the reaction between human immunoglobulin G (IgG) and goat-derived anti-immunoglobulin G (A-IgG) in a sodium phosphate buffer.

In a laboratory setting this reaction would be monitored for a period of several minutes to determine the rate of increase in the absorbance. However, due to the limited period of zero G on board the research aircraft, we had to find a way to accelerate the reaction rates. We wanted to have an absorbance change of approximately 0.15 to 0.20 over the first 20 seconds of reaction. To accomplish this we employed a buffer solution containing polyethylene glycol (PEG) that served as a catalyst to break down the structure of the water molecules and increase the rate of reaction. After trying a wide range of concentrations, it was determined that a PEG concentration of 7.5 mM added to the sodium phosphate buffer yields optimal absorbance during the 20-second interval at a wavelength of 280 nm. Consequently, a 7.5 mM solution of PEG and sodium phosphate was used to create the buffer solution in which the technical-grade IgG and the A-IgG would react to form immune complexes. The rate of absorbance for our optimal concentration is shown in figure 1. At this concentration, we achieved an absorbance change of 0.15 during the first 20 seconds of reaction. Another factor that became apparent during the initial phases of our work was the effect that massaging (i.e., pulling the combined fluid back into the syringe and re-injecting it into the cuvette) has on the uniformity of the reaction. Without massaging, the data were very oscillatory and non-repeatable. With only 2 massages using both syringes (see the equipment description below), we found a significant increase in the linearity of our data, and the results were consistent from one run to another.

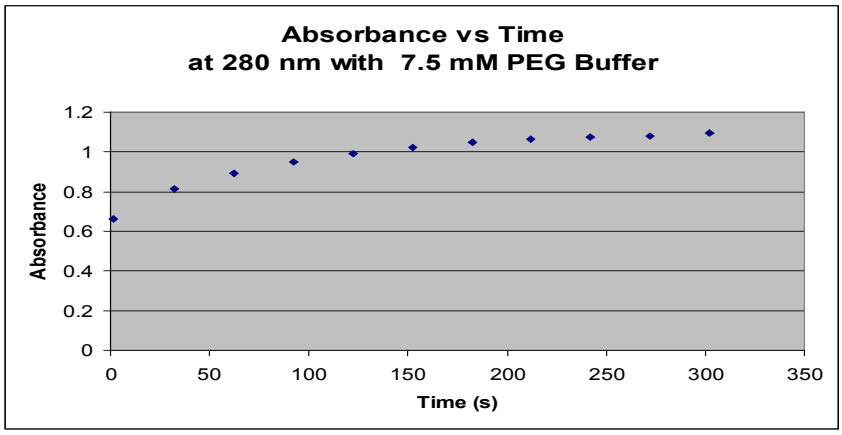

Figure. 1. Absorbance rate from the preliminary experiments to determine optimal PEG concentration. A 7.5 mM PEG buffer was found to provide an acceptable rate of reaction.

To measure the rate at which the complexes formed after both the IgG and the A-IgG solutions had been combined, we used an Ocean Optics CHEMUSB4-UV-VIS consisting of a USB4000 spectrometer with a combination deuterium tungsten halogen light source and a 1-cm cuvette holder interfaced with a PASCO Xplorer GLX Graphing Datalogger. This assembly was used to record the absorption measurements of both the zero-G flight data and the 1-G ground-truth data.

Figure 2. Front and inside view of the double-wall Lexan® glove box with two sets of industrial-strength rubber gloves. The glove box is shown with video camera mounting bar and top both removed.

While in flight, the experiment apparatus was housed in a double-walled Lexan® glove box, which allowed access by heavy-duty industrial-style rubber gloves (see figure 2). The immune complex formation (ICF) apparatus was constructed using two 1-mL syringes secured to a wooden piece by a retaining block (see figure 3). Each syringe had a 26-gauge needle secured to it. The two needles punctured a plastic cap that was sealed to a standard CVD-UV plastic 1 cm×1 cm×4.5-cm (4.5-mL) cuvette. The top of each cuvette was secured to the wooden piece by an aluminum retaining strip. Each ICF apparatus was secured vertically onto an ICF holder using industrial style Velcro®. Between each zero-G portion of the parabolas, 1 ICF was removed from the ICF holder and placed within the spectrophotometer. The IgG and A-IgG were mixed into the cuvettes, which contained the PEG buffer solution, on entering the zero-G portion. The 2

syringes were operated simultaneously, massaging the solution twice, and the absorption was recorded over the approximately 20-second zero-G period. We were able to acquire 5 usable runs on the first flight day and 7 usable runs on the second day. There were 2 primary reasons why we did not have more successful data: (1) the primary experiment operator on each day experienced motion sickness within the first 10 parabolas, and (2) the team experienced equipment malfunctions that required valuable flight time to correct.

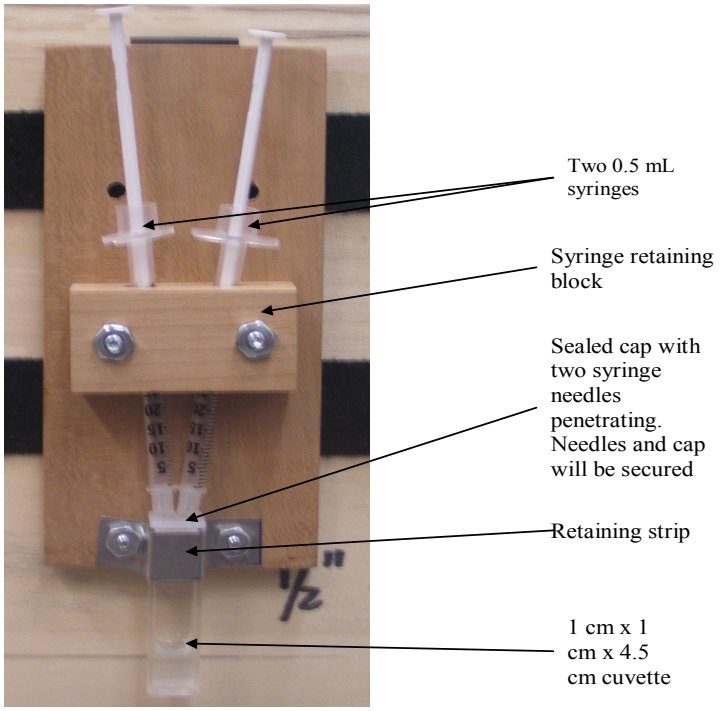

Figure 3. Immune complex formation apparatus.

RESULTS/DISCUSSION

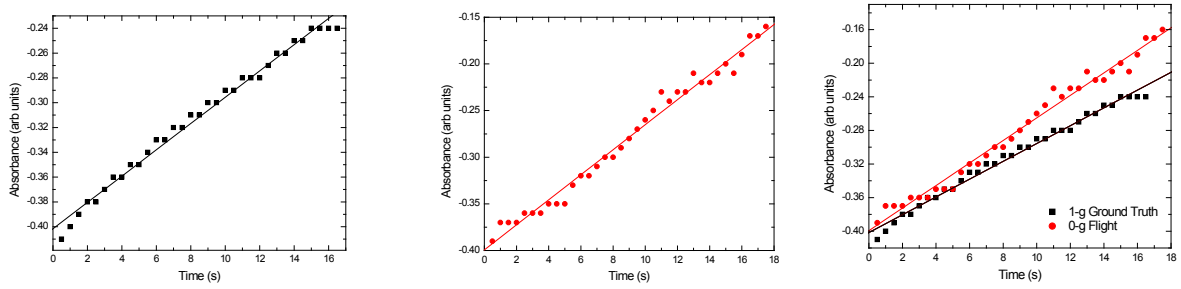

(a) **(b)** **(c)**

Figure 4. Absorbance as a function of time for two typical measurements: (a) 1-G ground-truth sample, (b) zero-G flight sample, and (c) both samples plotted together; (c) clearly shows the difference in absorbance rates measured in the two gravitational fields.

The ground-truth samples were measured in the laboratory postflight using the same equipment, concentrations, and procedures as during the flight. Figure 4(a) shows the absorbance as a function of time for a single representative run from the 1-G ground-truth samples. The start time

shown, set as zero, corresponds to the time period *after* the massaging process. Since the zero-G portion of each parabola was approximately 20 seconds, we only fit the absorbance rate over the same approximate range. The average rate change in the absorbance for all ground-truth data was 0.0101 s^{-1}. Figure 4(b) is a plot of absorbance versus time for a typical measurement made in zero G. The average rate change in the absorbance for all flight samples was 0.0122 s^{-1}. The data shown in figures 4(a) and 4(b) were chosen because their slope is close to the average values quoted above. These same 2 runs are plotted together in figure 4(c).

From figure 4, we see that one of our initial goals was achieved; that is, a reasonable total increase in absorbance over the first 20 seconds of each measurement was achieved. For the 1-G data, we measured an average change in absorbance of 0.19 over an average period of 16.8 seconds. This extrapolates out to a change of 0.23 over a period of 20 seconds. The flight data exhibited an even greater rate, with an average change in absorbance of 0.22 over an average period of 15.5 seconds. This projects out to a change of 0.28 over 20 seconds.

While the slopes of the curves are small values, there is a distinct change. This is convincingly shown in figure 4(c), where the 2 absorbance rates, 1 G and zero G, begin at approximately the same level but clearly diverge, with the zero-G measurements increasing at a faster rate than the ground-truth ones. The average slope value for the zero-G data is almost 21% larger than the average value for the 1-G data.

A concern of the group, when initially looking at the data, was the fact that we obtained negative values for the absorbance. The negative values were obtained during the second flight day and during the ground-truth measurements. We believe that this is due to a calibration error during the initial “dark” and “blank” scans. This has not been verified yet, but we still have confidence in the data since (1) our interest is in the change in the absorbance, not the absolute values; and (2) the data taken on the first flight day, which had positive absorbance values, had approximately the same slope values and changes in absorbance over the periods of interest as did the data with negative absorbance readings.

Overall, the greater slope of the zero-G absorbance data was a surprise to us as we initially expected to find a faster rate of reaction in the 1-G samples. At this time, we are trying to understand the mechanisms that could be responsible for the difference. Our initial conclusion is that the convection currents within the solution, present in the 1-G measurements, act to hinder, rather than enhance, the IgG/A-IgG reaction rate.

CONCLUSION

In this experiment we attempted to investigate the effects of microgravity on the immune system by looking at the binding rates of antigens and antibodies found in the human body. This was accomplished by measuring the absorbance rate of the reaction between human IgG and goat-derived A-IgG in a sodium phosphate buffer. The identical experiment was performed in zero G and 1 G to determine whether there is a gravitational effect on the rate of reaction. Our data clearly show a faster rate of absorbance, and, hence, a faster rate of reaction between the IgG and A-IgG in the zero-G environment versus the 1-G laboratory setting. We are continuing with this line of research and plan to repeat the 1-G measurements in the near future. The team also hopes

to have the opportunity to repeat the zero-G measurements on board the NASA parabolic flight aircraft. In addition to repeating the zero-G data, we hope to make measurements in the 0.38-G, 1.62-G, and 1.8-G environments available to see whether we can confirm our conclusion of a decreased reaction rate in an increased gravitational field.

ACKNOWLEDGMENTS

This research program would not have been possible without the generosity of Dr. Charles Harrington, the UNC Pembroke Provost; The North Carolina Space Grant; and the North Carolina section of the American Chemical Society.

REFERENCES

1. Borchers AT, Keen CL, Gershwin ME. Microgravity and Immune Responsiveness: Implications for Space Travel. *Nutr;* 18:889–898 (2002).
2. Dietrich DL, Ross HD, Shu Y, Chang P, Tien JS. *Comb Sci Tech*; 156:1–24 (2000).
3. Ronney PD. Combustion Phenomena at Microgravity. In: *Physics of Fluids in Microgravity*, ed. by R. Monti, Taylor & Francis Inc., New York, 2001.
4. Sonnenfeld G. The Immune System in Space and Microgravity. *Med Sci Sports Exerc;* 34:2021–2027 (2002).
5. Sonnenfeld G, Butel JS, Shearer WT. Effects of the Space Flight Environment on the Immune System. *Rev Environ Health;* 18:1–17 (2003).
6. Sonnenfeld G, Shearer WT. Immune function during space flight. *Nutrition;* 18:899–903 (2002).
7. Sundaresan A, Risin D, Pellis NR, *J Appl Physiol*; 96:2028–2033 (2004).
8. Wisniak J. *Indian J Chem Tech;* 7:319–326 (2001).

PHOTOGRAPHS

JSC2009EO16490
JSC2009EO16532 to JSC2009EO16530
JSC2009EO16536
JSC2009EO16555
JSC2009EO16570 to JSC2009EO16571
JSC2009EO16629
JSC2009EO16646 to JSC2009EO16647
JSC2009EO16662 to JSC2009EO16665
JSC2009EO16704
JSC2009EO16715 to JSC2009EO16717
JSC2009EO16725
JSC2009EO16754

VIDEO

- Zero-G flight week January 13–16, 2009, Master no.: 734616

Videos are available from the Imagery and Publications Office (GS4), NASA JSC.

CONTACT INFORMATION

Dr. Timothy M. Ritter, Ph.D.
Dept. of Chemistry and Physics
UNC Pembroke,
Pembroke, NC 28372
tim.ritter@uncp.edu

TITLE

Education Outreach Program – Sensorimotor Adaptation to Ambiguous Inertial Motion Cues: Tactile Cueing as a Gravitational Substitute for Spatial Navigation

FLIGHT DATES

January 14–16, 2009

PRINCIPAL INVESTIGATOR

Scott Wood, Universities Space Research Association

CO-INVESTIGATORS

Justin Barba, Texas A&M University
Kara Beaton, Johns Hopkins University
John Cackler, Stanford University
Stephanie Horsfield, Ohio University
Kathryn Montgomery, Rice University
Ji Son, University of California
R. Mercado-Young, Wyle Integrated Science and Engineering Group

GOAL

The purpose of this experiment was to examine how spatial awareness is impaired with changing gravitational cues during parabolic flight, and the extent to which vibrotactile feedback of orientation can be used to help improve spatial awareness.

OBJECTIVES

Our first objective was to examine how spatial navigation was impaired during parabolic flight. We hypothesized that one's ability to report one's orientation and point toward targets around one would be impaired during the microgravity phase of parabolic flight compared to 1-G control trials obtained on the ground. Our second objective was to examine how vibrotactile cueing of down relative to the aircraft improved spatial navigation. We hypothesized that tactile cueing would provide an effective gravitational substitute during the microgravity phase of parabolic flight that would improve spatial navigation ability. A third independent objective was to examine the overall shape of the heart and blood flow velocity in the left ventricle in response to changes in gravitational loading using portable echocardiography. We hypothesized a proportional increase in the sphericity of the left ventricle as a function of G-load.

METHODS AND MATERIALS

Spatial navigation requires an accurate awareness of orientation in one's environment, and then executing the appropriate motor behavior towards locations of interest. In this experiment we assessed spatial navigation by asking subjects to virtually point to remembered target locations around them. Subjects were restrained in a tilted position and placed at random positions ranging from nose up to nose down relative to the plane floor. Once placed in a new orientation, a target position was presented using a virtual-reality video mask. Subjects reported their orientation using verbal reports, and used a handheld controller to point to the desired target location. This spatial navigation task was repeated during the microgravity phases with and without constant tactile cueing of spatial vertical. The tactile cueing used a belt of 8 tactors placed around the mid-torso. The tactors closest to the floor of the plane were activated to indicate which direction was "down". Control measures were obtained during ground-testing so that spatial navigation performance during microgravity with tactile cueing could be compared with 1-G runs without tactile cueing.

Echocardiography measures: The effect of different levels of gravity on the size, shape, and function of the left ventricle was assessed with echocardiography using a 5-1 MHz phased array transducer (Philips Medical CX50, Andover, MA) during microgravity, lunar, and Martian phases of parabolic flight. Apical 4-chamber views and Doppler images were acquired with the subjects in the upright seated position, and images were stored on DVD. Analyses were performed postflight using off-line software (Q Lab, Philips Medical, Andover, MA) to determine left ventricular size and function.

RESULTS

Perceptual errors in verbal reports of position increased with increasing chair displacement without tactile cueing, based on the analysis to date. This is consistent with postflight debriefings in which the subjects indicated difficulty in maintaining spatial awareness for displacements larger than 45 degrees. Interestingly, the perceptual errors during microgravity were not consistently different than those that occurred while performing the task about an upright orientation on Earth. In contrast, perceptual errors of body orientation were negligible when the task was performed about a tilted axis on Earth, or during microgravity with tactile cueing of orientation. The perceptual errors in body orientation were correlated with errors in pointing to virtual targets. There were no significant differences in the time required to point toward the virtual targets across conditions.

Echocardiography measures: There was a close correlation between the circularity of the left ventricle (sphericity in a single plane) and the degree of gravitational force directed caudal to the longitudinal orientation of the body. Ejection time was inversely proportion to gravitational load.

DISCUSSION

Spatial navigation requires an accurate awareness of orientation in one's environment, and then execution of the appropriate motor behavior toward locations of interest (Benson, 2003). On Earth, low-frequency otolith and somatosensory neural activity provides information regarding our orientation relative to gravity. This sensory input is used by the central nervous system to maintain awareness of orientation and movement relative to a stable gravitoinertial reference frame. The absence of this input during microgravity can lead to perceptual illusions (e.g., inversion illusions) and impair one's ability to navigate within an orbiting spacecraft (Aoki et al., 2007). The microgravity phase of parabolic flight sequence provided a unique capability to assess spatial navigation capability without the normal gravity-receptors (e.g., otoliths, somatosensors) that are important for spatial orientation on Earth. We hypothesized that spatial awareness would be impaired during the microgravity phase of parabolic flight. This experiment also tested the extent to which tactile cueing of spatial vertical can be used to substitute for altered gravity-receptor input. The Tactile Situation Awareness System (TSAS) was developed in the U.S. Navy as a means of providing orientation information during altered sensory conditions in both helicopters and fixed-wing aircraft (Rupert, 2000). TSAS consists of a matrix of electromechanical tactile stimulators applied on the torso that can be used to convey orientation cues to the skin, such as an individual's position relative to gravity. We hypothesized that tactile cueing will provide an effective gravitational substitute during the microgravity phase of parabolic flight that will improve spatial navigation ability.

Our results demonstrated increased perceptual errors of tilt orientation and pointing errors during passive motion in microgravity or movements about an Earth-vertical axis, especially when these movements were greater than 45 degrees. In either case, cues from the otoliths and other somatosensory cues of gravitational loading were negligible. This demonstrates the importance of these gravitational sensors for maintaining spatial awareness on Earth, and the risk for losing awareness during transient periods of weightlessness with reduced visual information regarding one's surroundings. The lack of any differences in latency to point to targets was likely due to the

instruction set to perform the task "as quickly and accurately as possible". The perceptual errors of body orientation carried to errors in pointing toward virtual targets without affecting the speed at which subjects navigated to the new orientation.

These perceptual errors were reduced during movement about a tilted axis on Earth, indicating the importance of otolith and other somatosensory cues for maintaining spatial awareness. Since the perceptual errors were similarly reduced during microgravity trials with tactile cueing, the results are consistent with our hypothesis that vibrotactile cueing of down relative to the aircraft improves spatial navigation.

CONCLUSION

These results indicate that tactile cueing may improve navigation in operational environments, such as EVAs on a lunar surface. This type of sensory feedback may also prove beneficial as a navigation aid in patient populations, providing non-visual, non-auditory feedback of orientation or desired direction heading.

REFERENCES

1. Aoki H, Oman CM, Natapoff A. Virtual-reality-based 3D navigation training for emergency egress from spacecraft. *Aviat Space Environ Med*; 78:774–783, 2007.
2. Benson AJ. Spatial disorientation - general aspects. In: Ernsting J, Nicholson AN, Rainford DJ (eds) Aviation Medicine. Arnold, London, pp. 419–436, 2003.
3. Rupert AH. Tactile situation awareness system: proprioceptive prostheses for sensory deficiencies. *Aviat Space Environ Med;* 71:A92–99, 2000.

PHOTOGRAPHS

JSC2009EO16555 to JSC2009EO16556
JSC2009EO16563 to JSC2009EO16566
JSC2009EO16574
JSC2009EO16578 to JSC2009EO16579
JSC2009EO16591 to JSC2009EO16593
JSC2009EO16615 to JSC2009EO16515
JSC2009EO16620 to JSC2009EO16622
JSC2009EO16630 to JSC2009EO16632
JSC2009EO16635 to JSC2009EO16637
JSC2009EO16649 to JSC2009EO16649
JSC2009EO16655 to JSC2009EO16658
JSC2009EO16736 to JSC2009EO16739
JSC2009EO16744 to JSC2009EO16749

VIDEO

- Zero G flight week January 13–16, 2009, Master no.: 734616

Videos are available from the Imagery and Publications Office (GS4), NASA JSC.

CONTACT INFORMATION

Scott J. Wood
NASA Lyndon B. Johnson Space Center
Mail Code: SK
Houston, TX 77058
Mail Code: SK
281-483-7294
scott.j.wood@nasa.gov

TITLE

Education Outreach Program – Transpiration Rate in Reduced Gravity

FLIGHT DATES

January 15–16, 2009

PRINCIPAL INVESTIGATOR

Collin Witherspoon, Amarillo College

CO-INVESTIGATORS

Tina Lewis, Sam Houston Middle School, Amarillo, TX
Chris Sanders, Cinco Ranch High, Katy, TX
Richard Hobbs, Amarillo College, Amarillo, TX
Jeremy Hart, NASA Johnson Space Center, Houston, TX
Deborah Hutchings, San Jacinto College, Houston, TX

GOAL

The primary goal for this experiment was to measure the transpiration rate of a plant in a zero-G environment and determine if the rate differs from that in a 1-G environment.

OBJECTIVES

The objectives for this experiment were to measure plant transpiration in zero-G, 1/6-G (lunar), and 1/3-G (Martian) reduced-gravity environments by means of relative humidity (RH) and use these measurements to determine the transpiration rate.

METHODS AND MATERIALS

A plant transports water from its root system to other parts of the plant through a process called transpiration. If a root is sitting in a solution containing inorganic ions and water, the root cells will pump the ions into the xylem, producing a hypertonic solution inside the xylem. The cell walls of the plant are permeable to water and, due to the newly formed concentration gradient between the xylem and its exterior, water moves into the xylem by osmosis. The water in the xylem is pushed up a short distance by root pressure, but the primary mode of transportation is transpiration. Transpiration occurs when a water molecule leaves the leaf through a stoma. The cohesion of water molecules, by hydrogen bonding, forms a chain of water molecules from the stomata, through the xylem, down to the root system. A concentration gradient forms between the inside of a leaf and the surrounding air when the leaf contains more water than the air. When a stoma opens, a water molecule will be pulled off from the chain due to diffusion. The tension caused by this pulls the other water molecules in the chain up through the xylem. The question addressed in this experiment was whether gravity affects the rate of transpiration.

The experiment was performed using the transpiration chamber shown in figure 1. The chamber is constructed with 4 separable parts: the lower chamber, the inner chamber, the upper chamber, and the chamber attachment.

Figure 1. Transpiration chamber.

The lower chamber is a rectangular polyethylene container (4.75 in×4.625 in×7.25 in) glued to a rectangular acrylic board (15 in×10 in×0.1875 in). A TI-84 calculator (used as a data logger) was

attached to the board using Velcro®. The inner chamber is a cylindrical-polyethylene container (3 in×5.5 in). A one-hole rubber stopper is sealed into its neck using silicon caulking. The upper chamber is a rectangular polyethylene container (5.5 in×5 in×10 in). A Vernier RH sensor is pushed through a 1-hole rubber stopper and into a hole in the top of the container. A battery-powered electric fan is sealed into a hole on the left side of the container using silicon caulking, and a removable solid rubber stopper is in a hole on the right side. The chamber attachment consists of 2 lids fit the lower and upper chambers. The lids are glued top to top, and a 1-hole rubber stopper is sealed into a hole through the lids using silicon caulking.

The plant was pushed through the rubber stopper in the chamber attachment and the rubber stopper in the inside chamber. Silicon caulking and duct tape were used to seal the plant into both stoppers. This process provided double containment of the water in the inside container.

On the first flight (January 15, 2009), we collected RH samples for 18 zero-G parabolas, three 1/6-G parabolas, and two 1/3-G parabolas using the Vernier RH sensor and the TI-84 calculator. Each reduced-gravity portion of a parabola lasted approximately 18 seconds. The following steps were followed for each parabola:

1. If the fan is off, turn it on at the beginning of the reduced-gravity maneuver.
2. Seal the upper chamber with the solid rubber stopper at the beginning of the reduced-gravity maneuver.
3. Start the data log program on the TI-84 calculator. The program was configured to take one sample per second for 18 seconds.
4. At the end of the reduced-gravity maneuver, unseal the upper chamber.
5. Run data transfer program on the calculator to prepare it for the next reduced-gravity maneuver.
6. Turn the fan off if the RH drops too low.

On the second flight (January 16, 2009), we collected RH samples for 18 zero-G parabolas, three 1/6-G parabolas, and six 1/3-G parabolas using the Vernier RH sensor and the TI-84 calculator. Each reduced-gravity portion of a parabola lasted approximately 18 seconds. The fan was never turned off, and the upper chamber was sealed the entire time. The following steps were followed for each parabola:

1. Start the data log program on the TI-84 calculator. The program was configured to take one sample per second for 18 seconds.
2. Run data transfer program on the calculator to prepare it for the next reduced-gravity maneuver.

The changes in procedures from the first to the second flight were due to a change in environmental conditions that were outside of our control.

RESULTS

The change in RH was determined by the difference of final RH and initial RH:

$$R_f - R_i .$$

The change in time was always 18 seconds. The average rate of transpiration was determined by the ratio of change in RH by change in time:

$$ARC = \frac{R_f - R_i}{18} .$$

The following bar graph displays the zero-G trial data obtained on the first flight:

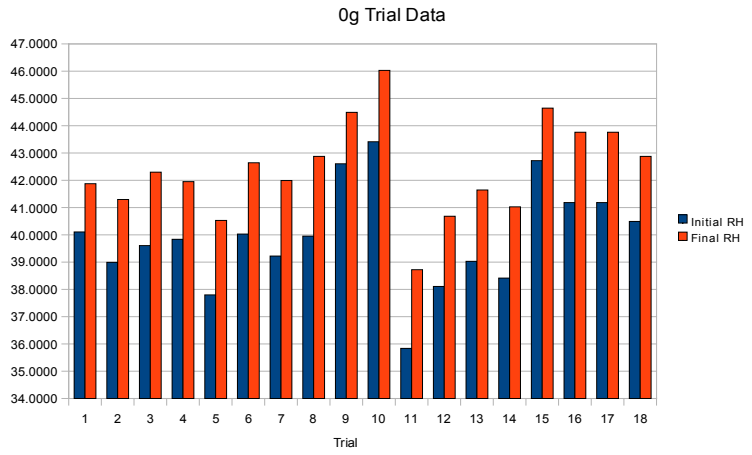

The average rate of change for each trial is shown in the following bar graph:

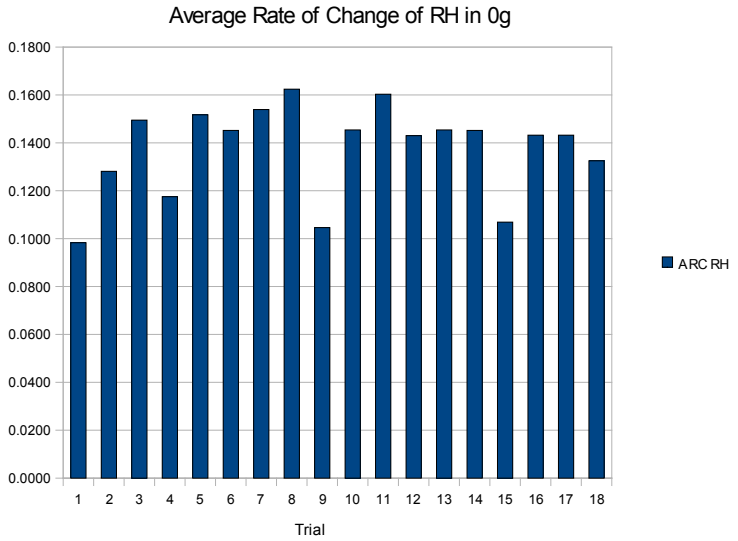

The mean rate of transpiration was 0.1376 ± 0.0190 %RH/sec.

The following bar graph displays the trial data obtained at Ellington Field (1 G) before the first flight:

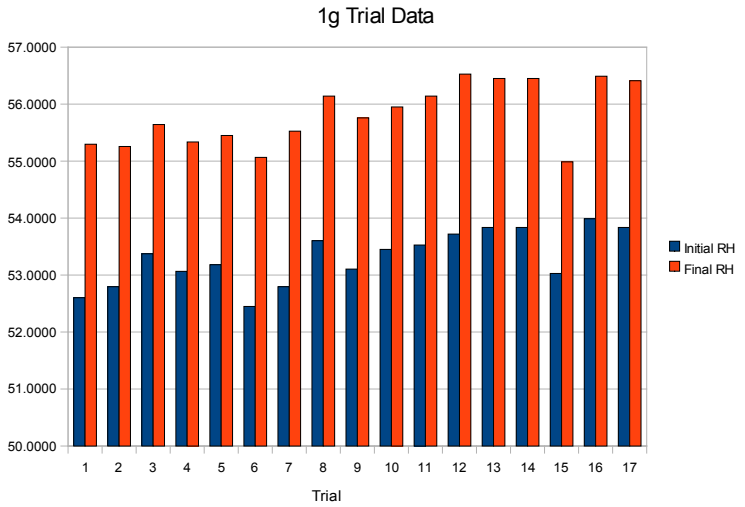

The average rate of change for each trial is shown in the following bar graph:

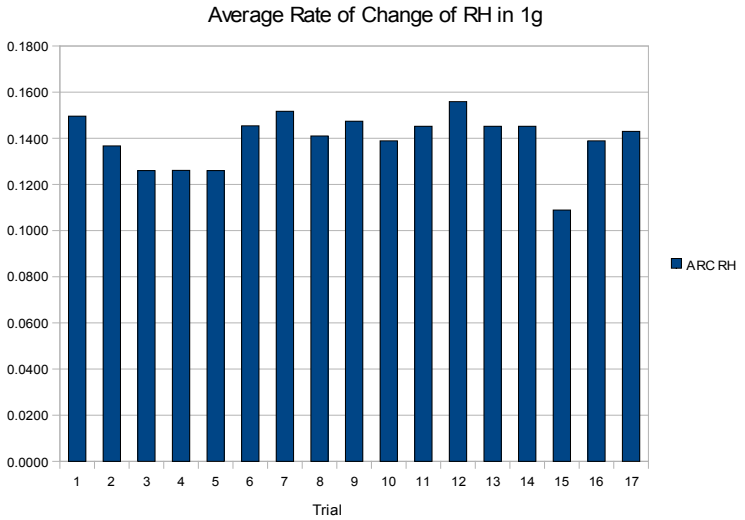

The mean rate of transpiration was 0.13333 ± 0.0193 %RH/sec.

The trial data for lunar and Martian gravity on the first and second flights are shown in the following bar graphs:

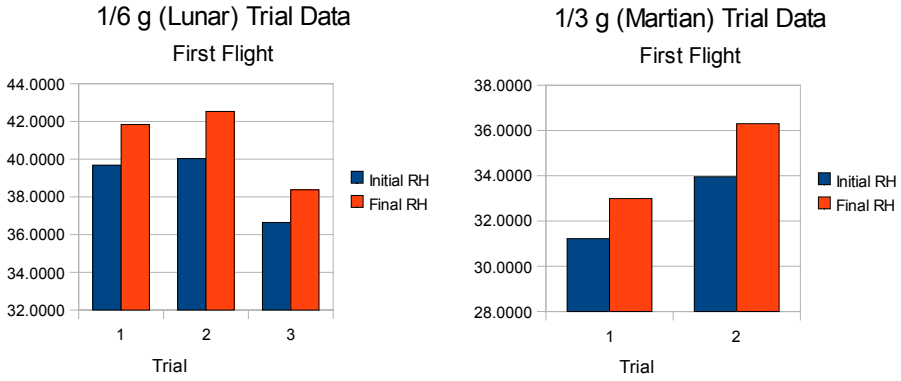

DISCUSSION

We compared the mean rates of change of RH in zero G and 1 G using the trial data obtained during the first flight and the trial data obtained at Ellington Field. We let the null hypothesis be that the average rate of change of RH in zero G is the same as that in 1 G, $H_0 : \mu_0 = \mu_1$. The alternative hypothesis was set up to be $H_a : \mu_0 > \mu_1$. Using a 2-sample t-test, we decided that the null hypothesis could not be rejected at a 95% confidence level.

CONCLUSION

The goal for this experiment was to measure the transpiration rate of a plant in a reduced-gravity environment. Based on our analysis, gravity appears to have no effect on the rate of transpiration within 18 seconds.

REFERENCES

Bibliographic information was not immediately available from investigators**.**

PHOTOGRAPHS

JSC2009E17470
JSC2009E17481 to JSC2009E17483
JSC2009E17504 to JSC2009E17506
JSC2009E17525 to JSC2009E17526
JSC2009E17598
JSC2009E17604 to JSC2009E17605
JSC2009E17637
JSC2009EO18047 to JSC2009EO18048
JSC2009EO18069 to JSC2009EO18070
JSC2009EO18083
JSC2009EO18086
JSC2009EO18132

VIDEO

- Zero G flight week 1/13–1/16/09, Master no.: 734616

Videos are available from the Imagery and Publications Office (GS4), NASA JSC.

CONTACT INFORMATION

Collin Witherspoon, Instructor
Mathematics and Engineering Department
Amarillo College
806-371-5142
fax: 806-345-5571
ccwitherspoon@actx.edu

TITLE

Education Outreach Program – The Effects of Center of Gravity Location on Locomotive Biomechanics: Implications for Spacesuit Portable Life Support System Design

FLIGHT DATES

January 15–16, 2009

PRINCIPAL INVESTIGATOR

Heather Paul, NASA Johnson Space Center

CO-INVESTIGATORS

Melanie Akheeba University of Houston, Clear Lake (UHCL)
Alexandria Burley, UHCL
Amanda Faye Culver, UHCL
Samuel Cyr, UHCL
Stanley Mukundi, UHCL
William Amonette, Faculty Advisor, UHCL

INTRODUCTION

In February 2003, President George W. Bush declared the new vision for the U.S. space program. He directed NASA to refocus its efforts and resources toward Exploration-class missions (Wikipedia, 2003). This vision involves completion of the ISS and retirement of the space shuttle by the year 2010, and the development of new vehicles and hardware to return humans to the Moon by 2020. The U.S. also plans to send humans to Mars. To fulfill this vision, NASA is using lessons learned from previous exploration programs and experience from long-duration missions on the ISS to design systems that will enable safe human exploration in these reduced-gravity environments.

Experience from long-duration spaceflight on board Skylab, the Russian space station Mir, and the ISS demonstrates that exposure to microgravity causes a variety of detrimental physiologic changes to the human body (Baldwin et al., 1996), including loss of bone mineral density, skeletal muscle, and aerobic capacity. After only 4 days of spaceflight, catabolic bone markers are increased (Smith and Heer, 2002), and after 14 days, losses of muscle cross-sectional area occur (Leblanc et al., 1995). Longer-duration exposure to microgravity results in bone remodeling with significant losses of bone mineral density in the weight-bearing areas of bones (i.e., the calcaneus, greater trochanter, femoral neck, and pelvis) (Organov et al., 1997). Losses of muscle mass and neuro-muscular disturbances result in decreases in muscular strength (Baldwin, 1996) and endurance (Hayes et al, 1991). Aerobic capacity is also compromised during spaceflight due to changes in blood volume and aerobic deconditioning (Trappe et al., 2005).

These physiologic changes will be hazardous to humans, especially when working in the reduced-gravity environments of the Moon and Mars. Decreased bone density in weight-bearing bones could result in fractures, which is problematic considering the limited medical support that will be available during these missions. Loss of aerobic capacity, muscle strength, and endurance could inhibit an astronaut's ability to perform EVAs that may require several hours of high metabolic activity.

Space-suit design is a critical element of human space exploration. The challenge of returning humans to the moon by 2020 has necessitated the development of a new space-suit system that will enable efficient and effective movement on the lunar surface during EVA. This space-suit system consists of the pressure garment and life support subsystems, each of which have their own unique design challenges.

Designs for the Portable Life Support System (PLSS) for lunar exploration have gone through several iterations. The focus of recent design efforts has been on packaging the thermal, ventilation, and oxygen subsystem components, with emphasis on mass and volume reduction for the overall architecture, as well as optimization of the center of gravity (CG). Figures 1 and 2 illustrate the PLSS-package design, including overall mass and volume data, as presented to NASA management in April 2008 (Thomas, 2008).

While the safety of the astronaut is of utmost importance in the design of a space-suit system, there is a significant human performance element as well. It is essential to understand the

biomechanical consequences of changing the PLSS-CG location to speculate on the potential for injury and/or the rising metabolic demand associated with each CG location. With previous evidence suggesting that humans lose bone, muscle, and aerobic capacity in microgravity environments, these data will be important to understand the potential forces that could be imparted to the skeletal system during suited EVAs. Additionally, because human physiology adaptations are specific to imposed physical demands, it may be necessary for crewmembers to perform locomotive exercise with simulated gravitational force acting on their bodies to prepare for work on the surface of the Moon and Mars while in transit to these destinations.

Therefore, the proposed research quantified the effect of varying CG location of the PLSS on locomotive biomechanics in lunar and Mars reduced-gravity environments. Comparisons were also made of the lunar and Mars data to microgravity test conditions in which CG was also varied, but resistance bands with a force equivalent to 1/3 G and 1/6 G times the subject's body weight were attached to the test subject and test equipment.

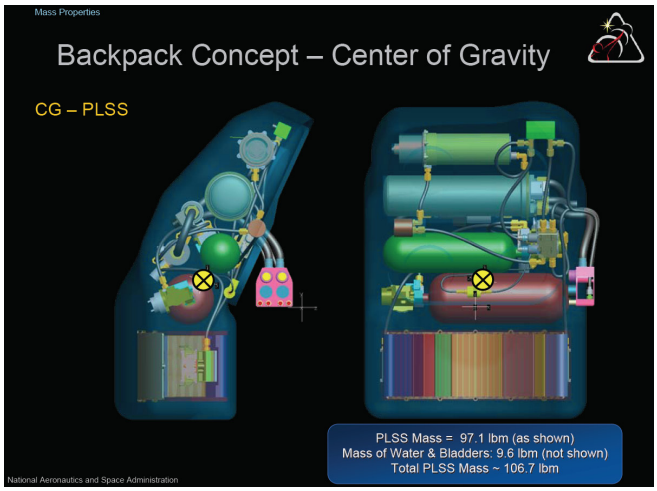

Figure 1. Location of PLSS CG and total PLSS mass in 1 G.

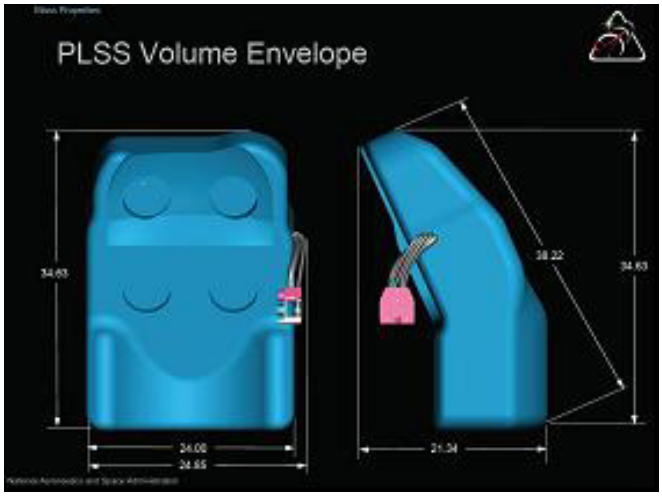

Figure 2. PLSS volume envelope.

Experiment Description

The primary purpose of this research was to quantify the biomechanical responses for 2 PLSS-CG locations at a 0% incline on a treadmill (Life Fitness 95Ti) in the reduced-gravity environment. The secondary purpose of this investigation was to quantify the biomechanics in microgravity with a resistance force equal to 1/3 G and 1/6 G while altering CG location for comparison to the lunar and Mars parabolic conditions.

A backpack, the "PLSS simulator" (figures 3 and 4), designed to simulate the total lunar volume of the PLSS, was worn by a test subject walking on a treadmill. Six weight bags (figure 5) were placed in the back and left pockets of the PLSS simulator to represent a CG offset to the respective location. Reflective markers were attached to the test subject's knees, ankles, and neck with double-sided tape. A camera videotaped the test subject's movement during parabolic flight; the resultant video was used for postflight evaluation of hip and knee joint angles. By varying the CG and evaluating the biomechanical changes, this research will help NASA make smarter design decisions for future development of the PLSS package. It may also provide input concerning the potential harmful effects of changing CG location during ambulation.

Figure 3. PLSS simulator: side view, back view, and front view.

Figure 4. PLSS simulator on test subject.

Figure 5. Weight bags for CG loading.

Hypotheses

This research quantified the effect of changes in the location of the CG of the PLSS on a test subject's movement at the trunk and lower extremities. The normal CG location is in line with the shoulders, hips, and knees when standing straight, and is typically located near a person's navel. When wearing a backpack, however, the CG shifts posterior, causing the person to alter biomechanics to compensate. Most guidelines indicate that backpacks should be packed such that the CG stays low and close to the hips, but with space-suit-PLSS design that may not be possible due to packaging constraints associated with enclosing heavy, large life-support components in a sturdy frame. In this test, since the weight of the simulated PLSS remained constant, the variation of the CG location may cause the test subject to compensate with altered biomechanics while walking on the treadmill. In addition, it was expected that the reduced-gravity environment would cause the test subject to compensate to a greater degree compared to 1-G testing. Finally, we expected that the locomotive biomechanics during treadmill exercise in microgravity with resistance bands to differ from the same exercise conditions in lunar and Mars parabolic flight.

Experiment Methods

During the reduced-gravity flight, biomechanics were measured for 2 CG locations at a treadmill incline of 0%. The 2 CG locations (back and left) were selected based on results from the UHCL 1-G testing conducted in the autumn of 2008. The 1-G testing evaluated 7 CG locations [center (unweighted PLSS simulator), top, bottom, left, right, front, and back]. The treadmill walking speed was set to 1.8 mph, which was the average walking speed that would have been required if the rover failed over 6 miles from the habitat and the crewmembers had needed to walk back during the Apollo missions.

The test subject wore tight-fitting clothing (i.e., compression tights, a sports top, and athletic shoes) that did not restrict body movements during testing. Reflective markers were attached to the test subject via double-sided tape bilaterally at the following locations: lateral malleolus, knee joint line, tibial tuberosity, and neck.

While wearing a backpack designed to simulate the total lunar volume of the PLSS, the "PLSS simulator", the test subject walked on a treadmill at 1.8 mph during parabolic maneuvers. The CG location of the subject was altered by repositioning the mass within the PLSS simulator via weight bags. Video data were collected continuously during ambulation by 1 video camera on the left side of the treadmill. Video footage was evaluated postflight using 2-dimensional motion capture software (Dartfish). The software was used to analyze the collected video data by comparing joint kinematics across the different CG and resistance levels.

During the microgravity parabolas, the subject was tethered to the treadmill using modified surgical tubing resistance bands. Prior to flight, load cells were used to determine the length of tubing necessary to create a force equal to 1/6 and 1/3 times the subject's body weight. The data collected during the microgravity parabolas were compared to the lunar and Mars parabolas, where the test subject was untethered.

Real-time data collection from the test subject also included rating of perceived exertion (figure 6). These values were used to analyze the qualitative effects of varying CG for each test subject at each test condition.

Exertion	Rating
	6
Very, very light	7
	8
Very light	9
	10
Fairly light	11
	12
Somewhat hard	13
	14
Hard	15
	16
Very hard	17
	18
Very, very hard	19
	20

Figure 6. Borg RPE scale (Adams and Beam, 2008).

RESULTS/DISCUSSION

Results of this research have been subdivided into 5 research areas, resulting in 4 abstracts for the 2009 UHCL 14th Annual Student Conference for Research and Creative Arts and 1 poster presented at the 2009 American Society of Exercise Physiologists (ASEP) national conference in Tyler, Texas. The following sections provide these results.

Research Area 1

Lower-extremity Kinematics in Terrestrial and Simulated Lunar Conditions

Purpose: The purpose of this research was to quantify lower-extremity and trunk biomechanics during terrestrial and simulated lunar ambulation with 2 center-of-mass (COM) locations.

Hypotheses:

1. When ambulating on a treadmill in simulated lunar gravitational conditions, stride length is increased compared to ambulation on Earth.
2. Shifting the COM to the back results in an increased knee and trunk angle in lunar gravitational conditions compared to Earth.
3. Shifting the COM to the side does not alter knee or trunk angle in lunar gravitational conditions compared to Earth.

Methods: Stride length was measured at left heel strike, and knee and trunk angles were analyzed during the mid-stance phase of gait using 2-dimensional motion capture software. Differences in means and effect sizes (Cohen's d) were calculated. Large differences were observed in the knee angles (0.63 deg, d=0.20) and trunk angles (14.70 deg, d=1.57) when comparing Earth gravity (Eg) and lunar gravity (Lg) in the back COM condition. Differences were observed for the left COM: knee angle (5.49 deg, d=1.11) and trunk angle (8.60 deg, d=1.40). Variations were also observed in stride length under both conditions: back (0.10m, d=1.45) and left (0.17m, d=2.12).

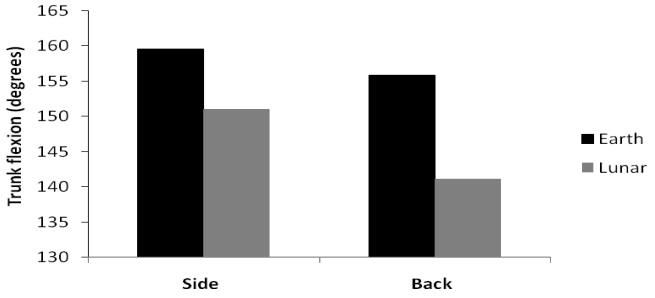

Figure 7. Trunk flexion angle at mid-stance phase.

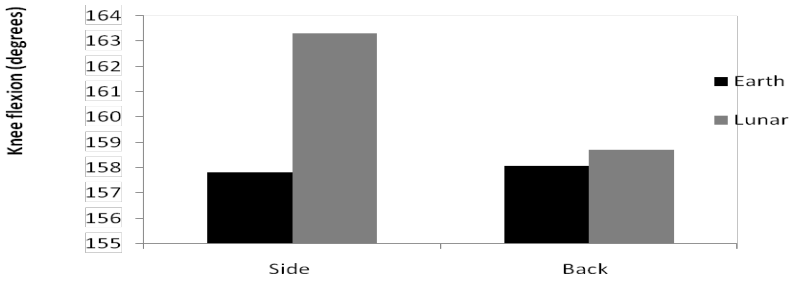

Figure 8. Knee flexion angle at mid-stance phase.

Figure 9. Variation in stride length.

Table 1. Differences in Stride Length, Knee Angle, and Trunk Angle in Simulated Lunar and Earth Gravitation Conditions

		Earth (Eg)	Lunar (Lg)	Difference	Cohen's d
Stride Length	Side	0.18 m	0.35 m	0.17 m	2.12
	Back	0.22 m	0.32 m	0.10 m	1.45
Knee Angle	Side	157.83°	163.32°	5.49°	1.11
	Back	158.07°	158.70°	0.63°	0.20
Trunk Angle	Side	159.60°	151.00°	8.60°	1.40
	Back	155.80°	141.10°	14.70°	1.57

Conclusion: These data indicate that when the COM is shifted to the left, there are large differences between Lg and Eg conditions. This suggests that NASA should ensure that the COM of the PLSS is positioned in line with the sagittal plane for the safety of the astronaut. Although an off-center design is not likely, the PLSS could shift during ambulation if it is not securely fastened to the pressure garment.

Under simulated lunar conditions, the increase in trunk angle was observed with the COM positioned to the back. This is likely a strategy aimed at maintaining balance while preserving velocity. Minimal differences were observed between the Lg and Eg conditions for knee angle with the COM shifted to the back. These differences are not substantial and would likely have no effect on the performance of the mission.

Research Area 2

Differences in Lower Body Biomechanics in Simulated Lunar and Martian Gravity and in Zero Gravity with Bungee Cords

Purpose: The purpose of this experiment was to measure the lower body biomechanics in simulated lunar and Martian conditions, and in zero gravity with bungee cords equal to the lunar and Martian gravitational vectors.

Hypothesis: There will be no difference in stride length, knee angle, and hip angle between the simulated bungee and actual conditions.

Methods: While walking in a microgravity environment simulated by parabolic flight, 2 test subjects were tethered to a treadmill by surgical tubing with a force equal to lunar gravity (Lg=1.6 m/s^2 BLg) and Martian gravity (Mg=3.7 m/s^2 BMg). These data were compared to the gait pattern in actual lunar (L) and Martian (M) conditions created by flight parabolas with differing trajectories.

Results: Mean data from the actual and simulated conditions were compared using effect size calculations (Cohen's d). Large effect sizes were observed for stride length in the BLg versus the actual L environment (d=1.36). Stride length in MMg and the actual M environment (d=0.92)

also demonstrated a large effect size. Minimal effect sizes were BLg for knee angle and that of L (d=0.11). When comparing BMg M, small effect sizes were observed (d=0.22). Measurements of hip angle for simulated BLg L (d=0.33) showed moderate effect size between conditions. Effect size comparisons of hip angle between BMg and M were moderate (d=0.57).

Effect Size Calculations		
Effect size: 0.01-0.29	0.30-0.69	0.70+
Stride Length		
1/6 versus lunar	1.3613530581585045	Large
1/3 versus Mars	0.9154434088701604	Large
Knee Angle		
1/6 versus lunar	0.10938089257489779	Small
1/3 versus Mars	0.22287100868595375	Small
Hip/Trunk Angle		
1/6 versus lunar	0.3282243184602572	Medium
1/3 versus Mars	0.5658896087151467	Medium

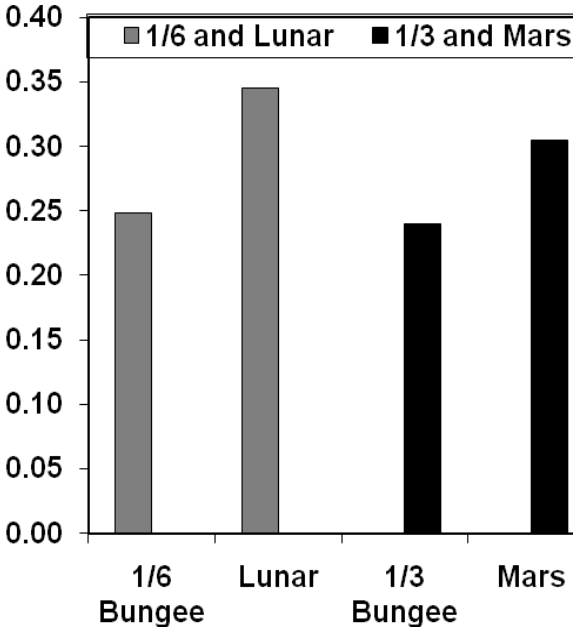

Figure 10. Stride length differences for simulated versus actual lunar and Mars gravity conditions.

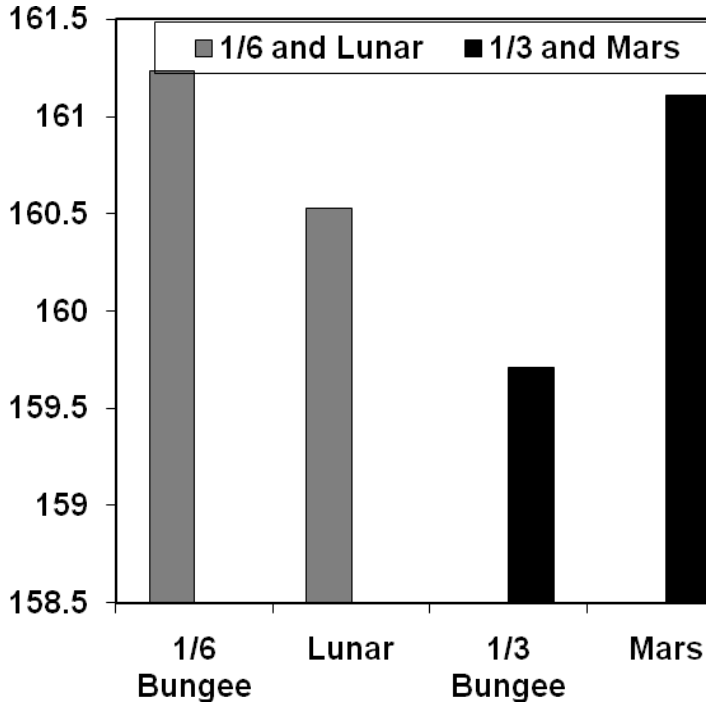

Figure 11. Knee angle differences for simulated versus actual lunar and Mars gravity conditions.

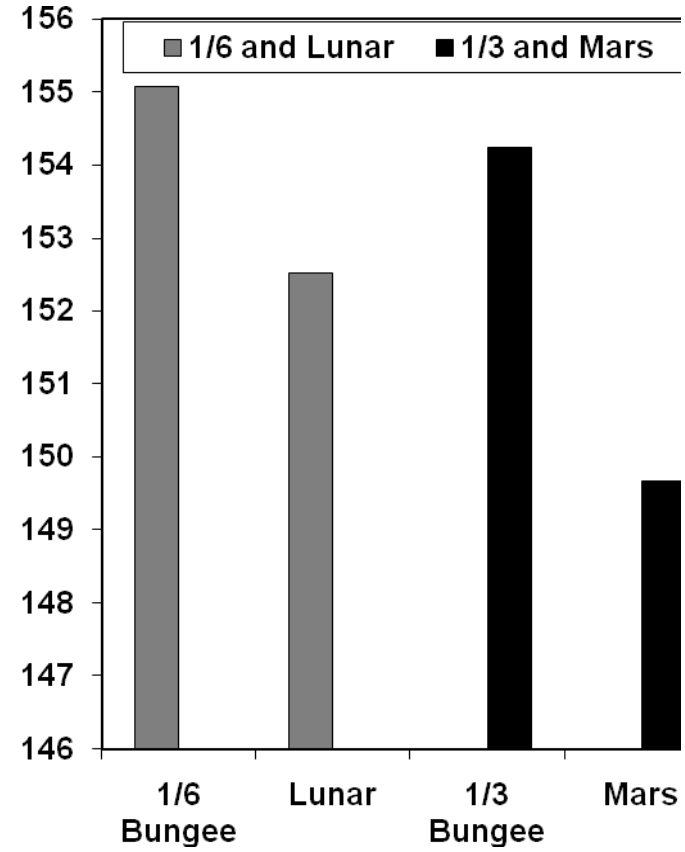

Figure 12. Trunk angle differences for simulated versus actual lunar and Mars gravity conditions.

Conclusion: These data indicate that gait patterns of stride length are most affected by different gravitational pulls. Effect size varied from small to large, depending on the measurement points. Small effect size was shown in the stride length. Medium effect size was shown in the trunk angle. Large effect size was shown in knee angle measurements. Error in effect size may be due to the precision required to calculate the correct weight and tension ratio of the simulated bungee. Scientists should investigate different types of bungee material, or a different method of construction should be investigated when developing the bungee weights. A balance of precise calculations and superior bungee material will reduce the effect size difference for future studies.

Research Area 3

Biomechanical Effects of COM Redistribution to Walking Kinematics in Bungee Simulated Lunar and Martian Conditions

Purpose: The purpose of this study was to determine whether CG changes while wearing bungees to simulate lunar or martian gravity within a microgravity environment affects lower body and trunk biomechanics.

Hypothesis: Movement of CG while wearing the bungees to simulate gravity would have minimal effect on lower-extremity biomechanics.

Methods: The mean knee angle, trunk angle, and stride length for the 3 conditions (CCOM, LCOM, and BCOM) were compared using effect size calculations (Cohen's d).

Results: Compared to the CCOM condition, minimal differences were observed in the knee angle for BCOM (d=0.05) and LCOM (d=0.16) conditions at bungee simulated Lg. In simulated Mg, BCOM (d=0.31) and LCOM (d=0.18) were minimally different. Moderate variations were observed in the hip angle for BCOM (d=0.79) and LCOM (d=1.15) for Lg and BCOM (d=0.44) and LCOM (d=0.69) for Mg compared to CCOM. Finally, moderate differences were observed for stride length at Lg: BCOM (d=0.60) and LCOM (d=0.97) and Mg; BCOM (d=0.90) and LCOM (d=0.91). When comparing LCOM to BCOM, the differences were negligible.

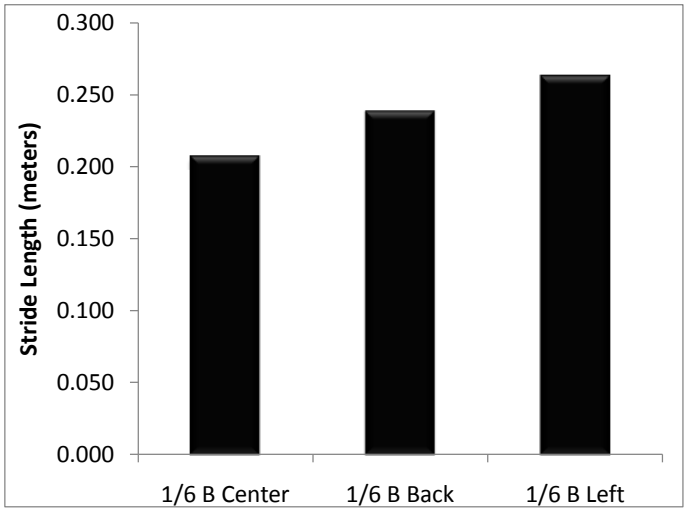

Figure 13. Stride length with 1/6 bungee.

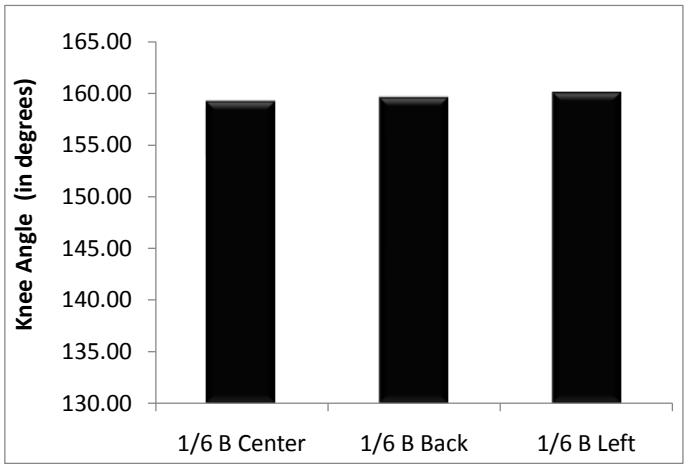

Figure 14. Knee angle with 1/6 bungee.

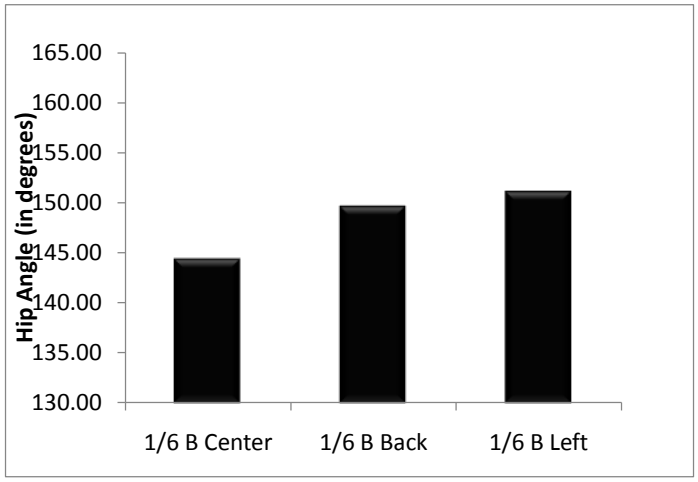

Figure 15. Hip angle with 1/6 bungee.

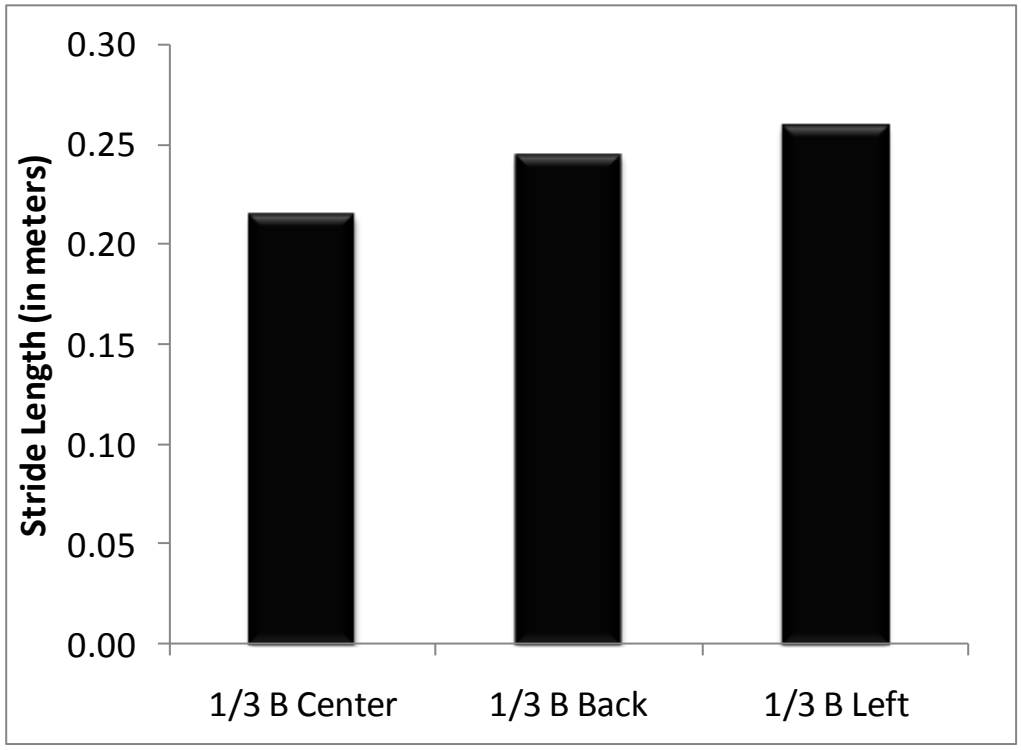

Figure 16. Stride length with 1/3 bungee.

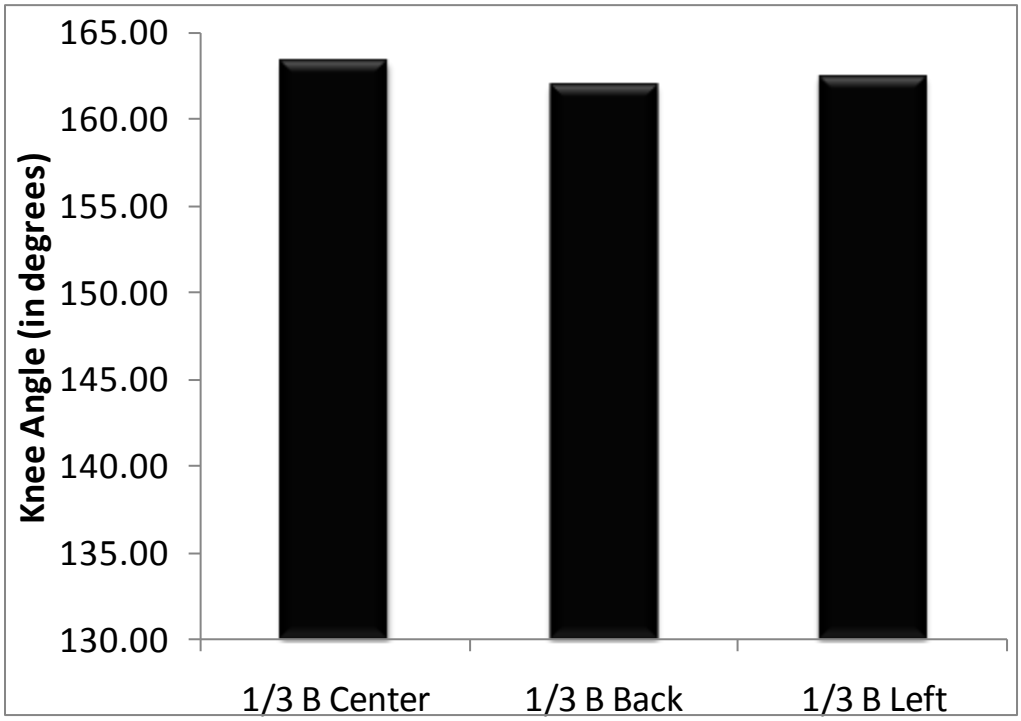

Figure 17. Knee angle with 1/3 bungee.

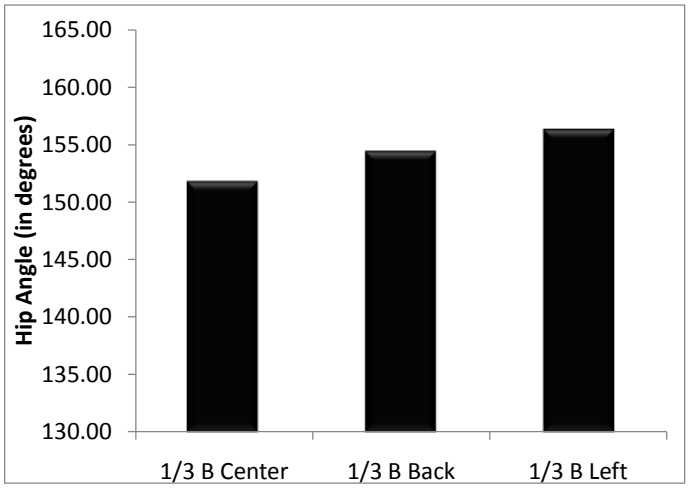

Figure 18. Hip angle with 1/3 bungee.

Conclusion: The data suggest that changing the COM of the PLSS under reduced-gravity conditions using bungees to simulate lunar and martian gravity alters biomechanics. More

research is warranted to determine the biomechanical impact of COM redistribution in these unique environmental conditions.

Research Area 4

Lower-extremity Biomechanics in Zero Gravity with Elastic Resistance

Purpose: The purpose of this research was to compare the walking kinematics in zero gravity using surgical tubing with static forces equal to 1/3 Earth gravity and 1/6 Earth gravity to normal walking kinematics on Earth.

Hypothesis: Simulated lunar and Martian gravitational conditions will result in altered kinematics compared to normal Earth gravitational conditions. Increases in stride length will also result in smaller knee and hip angles.

Methods: Lower-extremity and trunk kinematics were measured using motion-capture software (Dartfish). Effect size (Cohen's d) was calculated to determine differences between conditions. Additionally, Pearson's correlations were calculated to determine relationships between stride length and knee and hip angles.

Results: Large variations were observed between knee angles in Eg compared to Lg (d=0.83) and Mg (d=0.99). The differences in knee angle between Lg and Mg were negligible. For hip angle, large differences existed between Eg and Lg (d=3.40) and Eg and Mg (d=2.88); the differences between Mg and Lg (d=0.61) were moderate. Stride length differed between Eg and Lg (d=0.63) and Eg and Mg (d=1.16). Moderate differences were also observed between Lg and Mg (d=0.33). Stride length correlated poorly to knee (r=0.09) and hip angle in Lg (r=0.22). Moderate correlations were present between stride length (r=0.31) and knee and hip angle (r=0.30) in Mg. Using surgical tubing to create static forces similar to Lg and Mg significantly changes lower-extremity kinematics. The differences appear greater during the Mg conditions. Small to negligible differences were observed when comparing the Lg and Mg conditions. The variance observed in knee and hip angle during Lg cannot be explained by a change in stride length. The changes in stride length during Mg appear to have a greater impact on knee and hip angle.

Conclusion: Due to the significant changes in biomechanics with surgical tubing, scientists may want to explore other methods of tethering the astronaut to the treadmill in zero-G environments.

Research Area 5

Interrater Reliability of Lower-extremity and Trunk Kinematics Using a Two-dimensional Motion Capture Software

Purpose: Biomechanical analysis is an important subcomponent to understanding human performance. Two overall branches of biomechanics are kinematics and kinetics. Kinematics describes joint position, displacements, velocities, and acceleration irrespective of force, while kinetics measures the forces that cause human movement. To measure kinematics, cameras are used to record motion and software quantifies the positions, displacements, velocities, and accelerations. Sophisticated systems can calibrate 3-dimensional coordinates of markers in space, but they are impractical for many research environments. Dartfish is a 2-dimensional, motion-capture software that uses standard video cameras to record movement. It allows the user to analyze

performance using built-in measurement tools. However, there may be significant measurement error between individual raters.

Hypothesis: Therefore, the purpose of the research was to quantify the inter-rater reliability and standard error of mean (SEM) of 2-dimensional motion capture using Dartfish.

Methods: Four raters independently measured the knee and trunk angles and stride length during the mid-stance phase of gait in all conditions using Dartfish. These raters entered the data into an Excel® spreadsheet and were blinded to the scores of the other 3 raters. After all analyses were made, the principal investigator compiled the data into a single spreadsheet. SPSS 16.0 statistical software was used to calculate Cronbach's α on each dependent variable: knee angle, trunk angle, and stride length. SEM was calculated for each variable using the test standard deviations and α values. The mean knee angles for raters 1, 2, 3, and 4 were 161.04 deg ± 5.75, 161.34 deg ± 6.12, 161.21deg ± 5.89, and 161.12 deg ± 6.43; respectively. Interrater reliability for knee angle was high (α=0.96, SEM=1.48 deg). Minimum trunk angle measurements ranged from 128.6 to 134.5 deg between raters; the maximum values ranged from 166.6 to 170.6 deg (α=0.94, SEM=1.86 deg). Stride length measurements were also highly reliable (α=0.99, SEM=0.007 m) between rater 1 (0.26 ± 0.08 m), rater 2 (0.27 ± 0.08 m), rater 3 (0.26 ± 0.07 m), and rater 4 (0.26 ± 0.07 m).

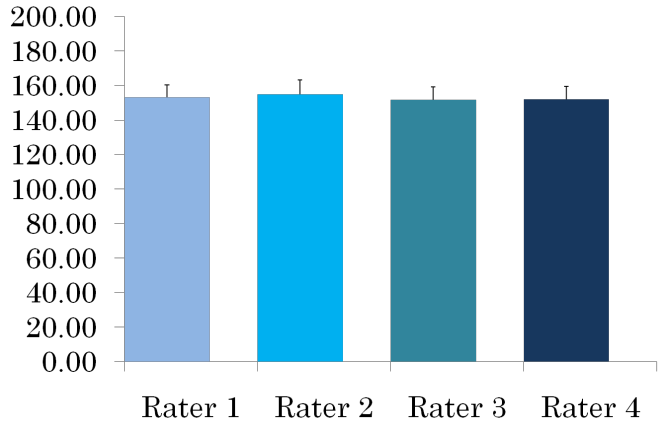

Figure 19. Variations of trunk angle measurements between raters.

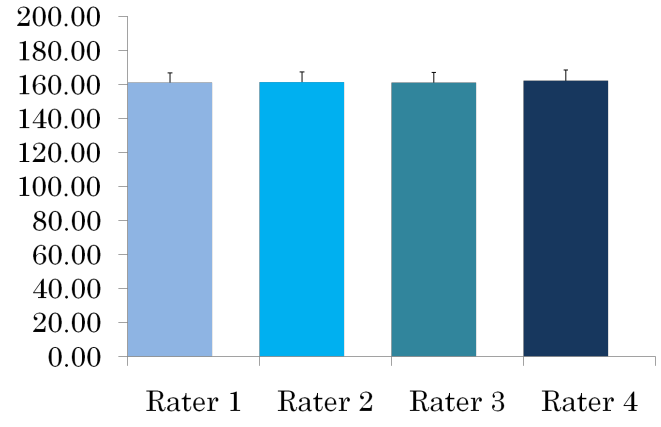

Figure 20. Variations of knee angle measurements between raters.

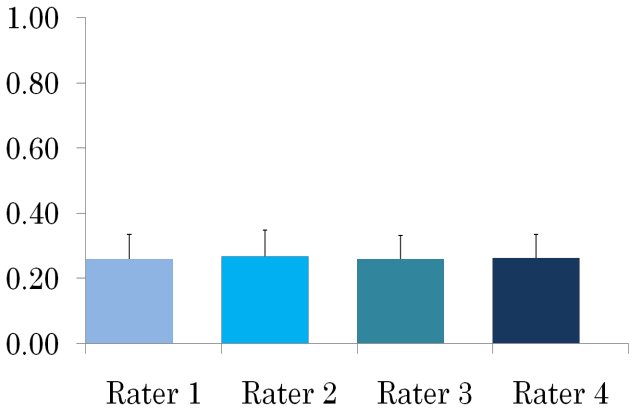

Figure 21. Stride length averages of the raters.

Conclusion: These data suggest that kinematic measurements are highly reliable between raters using the Dartfish software. The greater α values for knee and trunk angle were likely due to slight differences in the interpretation of the vertex and endpoints of the angles. Using the reported SEMs, scientists, and practitioners can be confident that measurement values obtained by different individuals are similar.

CONCLUSION

Flying on the ZERO-G® aircraft provided a unique environment in which to evaluate the effects of changing CG on locomotive biomechanics. Several lessons were learned from this experiment. Future research should include more test subjects, if possible, to provide a better representation of subject variability, and so that statistical evaluations can be conducted. Camera placement is critical, and, if possible, future research should ensure that the video camera is placed perpendicular to the sagittal plane of the test subject.

The challenge of returning humans to the moon involves the development of new spacesuit systems to enable efficient and effective movement on the lunar surface during EVA. This project determined that CG position affects locomotive biomechanics in reduced-gravity environments. These preliminary results indicate that it is essential to understand the biomechanical consequences of changing the PLSS-CG location to speculate on the potential for injury and/or the rising metabolic demand associated with each CG location. More research is also warranted to determine whether locomotive exercise in transit to the Moon and Mars is warranted, and, if so, what method of tethering is best to simulate gravitational force.

BIBLIOGRAPHY

1. Wikipedia. 23 Aug 2008: http://en.wikipedia.org/wiki/vision_for_space_exploration.
2. Baldwin KM., White TP, Arnaud SB, Edgerton VR, Kraemer WJ, Kram R, Raab-Cullen D, Snow CM. Musculoskeletal adaptations to weightlessness and development of effective countermeasures. *Med Sci Sports Exerc;* 28:1247–1253 (1996).
3. Smith SM, Heer M. Calcium and bone metabolism during space flight. *Nutrition;* 18:849–852 (2002).

4. Leblanc A, Rowe R, Evans H, Hendrick T. Regional muscle after short duration spaceflight. *Aviat Space Environ Med;* 66:1151–1154 (1995).
5. Organov V, Schneider V, Bakulin A, Voronin V, Morgun L, Shackelford A, LeBlanc L, Murashko V, Novikov V. The Future of Humans in Space. 12th Manin Space Symposium, 13 June 1997. Human bone tissue changes after long-term space flight: Phenomenology and possible mechanics.
6. Baldwin K. Effect of spaceflight on the functional, biochemical and metabolic properties of skeletal muscle. *Med Sci Sports Exerc;* 28:983–987 (1996).
7. Hayes JC, Roper, ML, McBrine JJ, Mazzocca AD, Siconolfi SF. Evaluation of skeletal muscle endurance following spaceflight. *Med Sci Sports Exerc;* 23 (1991).
8. Trappe T, Trappe S, Lee G, Widrick J, Fitts R, Costill D. Cardiorespiratory responses to physical work during and following 17 days of bed rest and spaceflight. *J Appl Physiol;* 100:951–957 (2005).
9. Thomas G. Portable Life Support System Design Status Review. Presentation to NASA Management. NASA Johnson Space Center, Houston. Apr 2008.
10. Adams GM, Beam WC. *Exercise Physiology: Laboratory Manual. 5th ed*. St. Louis: McGraw Hill, 2008.

ACKNOWLEDGMENTS

The research team thanks the NASA JSC RGO and Education Office for the amazing opportunity to conduct this research. We also thank our NASA mentor, Heather Paul, our faculty advisor, William Amonette, and Dr. Terry Dupler for their guidance and support throughout this project. Finally, we extend special thanks to Mallory Jennings, the NASA coop who volunteered her time and provided extensive support throughout the project.

PHOTOGRAPHS

JSC2009E17512 to JSC2009E17518
JSC2009E17523
JSC2009E17569
JSC2009E17571
JSC2009E17573
JSC2009E17575 to JSC2009E17576
JSC2009E17581 to JSC2009E17582
JSC2009E17586 to JSC2009E17589
JSC2009E17592 to JSC2009E17593
JSC2009E17613 to JSC2009E17630
JSC2009E175634
JSC2009EO17637
JSC2009EO18086
JSC2009EO18088
JSC2009EO18090 to JSC2009EO18092
JSC2009EO18102 to JSC2009EO18104
JSC2009EO18116
JSC2009EO18265 to JSC2009EO18273

VIDEO

- Zero G flight week 1/13–1/16/09, Master no.: 734616

Videos are available from the Imagery and Publications Office (GS4), NASA JSC.

CONTACT INFORMATION

William Amonette
University of Houston Clear Lake
2700 Bay Area Blvd
Houston, TX 77058

Heather Paul
NASA Lyndon B. Johnson Space Center
Mail Code: EC511
Houston, TX 77058

TITLE

Lab-On-a-Chip Applications and Development Portable Test System:
Testing New Swab System for ISS Operations beyond Expedition 18

FLIGHT DATES

February 24–25, 2009

PRINCIPAL INVESTIGATOR

Jake Maule, BAE Systems
Norm Wainwright, Charles River Labs

OBJECTIVE

Evaluate mixing and dispensing steps of new swab system in microgravity (with some additional tests in lunar and Martian gravity).

INTRODUCTION

The Lab-On-a-Chip Applications and Development Portable Test System (LOCAD PTS) was launched to the ISS aboard STS-116 on December 9, 2006.

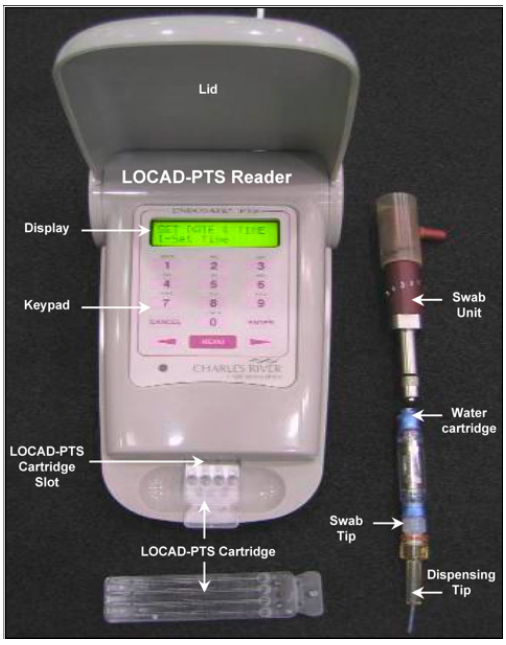

It has been used aboard the ISS during Expeditions 14 through 18 to monitor bacteria and fungi present on cabin surfaces.

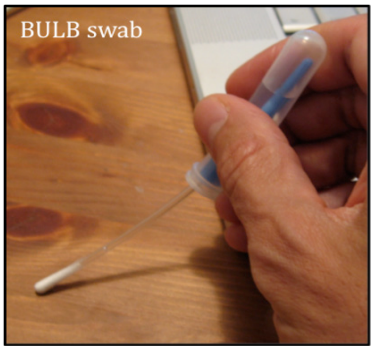

Samples are currently collected from ISS cabin surfaces with the swab system, which consists of the swab unit, water cartridge, swab tip, and dispensing tip.

Relevant Low-G Research to Date: KC-135 and C-9 tests between 2003 and 2009 have shown that the Lab-On-a-Chip instrument and swabbing/mixing steps function nominally in reduced

gravity. The function of all 3 types of LOCAD-PTS cartridge in reduced gravity was verified in April 2007.

METHODS AND MATERIALS

Mixing Tests: Each swab was spiked with 19.5 ng/mL of dye (p-nitroanaline). During zero-G onset, the bulb was snapped, water was squeezed down into the swab tube and was mixed during zero G for either 5 or 10 seconds. The complete volume of the mixed solution was then evacuated to an empty 2-mL Eppendorf tube. The absorbance (at 405 nm wavelength) was then read with a nano-drop spectrophotometer to evaluate the mixing efficiency during microgravity. The mixing process was videotaped and photographed to document the behavior of fluid within the swab tube and the influence of surface tension within the tube, and to determine how these factors affect hydration of the swab tip.

Dispensing Tests: These tests were performed to determine the dispensing accuracy of the BULB swab tool. They were performed with un-spiked BULB swabs. In hypergravity, the Bulb swab was snapped and fluid was squeezed down to the swab tip. At zero-G onset, 4 to 6 droplets were dispensed into 200-mL-volume, polymerase-chain reaction (PCR) tubes (see figure 1). The BULB swab system was positioned just a few millimeters from the rim of each tube, and each droplet adhered to the inside wall of the tube. At hypergravity onset, fluid was pulled down into the tube, after which each tube was capped to contain fluid during subsequent parabolas. The tubes were stored and the volume measured on the ground following landing. The process was repeated in 0.1 G and 0.38 G. All steps were documented by video and photography.

Figure 1. Dispensing droplets into PCR tubes during microgravity. Droplets remained in the tubes because of surface tension and were capped in hypergravity; the volumes were measured on the ground following landing.

RESULTS

Figure 2 shows the average volumes of droplets dispensed with the BULB swab system in 1 G (black columns), Martian gravity (red columns), lunar gravity (grey column), and microgravity (blue column).

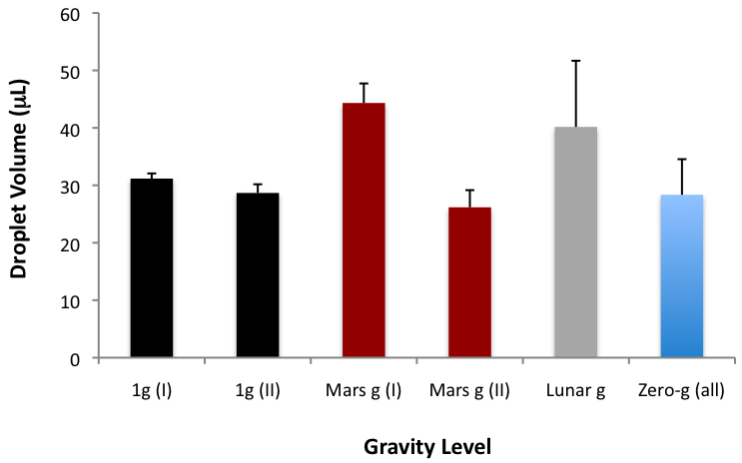

Figure 2. Effect of gravity level on droplet volume of BULB swab unit. Each column represents the average volume of droplets dispensed by the BULB swab unit (error bars = 1 standard deviation). For each 1 G, Mars G, and lunar G column, n=6 droplets were dispensed during one parabola. For the zero-G column, n=150 droplets) were dispensed during 26 separate parabolas.

In addition to gravity level, droplet volumes were dependent on technique used to dispense each droplet. For example, the distance between the pipette tip and the surface to which a droplet was dispensed (e.g., inner wall of a PCR tube or the cup of a sample well) was critical in determining the final droplet volume.

The blue column in figure 2 represents an overall average volume, derived from 150 separately dispensed droplets in zero G. These 150 droplets were dispensed in groups of 4 to 6 droplets during 26 separate parabolas. The average volume of each group of 4 to 6 droplets is shown in figure 3 (with error bar=1 SD). It can be seen from the error bars on each column that the variation in droplet volume in zero G is greater than in 1 G, but can be minimized, especially with the right technique to dispense a droplet at a consistent distance from a surface.

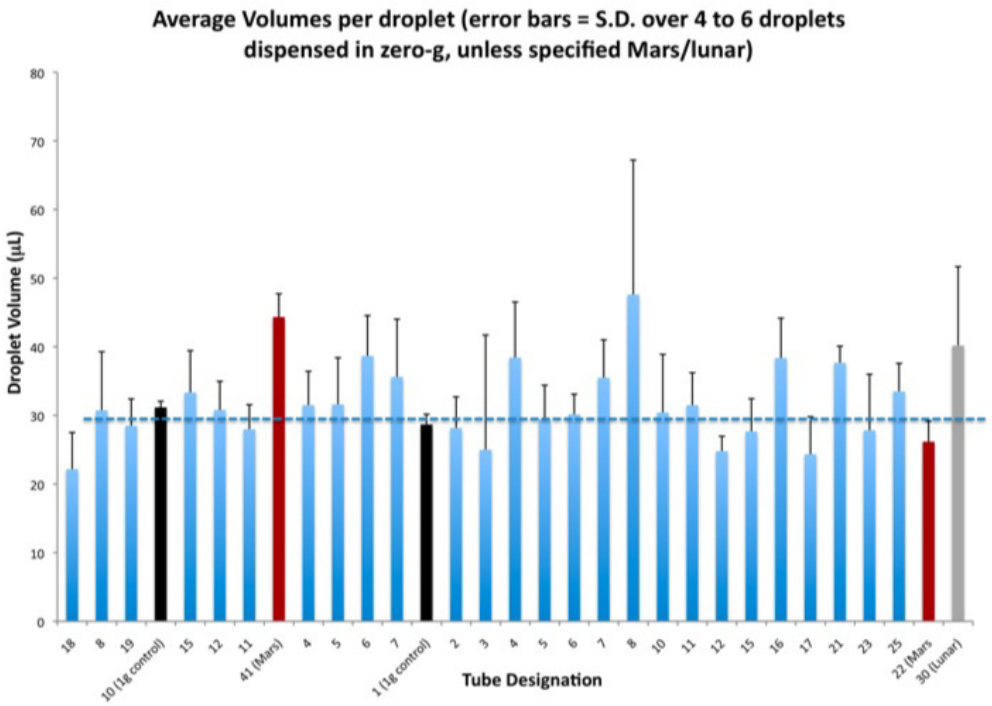

Figure 3. Individual average droplet volumes dispensed with the BULB swab unit. Average volumes are shown for 1 G (black columns), martian gravity (red columns), lunar gravity (grey columns), and zero G (blue columns) with error bar=1 standard deviation.

When a droplet was dispensed far from a surface in zero G, it would grow to almost 10 mm in diameter (see figure 4) before detaching by vibration or other forces imparted to the swab unit. This "droplet growth" could be prevented if the BULB swab pipette tip was positioned within 2 mm to 3 mm of the target surface (see figure 5).

Occasionally, the 1-mL volume in the bulb of the swab unit would pool in the upper portion of the swab tube, and dispensing would be impossible. This was simply rectified by a downward flick to move fluid toward the swab tip. The fluid would then remain at the end of the swab tube (by the swab tip) due to surface tension within the swab tube. Dispensing could then proceed.

On other occasions, on removal of the white end cap, fluid would stream out of the tip without any manual pressure on the bulb. This may have been due to built-up pressure in the bulb relative to the aircraft cabin (maintained around 8,000-feet-equivalent; note that ISS is sea-level-equivalent at 14.7 psi). This was rectified by slightly detaching the swab tube and removing that pressure differential before removing the white end cap.

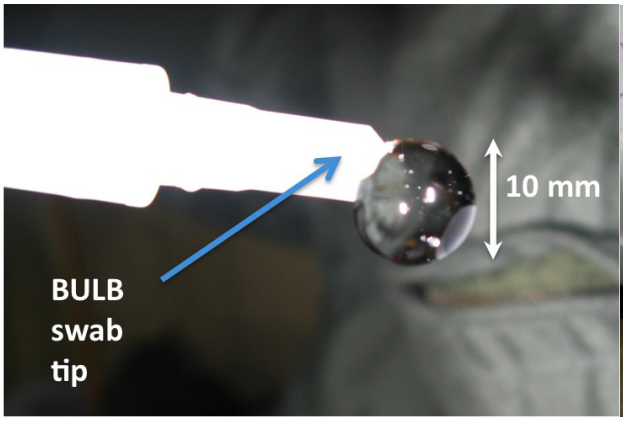

Figure 4. Droplet dispensed with BULB swab unit in microgravity away from the target surface.

Figure 5. Dispensing droplets into sample wells of a LOCAD-PTS cartridge with the BULB swab unit in zero G. Positioning of the pipette tip 2 to 3 mm from the sample well enabled consistent volumes to be dispensed.

DISCUSSION

The BULB swab unit has been proposed to replace the existing swab unit used for LOCAD-PTS operations aboard the ISS. In many ways, the BULB swab unit is simpler to use, is more streamlined, and has the capability to store a sample for later return to the ground and archiving at NASA JSC.

The BULB swab unit is a not a micropipette but a dropper-type dispenser. However, it dispenses consistent droplets in 1 G (average approximately 30 mL ± 2 mL). The tests performed here in microgravity show that, although the variation in droplet volumes increased, it was still within fairly narrow bounds (average approximately 30 mL ± 5 mL), which can be accounted for by the software in the LOCAD-PTS instrument.

Other issues, such as fluid remaining in the upper part of the swab tube (rectified by a flick) and automatic streaming of fluid from the pipette tip (rectified by a swab tube detach to remove pressure differential), were solved during each parabolic flight and can be built into future ISS procedures, if necessary. Complete mixing was performed in microgravity in fewer than 10 seconds without much difficulty.

PHOTOGRAPHS

JSC2009e047900 to JSC2009e047918
JSC2009e047925 to JSC2009e047943

VIDEO

- Zero G flight week 2/23–2/27, 2009, Master no.: DV1998

Videos are available from the Imagery and Publications Office (GS4), NASA JSC.

CONTACT INFORMATION

Jake Maule, Ph.D.
Principal Investigator, LOCAD-PTS Exploration
BAE Systems, NASA Marshall Space Flight Center
Huntsville, AL
256-961-7486
giles.maule-1@nasa.gov

TITLE

Effectiveness of Blunt Cannulas for Drug Administration in a Microgravity Environment

FLIGHT DATE

February 26, 2009

PRINCIPAL INVESTIGATORS

Melinda J. Hailey, R.N., BSN, Wyle Integrated Science and Engineering Group
Tina M. Bayuse, Pharm.D., Wyle Integrated Science and Engineering Group

GOALS

- Identify appropriate size vial required to withdraw a defined drug volume.
- Identify hardware that facilitates withdrawal of the appropriate volume of drug from vial (various-size blunt cannulas and syringes).
- Videotape procedure used to withdraw medication from a vial into a syringe for use with on-orbit procedure.

INTRODUCTION

The current system for injectable medications aboard the ISS has experienced a materials failure that requires a new system for injectable medications to be identified and flown. It is desired that this new system will fly medications for injection in their original manufacturer's packaging. This will allow the system to comply with USP guidelines while minimizing the frequency of resupply due to medication expiration. However, this change will require crew to draw liquid medications for injection from a vial into a syringe prior to injection.

This experiment will evaluate the effectiveness of 2 versions of a blunt cannula to facilitate the withdrawal of liquid medication from a medication vial into a syringe for injection within a microgravity environment. Other parameters to be assessed include: determining the ability to withdraw the required amount of medication and whether this is dependent on vial size, liquid, or the total volume of the fluid within the vial. Liquid medications proposed for flight on ISS will be used for this experiment.

DISCLAIMER

The content of this report should not be considered final and binding. Formal review and evaluation of all data collected will be the subject of final reports and publications when deemed appropriate. The content of this report should permit the reader to become familiar with the procedures followed and the preliminary observations and lessons learned. This document neither endorses nor rejects the performance of any commercial products used.

Medications for injection are commercially available in a variety of forms, including glass/plastic single-dose vials, glass/plastic multi-dose vials, and prefilled syringes. Whenever possible, it is desired that injectable medications for use on the ISS be delivered in a prefilled syringe to limit the need for astronauts to manipulate the medication prior to administration. However, the healthcare market is constantly evolving based on new evidence sources and changing standards of care, meaning that medications are not consistently available at the desired strengths or volumes in the same packaging over a period of time.

In the event medications must be supplied in a vial, a system is required that allows for the safe withdrawal of medication from the vial into a syringe for administration. Traditionally, this method of withdrawal requires the use of a needle. In an effort to limit risk of inadvertent needle sticks, the healthcare marketplace has a variety of blunt cannulas and vial adaptors that allow direct connection of a syringe to a medication vial, eliminating the need for a sharp to pierce the vial septum.

Figure 1. Carpuject (current method of injectable meds on the ISS).

Figure 2. Single-dose and multi-dose medication vials (current method of injectable meds on the ISS).

Figure 3. Commercially prepared pre-filled medication syringes.

Figure 4. Trapping of fluid in medication vial due to fluid adhesion.

A November 2008 ZERO-G® flight was used to conduct a hardware evaluation of various needleless vial adaptors. The flight evaluation revealed that while the needleless vial adaptors are appropriate for use with multi-dose vials, single-dose medication vials with volumes <5 mL pose a greater challenge in accessing the entire drug volume required for administration. At issue is the manufacturer's air bubble in the vial. In microgravity, this air bubble traps fluid along the sides and base of the vial despite effective air/fluid separation prior to medication withdrawal. Manufacturers typically provide some overfill of the vial, but this volume is not predictable. Terrestrially, any fluid that is not immediately at the septum may be "chased" using a needle that can be manipulated to the liquid bubble. Both vial adaptors tested limited the ability to chase pockets of medication in vial, either due to the locking mechanisms on the vial top or the length of the spike. The spike-vial adaptor length was also limiting in vials holding <3 mL of fluid. The spike length in relation to where the fluid ports on the spike are was too long to allow access to all of the fluid in the vial. Use of single-dose vials without the ability to "chase" fluid risks the possibility of the inability to access all of the desired medication from the vial. Thus, this February 2009 flight was used to evaluate the effectiveness of blunt cannulas to "chase" the fluid volume in smaller-unit-dose vials of medications.

OBJECTIVE

Identify issues related to withdrawal of liquid medication for injection from a glass medication vial into a syringe within a microgravity environment using a blunt cannula.

METHODS AND MATERIALS

A market survey of blunt cannulas was performed, and 2 primary pieces of hardware were selected for further testing. A metal blunt cannula (17 G×1.5 in Kendall MONOJECT) was selected for its length as well as diameter, and a plastic blunt cannula (approximately 16 G×0.5 in, Monoject SmarTip™) was selected as a representative market sample for comparison.

Figure 5. Metal blunt cannula.

Figure 6. Plastic blunt cannula.

Hardware testing was completed using the identified blunt cannulas (metal and plastic) as well as medications in similar volume and concentration to those currently flown on the ISS. Due to delivery delays of the metal blunt cannula, ground-based preflight testing was completed using an 18 G×1.5-in, metal needle as a substitute. The flight portion of the evaluation was designed to be completed within 20 parabolas, lasting approximately 20 seconds each, with testing divided into three segments: Segment 1 – fluid withdrawal from vial; Segment 2 – fluid isolation within a syringe; Segment 3 – video documentation of procedure steps required to withdraw medication from vial into syringe. Two participants were used to conduct all tests. One fixed video camera was used to document the experiment. Feedback on each medication and device was captured by activated microphones attached to both participants. Materials were immobilized using Velcro® and foam blocks for safety during periods of aircraft turbulence and during microgravity portions of the flight. Potential sharp objects (e.g., medication vials) were disposed of in a sharps container that was attached to the table used in the experiment. Any liquids that were inadvertently released during microgravity portions of the flight were captured using towels secured to the work surface. Postflight testing using the metal blunt cannula was completed with a smaller-diameter cannula due to problems discovered in flight.

RESULTS/DISCUSSION/CONCLUSION

Based on findings from the November 2008 flight as well as this flight, there are 3 areas of discussion for this report: (1) ability to withdraw required amount of medication from vial, (2)

air/fluid separation within syringe, and (3) medication characteristics posing issues in microgravity.

(1) **Withdrawal of medication from vial**: Two general areas for discussion were observed during this portion of the testing.

a. ***Piercing the medication vial septum*** – Due to a delay in delivery of required hardware, ground-based testing of the metal blunt cannula was not possible. A substitution was made, and the preflight ground-based testing used an 18 G×1.5-in needle instead. Both the needle and the plastic cannula easily pierced through the vial septum in 1-G testing. In flight, however, it was discovered that the diameter of the blunt metal cannula caused a disruption of fluid at the septum, thus negating the effects of a good fluid/air separation maneuver. This, coupled with the short duration of zero-G parabolas (<20 seconds each) limited the amount of data collected, as time was spent in zero G trying to re-isolate fluid as well as chase fluid from around the vial sides. The plastic blunt cannula performed consistently well with septum perforation due to the narrowed tip, which facilitates an efficient, non-coring pierce to the septum.

b. ***Withdrawal of fluid from the vial*** – A 1-G evaluation of the hardware revealed that both the metal and the plastic blunt cannulas were capable of withdrawing the required volume from all of the tested medication vials. It was observed that the metal blunt cannula was able to reach the bottom corners of ≤3-mL vials, thus allowing the operator to "chase" the medication in all areas within the vial. Due to the short length of the plastic blunt cannula, this was not possible. Inflight test results for both pieces of hardware were inconsistent. Some medications were better withdrawn with the plastic cannula and others with the metal cannula. It is hypothesized that this inconsistency could be attributed to the additional time required for fluid isolation within the vial due to the challenges mentioned above related to spiking the blunt metal cannula as well as the time required to re-isolate fluid in the vials used with the blunt plastic cannula due to its shortened length.

Figure 7. Metal blunt cannula in 2-mL vial (cap vial adaptor).

Figure 8. Plastic blunt cannula in 2-mL vial (cap vial adaptor).

(2) **Air/fluid separation in syringe**: Due to dead space within vial adaptors and blunt cannulas, despite effective fluid isolation in vial some air will inevitably be mixed into medications as they are withdrawn into a syringe. This air, combined with any microbubbles that are possibly still in solution, will require a second effort on the part of the astronaut to isolate fluid in the

syringe prior to medication administration. Selection of a syringe size larger than the volume of medication required is considered to be helpful so that a larger volume than necessary may be withdrawn, followed by fluid and air being isolated and then extra air ejected from syringe. For this flight, air/fluid separation was evaluated in syringes that were prefilled with a defined volume prior to the flight start. It was observed that, when the ratio of fluid-to-volume within a syringe increased, the more challenging it was to isolate fluid from air. Given the short duration of microgravity parabolas, it is hypothesized that repeated attempts at fluid isolation will make it possible to achieve sufficient separation no matter what size syringe is used. However, it is felt that a larger syringe volume than medication volume should be considered when selecting hardware for use with injection.

CONCLUSIONS/RECOMMENDATIONS

1. Plastic tip and blunt metal cannulas both facilitate the effective removal of medication from single-dose medication vials ≤3 mL. However, it is proposed that hardware selected for use with single-dose vials ≤3 mL within a microgravity environment have the ability to reach the entire interior surface to facilitate "chasing" of medication. This selection will limit the number of attempts to isolate fluid in vial for one-dose withdrawal, as well as limit repeated punctures to the vial septum.
2. The diameter of the metal blunt cannula was a limiting factor in the microgravity portion of this evaluation. It is the investigators' recommendation that a ground-based evaluation of a smaller-diameter blunt cannula be performed to see whether perforation of the vial septum is easier. If it is found that this smaller cannula does not facilitate an easier perforation, it would be our recommendation that the plastic blunt cannula be flown.
3. Fluid isolation within a syringe is easier to achieve with a syringe volume that is greater that the medication volume. For example,
   a. 1-mL to 2-mL medication volume should use a ≥3-mL syringe.
   b. 3-mL medication volume should use a ≥5-mL syringe.
   c. ≥4-mL medication volume should use a ≥10-mL syringe.

Limitations of evaluation:

1. Parabola length was too short to evaluate all of the steps required to withdraw medications from a vial, taking into consideration fluid bubble management. These steps are required in full sequence in microgravity to fully assess the time impact required to withdraw the medications.
2. Bubbles and microbubbles that could be formed during the agitation of launch and subsequent continuous microgravity could not be realized in this study due to the aircraft pullouts.

ACKNOWLEDGMENTS

The investigators would like to acknowledge the following persons/groups for their support with flight preparation and execution for this evaluation: Terry Guess and David Ham along with the Advanced Projects team at Wyle Integrated Science and Engineering Group, Crew Health Hardware Integration and Program Support Team (Wyle), the NASA Health Maintenance System Management team, and the NASA JSC Pharmacy. Finally, the investigators also acknowledge the valued support and guidance from the NASA JSC RGO.

PHOTOGRAPHS

JSC2009E048793 to JSC2009E048796

VIDEO

- Zero-G flight week 2/23–2/27/09, Master no.: DV1998

Videos are available from the Imagery and Publications Office (GS4), NASA JSC.

CONTACT INFORMATION

Melinda J. Hailey, R.N., BSN
HMS Instructor, Space Medicine Training
Wyle Integrated Science and Engineering Group
1290 Hercules Avenue, Suite 120 (MC: W1A)
Houston, TX 77058
281-212-1355
Melinda.j.hailey@nasa.gov

Tina M. Bayuse, Pharm.D.
Lead Pharmacist, JSC Pharmacy
Wyle Integrated Science and Engineering Group
NASA-Johnson Space Center
2101 NASA Parkway (MC: SD38)
Houston, TX 77058
281-244-1632
Tina.M.Bayuse@nasa.gov

TITLE
Education Outreach Program – Medical Injections for Emergency Extended EVA Suit

FLIGHT DATE
April 3, 2009

PRINCIPAL INVESTIGATOR
John McQuillen, University of Kentucky

CO-INVESTIGATORS
Allyson Durborow, University of Kentucky
John Whitt, University of Kentucky
Hannah Grise, University of Kentucky
Daniel Moore, University of Kentucky
Tyler Young, University of Kentucky
Travis Ray, University of Kentucky

GOAL

This University of Kentucky experiment dealt with the development and design for the next-generation EVA suits for Constellation missions to the Moon. The Human Research Program is currently conducting preliminary studies to examine feasibility issues associated with extended continuous use of EVA suits of up to 144 hours. The purpose of this study is to determine how to handle an emergency situation that would occur if the spacecraft cabin atmosphere becomes unsuitable to sustain life.

A partial or complete loss of cabin pressure could cause a spacecraft fire, which could render the cabin atmosphere incompatible with life. In the event that an emergency does occur, the astronauts will need medication. The purpose of this experiment is to determine how it would be possible to deliver medications to the astronauts. This is important because an injury could occur during the extended duration within the suit. There are multiple microgravity issues such as dosage preparation, penetration of the syringe needle through the suit portal, foreign objects within the syringe needle, and targeting the appropriate tissue for injection. It is important to move the air bubble in the syringe to the top of the syringe so that it will not cause harm to the astronauts. If it is not moved out of the syringe, air embolism can occur. Air embolism, which is a medical condition caused by gas bubbles in the bloodstream, can cause death if a gas bubble becomes lodged in the heart and stops blood flow.

OBJECTIVES

The University of Kentucky's main objectives with this experiment were to see movement of the bubble in all the syringes, the bubble moved to the top of the syringe, which speed (rpm) worked better for the movement of the bubble, and how the small and large bubbles moved in the different syringe sizes.

METHODS AND MATERIALS

The University of Kentucky's research began with internet research to gain a better understanding of the experiment problem. The team also worked with the assigned NASA mentor to grasp an idea of what was expected to obtain successful data. Once a good understanding of the experiment was obtained, the team consulted with our University of Kentucky mentor and various University of Kentucky professors to talk through design ideas. Talking with the assigned NASA mentor, University of Kentucky mentor, and University of Kentucky professors was very helpful because the team was then able to begin sketching and modeling preliminary designs for the experiment.

After running through many preliminary designs, one design was decided on. This design uses a rotating aluminum shaft with 2 steel circular disks driven by a stepper motor. The first circular disk contains 0.5-mL, 1-mL, 3-mL, 6-mL, and 10-mL syringes of water and glycerin that are set at a 15-degree angle from the horizontal. The second circular disk, which is placed directly above the disk with the syringes, has 4 digital video cameras to record the movement of the bubbles in the syringes. Each of the syringes is filled with food coloring and either a large or small bubble size. Table 1 describes this labeling system. The shaft and disks are all completely

enclosed in a Plexiglas® box that is mounted on a metal rack that was provided by our NASA mentor.

Table 1

Parabola	Rate	Syringe Size	Syringe Content			
1	(1) Slow	10 mL	Big – Water	Small – Water	Big – Glycerin	Small – Glycerin
2	(2) Fast	10 mL	Big – Water	Small – Water	Big – Glycerin	Small – Glycerin
3	(3) Fast-Stop	10 mL	Big – Water	Small – Water	Big – Glycerin	Small – Glycerin
4	(4) Medium	10 mL	Big – Water	Small – Water	Big – Glycerin	Small – Glycerin
5	(5) Slow-Stop	10 mL	Big – Water	Small – Water	Big – Glycerin	Small – Glycerin
6	(6) Medium-Stop	10 mL	Big – Water	Small – Water	Big – Glycerin	Small – Glycerin
7	(1) Slow	0.5 mL	Big – Water	Small – Water	Big – Glycerin	Small – Glycerin
8	(2) Fast	0.5 mL	Big – Water	Small – Water	Big – Glycerin	Small – Glycerin
9	(3) Fast-Stop	0.5 mL	Big – Water	Small – Water	Big – Glycerin	Small – Glycerin
10	(4) Medium	0.5 mL	Big – Water	Small – Water	Big – Glycerin	Small – Glycerin
11	(5) Slow-Stop	0.5 ml	Big – Water	Small – Water	Big – Glycerin	Small – Glycerin
12	(6) Medium-Stop	0.5 mL	Big – Water	Small – Water	Big – Glycerin	Small – Glycerin
13	(1) Slow	3 ml	Big – Water	Small – Water	Big – Glycerin	Small – Glycerin
14	(2) Fast	3 mL	Big – Water	Small – Water	Big – Glycerin	Small – Glycerin
15	(3) Fast-Stop	3 mL	Big – Water	Small – Water	Big – Glycerin	Small – Glycerin
16	(4) Medium	3 mL	Big – Water	Small – Water	Big – Glycerin	Small – Glycerin
17	(5) Slow-Stop	3 mL	Big – Water	Small – Water	Big – Glycerin	Small – Glycerin
18	(6) Medium-Stop	3 mL	Big – Water	Small – Water	Big – Glycerin	Small – Glycerin
19	(1) Slow	1 mL	Big – Water	Small – Water	Big – Glycerin	Small – Glycerin
20	(2) Fast	1 mL	Big – Water	Small – Water	Big – Glycerin	Small – Glycerin
21	(3) Fast-Stop	1 mL	Big – Water	Small – Water	Big – Glycerin	Small – Glycerin
22	(4) Medium	1 mL	Big – Water	Small – Water	Big – Glycerin	Small – Glycerin
23	(5) Slow-Stop	1 mL	Big – Water	Small – Water	Big – Glycerin	Small – Glycerin
24	(6) Medium-	1 mL	Big – Water	Small –	Big –	Small –

Table 1						
Parabola	Rate	Syringe Size	Syringe Content			
	Stop			Water	Glycerin	Glycerin
25	(1) Slow	6 mL	Big – Water	Small – Water	Big – Glycerin	Small – Glycerin
26	(2) Fast	6 mL	Big – Water	Small – Water	Big – Glycerin	Small – Glycerin
27	(3) Fast-Stop	6 mL	Big – Water	Small – Water	Big – Glycerin	Small – Glycerin
28	(4) Medium	6 mL	Big – Water	Small – Water	Big – Glycerin	Small – Glycerin
29	(5) Slow-Stop	6 mL	Big – Water	Small – Water	Big – Glycerin	Small – Glycerin
30	(6) Medium-Stop	6 mL	Big – Water	Small – Water	Big – Glycerin	Small – Glycerin

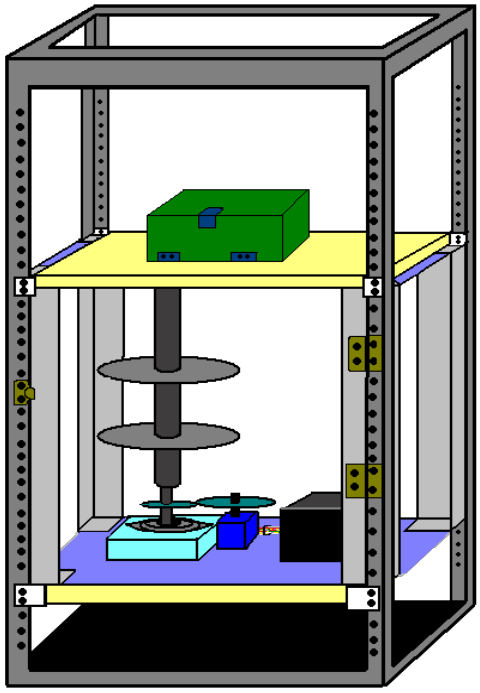

Illustration of the test rig.

After researching and constructing the design, the University of Kentucky team made hypotheses about the experiment. These hypotheses were as follows:

- If an astronaut flicks his or her wrist quickly, the bubble will move.
- If the syringes are spun at fast speeds on the disks, the bubble will move.

RESULTS

The air bubble was observed to move with certain combinations of syringe diameter, fluid viscosity, and rotation speed. Bubble motion was recorded at all 3 rotation speeds in the second

flight. These speeds were 26 rpm, 44 rpm, and 54 rpm. In the first flight, the rotation speeds of 6 rpm, 16 rpm, and 26 rpm yielded no bubble movement. While 26 rpm was evaluated in both flights, movement was observed only in the second flight due to an increase in rotation duration from the first flight. The increase of 5 seconds in the rotation time allowed for an increase in momentum sufficient to move the air bubble.

The tables and graphs below show the results for the various syringes for both flight days.

Water – Big Bubble

Slow	Syringe Volume (mL)	Start Location (mL)	Final Location (mL)	Displacement (mL)	Did bubble move all the way to the needle?
	0.5	0.5	0.5	0	No
	1	1	1	0	No
	3	2.4	0.7	1.7	No
	6	No Data	No Data	No Data	--
	10	No Data	No Data	No Data	--

Fast	Syringe Volume (mL)	Start Location (mL)	Final Location (mL)	Displacement (mL)	Did bubble move all the way to the needle?
	0.5	0.5	0.5	0	No
	1	1	1	0	No
	3	2.4	0	2.4	Yes
	6	No Data	No Data	No Data	--
	10	7.4	0	7.4	Yes

Fast-Stop	Syringe Volume (mL)	Start Location (mL)	Final Location (mL)	Displacement (mL)	Did bubble move all the way to the needle?
	0.5	0.5	0.5	0	No
	1	1	1	0	No
	3	No Data	No Data	No Data	--
	6	3.8	0	3.8	Yes
	10	7.3	0	7.3	Yes

Medium	Syringe Volume (mL)	Start Location (mL)	Final Location (mL)	Displacement (mL)	Did bubble move all the way to the needle?
	0.5	0.5	0.5	0	No
	1	1	1	0	No
	3	2.3	0	2.3	Yes
	6	3.8	0	3.8	Yes
	10	7.4	0	7.4	Yes

Slow-Stop	Syringe Volume (mL)	Start Location (mL)	Final Location (mL)	Displacement (mL)	Did bubble move all the way to the needle?
	0.5	0.5	0.5	0	No
	1	1	1	0	No
	3	2.4	1.3	1.1	No
	6	3.8	0	3.8	Yes
	10	7.5	0	7.5	Yes

Medium-Stop	Syringe Volume (mL)	Start Location (mL)	Final Location (mL)	Displacement (mL)	Did bubble move all the way to the needle?
	0.5	0.5	0.5	0	No
	1	1	1	0	No
	3	2.4	1.3	1.1	No
	6	3.8	0	1.3	Yes
	10	7.4	0	7.4	Yes

Water – Small Bubble

Slow	Syringe Volume (mL)	Start Location (mL)	Final Location (mL)	Displacement (mL)	Did bubble move all the way to the needle?
	0.5	0.5	0.5	0	No
	1	No Data	No Data	No Data	--
	3	3	3	0	No
	6	No Data	No Data	No Data	--
	10	No Data	No Data	No Data	--

Fast	Syringe Volume (mL)	Start Location (mL)	Final Location (mL)	Displacement (mL)	Did bubble move all the way to the needle?
	0.5	0.5	0.5	0	No
	1	No Data	No Data	No Data	--
	3	2.4	0	2.4	Yes
	6	No Data	No Data	No Data	--
	10	7.4	0	7.4	Yes

Fast-Stop	Syringe Volume (mL)	Start Location (mL)	Final Location (mL)	Displacement (mL)	Did bubble move all the way to the needle?
	0.5	0.5	0.5	0	No
	1	No Data	No Data	No Data	--
	3	No Data	No Data	No Data	--
	6	4.8	0	4.8	Yes
	10	7.4	0	7.4	Yes

Medium	Syringe Volume (mL)	Start Location (mL)	Final Location (mL)	Displacement (mL)	Did bubble move all the way to the needle?
	0.5	0.5	0.5	0	No
	1	No Data	No Data	No Data	--
	3	3	3	0	No
	6	4.8	0	4.8	Yes
	10	7.4	0	7.4	Yes

Slow-Stop	Syringe Volume (mL)	Start Location (mL)	Final Location (mL)	Displacement (mL)	Did bubble move all the way to the needle?
	0.5	0.5	0.5	0	No
	1	No Data	No Data	No Data	--
	3	3	3	0	No
	6	4.8	0	4.8	Yes
	10	7.4	0	7.4	Yes

Medium-Stop	Syringe Volume (mL)	Start Location (mL)	Final Location (mL)	Displacement (mL)	Did bubble move all the way to the needle?
	0.5	0.5	0.5	0	No
	1	No Data	No Data	No Data	--
	3	3	3	0	No
	6	4.8	0	4.8	Yes
	10	7.4	0	7.4	Yes

Glycerin – Big Bubble

Slow	Syringe Volume (mL)	Start Location (mL)	Final Location (mL)	Displacement (mL)	Did bubble move all the way to the needle?
	0.5	0.5	0.5	0	No
	1	1	1	0	No
	3	2.5	2.2	0.3	No
	6	No Data	No Data	No Data	--
	10	No Data	No Data	No Data	--

Fast	Syringe Volume (mL)	Start Location (mL)	Final Location (mL)	Displacement (mL)	Did bubble move all the way to the needle?
	0.5	0.5	0.5	0	No
	1	1	1	0	No
	3	2.5	1.2	1.3	No
	6	No Data	No Data	No Data	--
	10	5.8	0	5.8	Yes

Fast-Stop	Syringe Volume (mL)	Start Location (mL)	Final Location (mL)	Displacement (mL)	Did bubble move all the way to the needle?
	0.5	0.5	0.5	0	No
	1	1	1	0	No
	3	No Data	No Data	No Data	--
	6	4	2.8	1.2	No
	10	5.8	2.8	3	No

Medium	Syringe Volume (mL)	Start Location (mL)	Final Location (mL)	Displacement (mL)	Did bubble move all the way to the needle?
	0.5	0.5	0.5	0	No
	1	1	1	0	No
	3	2.5	1.7	0.8	No
	6	4	0.6	3.4	No
	10	5.8	0	5.8	Yes

Slow-Stop	Syringe Volume (mL)	Start Location (mL)	Final Location (mL)	Displacement (mL)	Did bubble move all the way to the needle?
	0.5	0.5	0.5	0	No
	1	1	1	0	No
	3	2.5	1.9	0.6	No
	6	4	3.4	0.6	No
	10	5.8	3.2	2.6	No

Medium-Stop	Syringe Volume (mL)	Start Location (mL)	Final Location (mL)	Displacement (mL)	Did bubble move all the way to the needle?
	0.5	0.5	0.5	0	No
	1	No Data	No Data	No Data	--
	3	2.5	1.8	0.7	No
	6	4	3	1	No
	10	5.8	3.2	2.6	No

Glycerin – Small Bubble

Slow	Syringe Volume (mL)	Start Location (mL)	Final Location (mL)	Displacement (mL)	Did bubble move all the way to the needle?
	0.5	0.5	0.5	0	No
	1	1	1	0	No
	3	2.4	2.2	0.2	No
	6	No Data	No Data	No Data	--
	10	No Data	No Data	No Data	--

Fast	Syringe Volume (mL)	Start Location (mL)	Final Location (mL)	Displacement (mL)	Did bubble move all the way to the needle?
	0.5	0.5	0.5	0	No
	1	1	1	0	No
	3	2.4	1.2	1.2	No
	6	No Data	No Data	No Data	--
	10	6.4	0	6.4	Yes

Fast-Stop	Syringe Volume (mL)	Start Location (mL)	Final Location (mL)	Displacement (mL)	Did bubble move all the way to the needle?
	0.5	0.5	0.5	0	No
	1	1	1	0	No
	3	No Data	No Data	No Data	--
	6	4.6	3.6	1	No
	10	6.4	2.6	3.8	No

Medium	Syringe Volume (mL)	Start Location (mL)	Final Location (mL)	Displacement (mL)	Did bubble move all the way to the needle?
	0.5	0.5	0.5	0	No
	1	No Data	No Data	No Data	--
	3	3.2	1.8	0.6	No
	6	4.6	3.5	1.1	No
	10	6.6	0	6.6	Yes

Slow-Stop	Syringe Volume (mL)	Start Location (mL)	Final Location (mL)	Displacement (mL)	Did bubble move all the way to the needle?
	0.5	0.5	0.5	0	No
	1	1	1	0	No
	3	2.4	2.2	0.2	No
	6	4.6	3.8	0.8	No
	10	6.8	4	2.8	No

Medium-Stop	Syringe Volume (mL)	Start Location (mL)	Final Location (mL)	Displacement (mL)	Did bubble move all the way to the needle?
	0.5	0.5	0.5	0	No
	1	1	1	0	No
	3	2.4	2.3	0.1	No
	6	4.5	0.4	4.1	No
	10	6.8	4	2.8	No

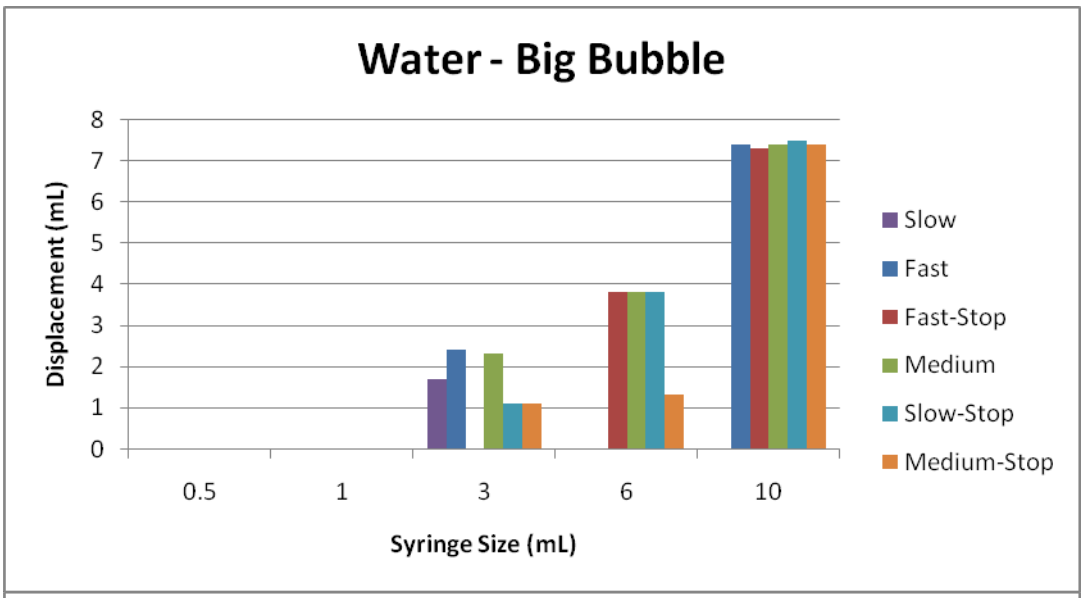
Water - Big Bubble
Displacement (mL)
0
1
2
3
4
5
6
7
8
0.5
1
3
6
10
Syringe Size (mL)
Slow
Fast
Fast-Stop
Medium
Slow-Stop
Medium-Stop

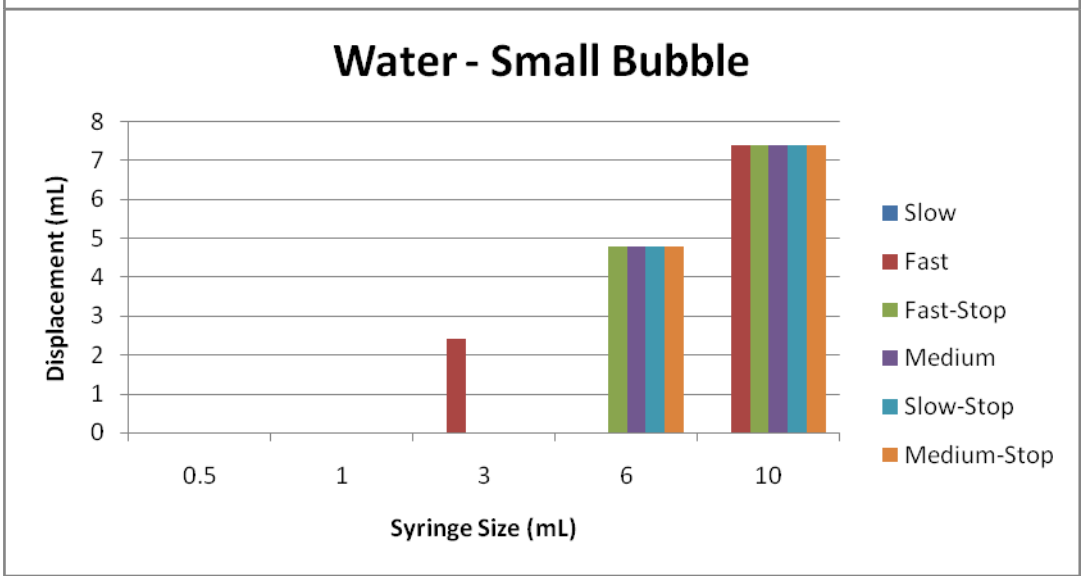
Water - Small Bubble
Displacement (mL)
0
1
2
3
4
5
6
7
8
0.5
1
3
6
10
Syringe Size (mL)
Slow
Fast
Fast-Stop
Medium
Slow-Stop
Medium-Stop

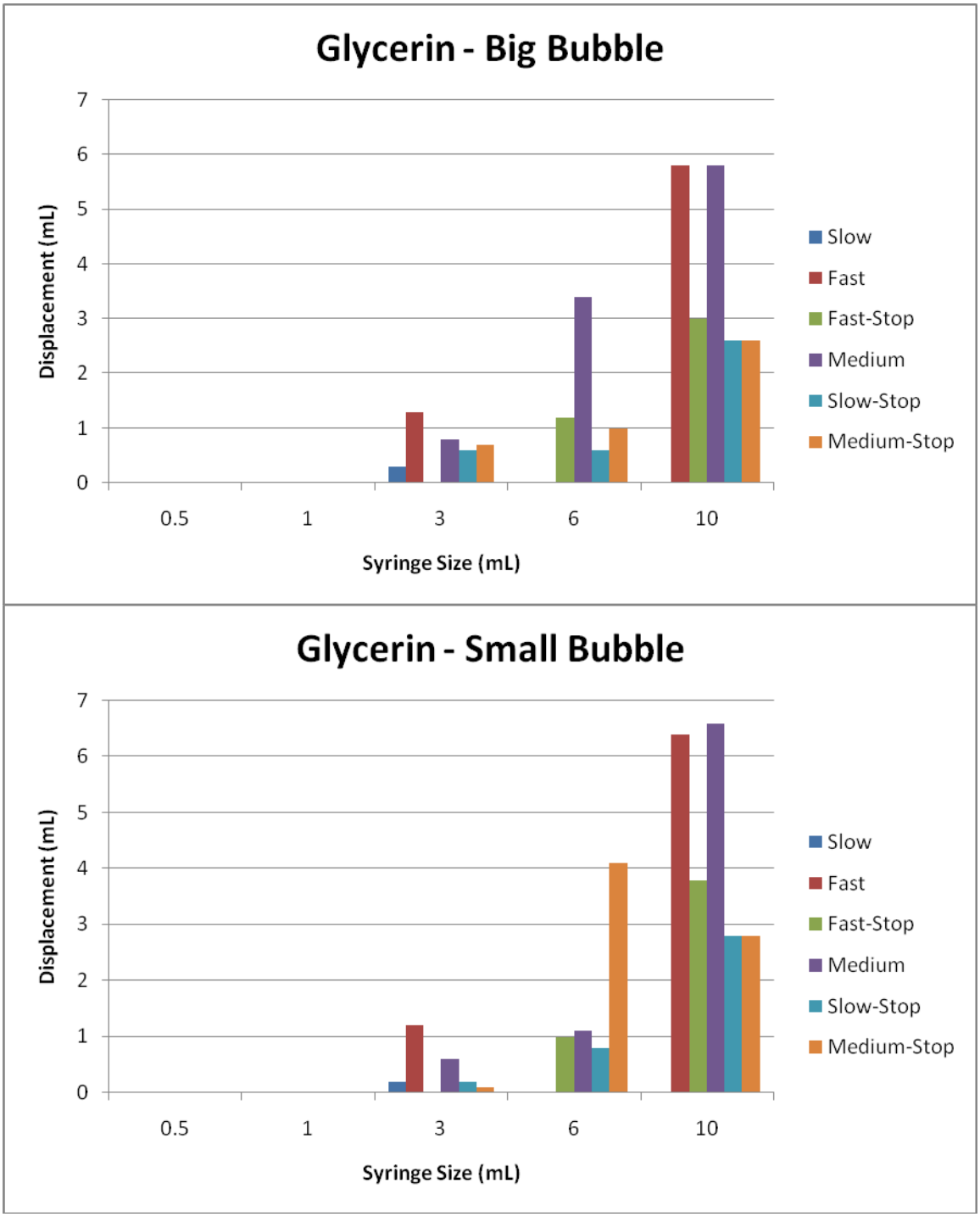

*See Appendix for conversion from mL to in.
**Results with no data are given a value of 0 on graphs.

The force acting at the center of the syringes increases with rotation speed. The G-forces acting on the syringes for each of the tested rpm's are:

0.0026 Gs for 6 rpm
0.0070 Gs for 16 rpm

0.0113 Gs for 26 rpm
0.0192 Gs for 44 rpm
0.0235 Gs for 54 rpm

These G-forces were found using the following equation:

$G = (1.118 \times 10^{-5})\ R\ S^2$

where *G* is the G-force created by the centrifugal force, R is the radius of the rotor in centimeters, and S is the rpm's at which the syringe was rotated.

The following is a sample calculation of the G-force acting on a syringe rotating at 26 rpm:

S = 26 rpm
R = 2.5 in * (2.54cm/ 1in) = 6.35cm
$G = (1.118 \times 10^{-5})$ (26 rpm) $(6.35\text{cm})^2$
G = 0.0117 Gs

Due to the fact that the syringes were placed on wedges, the component of the G-force, which acts in the direction of the syringe, must be calculated as follows:

c = *g*cos15º

where c is the component of the G-force that acts in the direction of the syringe and *g* is still the G-force created by the centrifugal force.

c = *g*cos15º
c = 0.0113 Gs

DISCUSSION

This experiment provided many challenging opportunities for the team members involved. The proper alignment of the shaft in the bearings proved to be quite problematic. We were unable to acquire the highly accurate measuring tools required to gain the precise alignment necessary for the bearings. Without the proper alignment the bearings were unable to reduce the friction enough to allow for shaft movement. Using the tools we had access to, we secured the bearings in as close to the correct alignment as possible. Because we could not find the perfect alignment, there was a slight wobble in the shaft. To stop the shaft from wobbling, the motor had to be allowed to wobble. The challenge we faced was finding a way to secure the motor but still allow for it to wobble. We solved the problem of securing the motor by using a vice clamp. The clamp secured the motor in place while allowing enough movement in the motor to correct the wobble in the shaft.

Another challenge we encountered was the proper propositioning of the air bubble. To observe the effects of the centrifugal forces on the air bubble, the bubble had to begin at the end of the syringe that was furthest from the center of rotation. To solve this problem, the syringes were placed on wedges. The incline of the wedges allowed the bubble to be forced to the top of the

syringe when gravity acted on the fluid in the syringe. This solution effectively allowed the bubble to preposition automatically between each parabola.

CONCLUSION

As can be seen from the graphs and charts on the previous pages, the bubble moved in the larger-size syringes, which were the 3-mL, 6-mL, and10-mL syringes. There was very little movement in the 0.5-mL and 1-mL syringes. The bubble also moved more easily in water than in glycerin. The medium to fast speeds moved the bubble the most in the syringes. For the slower speeds, the bubble did not move. For water, the big bubble and the small bubble were very similar displacement wise. The displacement in glycerin of the big bubble and the small bubble was also very similar.

APPENDIX

The dimensions of the 6 tested syringes are as follows:

Volume (mL)	Diameter (mm)	Diameter (in)	Length (in)	Number of tick marks on each syringe	Distance between each tick mark (in)	Number of inches corresponding to 1 mL on the syringe
0.5	4.64	0.18	1.16	50	0.023	2.33
1	4.78	0.19	2.19	100	0.022	2.19
3	8.66	0.34	2.01	30	0.067	0.67
6	12.7	0.50	1.86	30	0.062	0.31
10	14.5	0.57	2.38	50	0.048	0.24

The last column of the table above can be used to convert the displaced volume to the actual distance the bubble moved in the syringe.

PHOTOGRAPHS

JSC2009E070199 to JSC2009E0070202
JSC2009E070224
JSC2009E 070298
JSC2009E070339
JSC2009E070342
JSC2009E070349
JSC2009E070351
JSC2009E070353
JSC2009E070354
JSC2009E070372
JSC2009E070373

VIDEO

- Zero-G flight week 3/30–4/03/09, Master no.: DV2062

Videos are available from the Imagery and Publications Office (GS4), NASA JSC.

CONTACT INFORMATION

Hannah.Grise@uky.edu
John.B.McQuillen@nasa.gov

Appendix

Background Information about the C-9 and the Reduced Gravity Program

The Reduced Gravity Program, operated by NASA JSC, provides engineers, scientists, and astronauts alike a unique opportunity to perform testing and training in a weightless environment without ever having to leave the confines of the Earth's orbit. Given the frequency of space shuttle missions and the construction and habitation of the new ISS, the Reduced Gravity Program provides a truly ideal environment in which to test and evaluate space hardware and experimental procedures prior to launch.

The Reduced Gravity Program was established in 1959 to investigate the reactions of humans and hardware during operations in a weightless environment. A specially modified turbojet, flying parabolic arcs, produces periodic episodes of weightlessness lasting 20 seconds to 25 seconds. The aircraft is sometimes also flown to provide short periods of lunar (1/6) and Martian (1/3) gravity. Over the last 50 years, more than 100,000 parabolas have been flown in support of Project Mercury and the Gemini, Apollo, Skylab, Space Shuttle, and International Space Station Programs.

Excluding the C-9 flight crew and the Reduced Gravity Program test directors, the NASA C-9 aircraft accommodates seating for a maximum of 20 other passengers. The C-9 cargo bay provides a test area that is approximately 45-ft long, 104-in wide, and 80-in high.

NASA has also recently transitioned to using the ZERO-G® 727 aircraft, which will hold up to 30 investigators. The ZERO-G® 727 is nearly identical in size and volume to the KC-135 aircraft that was previously used by NASA to support the Reduced Gravity Program. This Boeing 727 has a larger cargo door to accommodate large payloads and provides a test area that is approximately 70 ft long, 140 in wide, and 86 in high.

Both aircraft are equipped with electrical power for test equipment and photographic lights. When requested, professional photography and video support can be scheduled to document activities in flight.

A typical flight lasts 2 hours to 3 hours and consists of 30 parabolas to 40 parabolas. The parabolas are flown in succession or with short breaks between maneuvers to allow time for reconfiguration of test equipment.

For additional information concerning flight weeks sponsored by the JSC Human Adaptation and Countermeasures Division or other Reduced Gravity Program opportunities, please contact:

Todd Schlegel, M.D.
Technical Monitor, Human Adaptation
and Countermeasures Division
NASA Lyndon B. Johnson Space Center
Mail Code: SK
Houston, TX 77058
Telephone: 281-483-9643

Dominic Del Rosso
Test Director
NASA Lyndon B. Johnson Space Center
Reduced Gravity Office, Ellington Field
Mail Code: CC43
Houston, TX 77034
Telephone: 281-244-9113

Explore the Zero-Gravity Experiments and Aircraft Operations Web pages at:
http://zerog.jsc.nasa.gov/
http://jsc-aircraft-ops.jsc.nasa.gov